

**“ROLE OF ULTRASONOGRAPHY AND  
ELASTOGRAPHY IN EVALUATION OF SOLID  
THYROID NODULES”**

By

**Dr. SHABARISH D V**

Dissertation submitted to the

**B.L.D.E. UNIVERSITY VIJAYPUR, KARNATAKA**



In partial fulfillment of the requirements for the degree of

**DOCTOR OF MEDICINE**

In

**RADIO-DIAGNOSIS**

Under the guidance of

**DR. RAMESH C PATTANSHETTI**<sub>M.D.</sub>

PROFESSOR and HOD

DEPARTMENT OF RADIO-DIAGNOSIS

B.L.D.E.U'S SHRI B. M.PATIL MEDICAL COLLEGE

HOSPITAL & RESEARCH CENTRE, VIJAYPUR

KARNATAKA

**2021**

**B.L.D.E. UNIVERSITY'S**  
**SHRI B. M. PATIL MEDICAL COLLEGE, HOSPITAL &**  
**RESEARCH CENTRE, VIJAYPUR**

**DECLARATION BY THE CANDIDATE**

I, **Dr. SHABARISH D V**, hereby declare that this dissertation entitled  
**“ROLE OF ULTRASONOGRAPHY AND ELASTOGRAPHY IN**  
**EVALUATION OF SOLID THYROID NODULES”** is a bonafide and  
genuine research work carried out by me under the guidance of **Dr.**  
**RAMESH C PATTANSHETTI** Professor and HOD, Department of  
Radiodiagnosis, B.L.D.E.U's Shri B. M. Patil Medical College Hospital  
and Research Centre, Vijaypur.

Date:23-10-2020

Place: Vijaypur



**Dr. SHABARISH D V**  
Post Graduate Student,  
Department of Radiodiagnosis,  
B.L.D.E.U's Shri B. M. Patil Medical  
College, Hospital & Research Centre,  
Vijaypur.

**B.L.D.E. UNIVERSITY'S**  
**SHRI B. M. PATIL MEDICAL COLLEGE, HOSPITAL &**  
**RESEARCH CENTRE, VIJAYPUR**

**CERTIFICATE BY THE GUIDE**

This to certify that the dissertation entitled “**ROLE OF ULTRASONOGRAPHY AND ELASTOGRAPHY IN EVALUATION OF SOLID THYROID NODULES**” is a bonafide research work done by **Dr. SHABARISH D V**, under my overall supervision and guidance, in partial fulfilment of the requirements for the degree of M. D. in Radiodiagnosis.

Date:23-10-2020



Place: Vijaypur **Dr. RAMESH C PATTANSHETTI**<sub>M.D.</sub>  
Professor and HOD  
Department of Radiodiagnosis,  
B.L.D.E.U's Shri B. M. Patil Medical College,  
Hospital & Research Centre, Vijaypur.

**B.L.D.E. UNIVERSITY'S**  
**SHRI B. M. PATIL MEDICAL COLLEGE, HOSPITAL &**  
**RESEARCH CENTRE, VIJAYPUR**

**ENDORSEMENT BY THE HEAD OF DEPARTMENT**

This to certify that the dissertation entitled “**ROLE OF ULTRASONOGRAPHY AND ELASTOGRAPHY IN EVALUATION OF SOLID THYROID NODULES**” is a bonafide research work done by **Dr.SHABARISH D V** under the guidance of **Dr. RAMESH C PATTANSHETTI** Professor,& Head of Department of Radiodiagnosis at B.L.D.E.U's Shri B. M. Patil Medical College Hospital and Research Centre, Vijaypur.

Date:23-10-2020

Place: Vijaypur



**Dr. RAMESH C PATTANSHETTI** M.D.  
Professor and HOD  
Department of Radiodiagnosis,  
B.L.D.E.U's Shri B. M. Patil Medical College,  
Hospital & Research Centre, Vijaypur.

**B.L.D.E. UNIVERSITY'S**  
**SHRI B. M. PATIL MEDICAL COLLEGE, HOSPITAL &**  
**RESEARCH CENTRE, VIJAYPUR**

**ENDORSEMENT BY THE PRINCIPAL**

This to certify that the dissertation entitled “**ROLE OF ULTRASONOGRAPHY AND ELASTOGRAPHY IN EVALUATION OF SOLID THYROID NODULES**” is a bonafide research work done by **Dr. SHABARISH D V** under the guidance of **Dr. RAMESH C PATTANSHETTI** Professor and HOD, Department of Radiodiagnosis at B.L.D.E.U's Shri B. M. Patil Medical College Hospital and Research Centre, Vijaypur.

Date: **23-10-2020**



Place: Vijaypur.

**Dr. ARAVIND PATIL**  
Principal, B.L.D.E.U's  
Shri B. M. Patil Medical College,  
Hospital & Research Centre, Vijaypur.

**B.L.D.E. UNIVERSITY'S  
SHRI B. M. PATIL MEDICAL COLLEGE, HOSPITAL &  
RESEARCH CENTRE, VIJAYPUR**

**COPYRIGHT**

**DECLARATION BY THE CANDIDATE**

I hereby declare that the B.L.D.E. UNIVERSITY, VIJAYPUR, Karnataka shall have the rights to preserve, use and disseminate this dissertation/thesis in print or electronic format for academic/research purposes.

Date:23-10-2020

Place: Vijaypur



**Dr. SHABARISH D V**  
Post Graduate Student,  
Department of Radiodiagnosis,  
B.L.D.E.U's Shri B. M. Patil Medical  
College, Hospital & Research Centre,  
Vijaypur.

## **ACKNOWLEDGEMENT**

*This piece of work has been accomplished with the grace of almighty God. It gives me immense pleasure to express my heartfelt gratitude to all. I dedicate this page to each and everyone who has helped me to explore the expanses of knowledge.*

*I express my profound gratitude and sincere thanks to my guide, **Dr. Ramesh C Pattanshetti** M.D., Professor & Head, Department of Radiology, B.L.D.E.U's Shri B. M. Patil Medical College, Vijaypur, for his constant and unfailing support, professional insight, valuable suggestions, motivation and exemplary guidance to carry out and complete this dissertation. I am deeply grateful to him for providing me necessary facilities and excellent supervision to complete this work.*

*I offer my sincere thanks to **Dr. M.S.Biradar**, Vice Chancellor, **Dr. Aravind Patil**, Principal and **Dr. Rajesh M Honnutagi**, Medical Superintendent B.L.D.E.U's Shri B. M. Patil Medical College, Vijaypur, for their support and inspiration.*

*My thanks to **Dr Shivanand V Patil** M.D., **Dr. Satish D Patil** M.D., Associate professors, **Dr. Ravi Kumar** DNB Assistant professor, **Dr. M M Patil** DMRD, **Dr. Vishal S. Nimbal** DNB & **Dr. Suresh Kanamadi** MD, Senior Resident, Department of Radio-diagnosis, B.L.D.E.U's Shri B. M. Patil Medical College, Vijaypur, for their valuable suggestions and encouragement which have definitely helped me improve my research work.*

*I acknowledge my gratitude to My seniors **Dr Iranna**, **Dr Shivu**, **Dr Karthik**, **Dr Namit**, **Dr Suhas C N**, **Dr Srikalyan D**, **Dr Shantala P**, **Dr Siddaling B M**, my colleagues **Dr.Mohit lohey**, **Dr. Arjun kamath**, **Dr.Prakriti R P**, my juniours **Dr Harish**, **Dr Amruth**, **Dr Nagabhavani**, **Dr Manasa**, Postgraduate colleagues, Department of Radiology, B.L.D.E.U's Shri B. M. Patil Medical College, Vijaypur, for their support, advice and help in data collection.*

*I thank **Mr. Mohammad S**, Statistician for his masterly guidance and statistical analysis.*

*I sincerely acknowledge the support and kindness shown towards me by all the staff of Central Library, Shri B. M. Patil Medical College, Vijaypur, at all times.*

*My heartly thanks to my grand father **Mr. Narayanappa**, my beloved parents **Mr. D N Venkata Reddy and Mrs. T B Bhagyamma**, my brother **Mr Ravi teja** and my wife **Dr Gouthami Shabarish** for their encouragement, support and sacrifices.*

*Last but not the least, my sincere thanks to all the patients of this study for their cooperation without which this study would not have been possible.*

*Date: 23-10-2020*

*Place: Vijayapur.*



**Dr. Shabarish D V**



**LIST OF ABBREVIATIONS**

<b>ACR</b>	<b>American College of Radiology</b>
<b>ATA</b>	<b>American Thyroid Association</b>
<b>CAL</b>	<b>Calcifications</b>
<b>CT</b>	<b>Computed Tomography</b>
<b>FNA</b>	<b>Fine Needle Aspiration</b>
<b>HYPO</b>	<b>Hypoechoic</b>
<b>MNG</b>	<b>Multinodular Goiter</b>
<b>MEN</b>	<b>Multiple Endocrine Neoplasia</b>
<b>MRI</b>	<b>Magnetic Resonance Imaging</b>
<b>MTC</b>	<b>Medullary Thyroid Carcinoma</b>
<b>M HYPO</b>	<b>Markedly Hypoechoic</b>
<b>MICRO</b>	<b>Micro calcifications</b>

<b>NPV</b>	<b>Negative Predictive Value</b>
<b>NHL</b>	<b>Non-Hodgkin's Lymphoma</b>
<b>n</b>	<b>Number</b>
<b>PD</b>	<b>Poorly defined</b>
<b>PPV</b>	<b>Positive Predictive Value</b>
<b>PET</b>	<b>Positron Emission Tomography</b>
<b>SPECT</b>	<b>Single Photon Emission Computed Tomography</b>
<b>SN</b>	<b>Sensitivity</b>
<b>SP</b>	<b>Specificity</b>
<b>TSH</b>	<b>Thyroid Stimulating Hormone</b>
<b>T3</b>	<b>Triiodothyronine</b>
<b>T4</b>	<b>Thyroxine</b>
<b>TIRADS</b>	<b>Thyroid Imaging Reporting and Data System</b>

## **ABSTRACT**

### **ROLE OF ELASTOGRAPHY IN EVALUATION OF THYROID NODULES**

#### **OBJECTIVES:**

To characterize the thyroid nodules on shear wave elastography by virtual touch tissue quantification (VTQ) technique using acoustic radiation force impulse (ARFI).

To correlate the observations of elastography with cytological and/or histopathological diagnosis and establish a reference value of elastographic parameters for benignancy and malignancy.

To compare the accuracy of shear wave elastography in differentiating benign and malignant thyroid nodules with that of grey scale ultrasound and Doppler findings using pathological diagnosis as a reference standard.

#### **MATERIALS AND METHODS:**

This is a prospective study that has been carried out on 60 patients who were detected to have a thyroid nodule on ultrasound in Sri B M Patil medical college, Vijayapura. The ultrasound characteristic of each nodules were determined and classified using TIRADS and then these nodules were evaluated using shear wave elastography. The findings of ultrasound and elastography were correlated with histopathological diagnosis. The sensitivity, specificity, positive predictive value and negative predictive value of ultrasound features and shear wave elastography and then were compared with each other.

#### **RESULTS:**

Out of the 60 patients evaluated for the thyroid nodules. The nodules were most commonly seen in the females with gender distribution of (8:1), among which there was no significant correlation of the gender predilection to the malignancy. There is

statistical significance of the shear wave velocity in determining the malignant nodule with  $p < 0.05$ . There is also statistical significance among some of the ultrasound features including hypoechogenicity, taller than wide, microcalcification, lobulated or poorly defined margins and lymphadenopathy in determining the malignant thyroid nodules ( $p < 0.05$ ). The shear wave velocity has a higher sensitivity and specificity in determining the malignant nodules as compared to the USG using TIRADS; with SWV showing a sensitivity of 93.3 % and specificity of 80 %.

### **CONCLUSION:**

The shear wave elastography technique using virtual touch tissue quantification technique (VTQ) considering shear wave velocity and black and white color coding of the thyroid nodule, is more sensitive and specific modality in differentiating benign and malignant thyroid nodules than the US TIRADS. Considering 2.83 cm/s as a cutoff value of SWV there is high sensitivity of 93 % and specificity of 80 % in differentiating the benign and malignant nodules.

**TABLE OF CONTENTS**

<b>SR NO.</b>	<b>CONTENTS</b>	<b>PAGE NO.</b>
<b>1.</b>	<b>INTRODUCTION</b>	<b>8</b>
<b>2.</b>	<b>OBJECTIVES</b>	<b>10</b>
<b>3.</b>	<b>REVIEW OF LITERATURE</b>	<b>11</b>
<b>4.</b>	<b>METHODOLOGY</b>	<b>48</b>
<b>5.</b>	<b>RESULTS</b>	<b>49</b>
<b>6.</b>	<b>DISCUSSION</b>	<b>79</b>
<b>7.</b>	<b>CONCLUSION</b>	<b>96</b>
<b>8.</b>	<b>SUMMARY</b>	<b>98</b>
<b>9.</b>	<b>BIBLIOGRAPHY</b>	<b>100</b>
<b>10.</b>	<b>ANNEXURES</b>	<b>110</b>

**LIST OF TABLES**

<b>Sl. No.</b>	<b>Title</b>
1.	Shear wave velocities in normal tissue and parenchyma
2.	Black and white virtual touch tissue imaging
3.	Shear wave velocity map
4.	Sonographical suspicious criteria for malignancy
5.	TIRADS classification of thyroid nodules.
6.	Age distribution of nodules
7.	Gender distribution of nodules
8.	Lobe distribution of nodules
9.	Shape of the thyroid nodules
10.	Margins of thyroid nodules
11.	Pattern of vascularity among the thyroid nodules
12.	Association of cervical lymphadenopathy
13.	Shear wave elastography among thyroid nodules
14.	Age and gender distribution among benign and malignant nodules
15.	Gender distribution among benign and malignant nodules
16.	Shape distribution in malignant and benign thyroid nodule
17.	Margin distribution in benign and malignant nodules
18.	Calcification in benign and malignant nodules
19.	Pattern of vascularity in benign and malignant nodules
20.	Association of cervical lymphadenopathy with thyroid nodules
21.	Shear wave elastography of benign and malignant nodules
22.	Black and white color coding
23.	Shear wave velocity color coding

24.	Comparison of US diagnosis and FNA/HPR results
25.	Comparison of US diagnosis with FNA/HPR
26.	Comparison of shear wave elastography among different studies

### LIST OF FIGURES

Sl. No.	Title
1.	Thyroid embryology
2.	Development and migration of thyroid gland
3.	Anatomical relations of thyroid gland
4.	Blood supply of thyroid
5.	Normal ultrasound anatomy of thyroid gland
6.	Normal thyroid gland on color Doppler
7.	Normal spectral waveform of thyroid gland
8.	Shear and strain elastography diagrammatic representation
9.	Mechanism of elastography
10.	Score system in strain wave elastography
11.	Strain changes displayed as a gray-scale image
12.	Point and 2D shear wave elastography
13.	Hyperechoic nodule showing color doppler and SWV
14.	Papillary carcinoma of thyroid
15.	Scintigraphy image of multinodular goiter
16.	Multinodular goiter US and CT scan
17.	Papillary carcinoma of thyroid US image
18.	Follicular carcinoma of thyroid US image
19.	Anaplastic carcinoma of thyroid US image
20.	Medullary carcinoma of thyroid
21.	Primary thyroid lymphoma
22.	Metastatic lung carcinoma



23.	Adenomatous nodule
24.	Chronic lymphocytic thyroiditis
25.	Hurthle cell neoplasm
26.	US guided FNA of thyroid nodule
27.	Case 1 : colloid nodule
28.	Case 2 : papillary carcinoma of thyroid
29.	Case 3 : anaplastic carcinoma of thyroid
30.	Case 4 : Hurthle cell carcinoma
31.	Case 5 : Follicular carcinoma of thyroid
32.	Case 6 : Medullary carcinoma of thyroid

## LIST OF GRAPHS

Graph no	List of graphs
1	Age distribution of nodules
2	Gender distribution of nodules
3	Lobe distribution of nodules
4	Shape of the thyroid nodules
5	Margins of thyroid nodules
6	Pattern of vascularity among the thyroid nodules
7	Association of cervical lymphadenopathy
8	Shear wave elastography among thyroid nodules
9	Age and gender distribution of nodules
10	Gender distribution of nodules
11	Shape distribution of nodules
12	Margin distribution in benign and malignant nodules
13	Calcification in benign and malignant nodules
14	Pattern of vascularity in benign and malignant nodules
15	Association of lymphadenopathy with thyroid nodules
16	Shear wave elastography of nodules
17	Black and white color coding
18	ROC Curve
19	Diagnostic accuracy of us findings for malignant nodules
20	Bar graph comparing TIRADS with FNAC/ HPR

## INTRODUCTION

The term "thyroid nodule" is defined as a distinct lesion that is palpable or radiologically distinct from surrounding normal thyroid parenchyma. The Thyroid nodules are common, in about 8.5% of the population with incidence more common among women. Among the Indian population the prevalence of thyroid nodule is approximately 12.2%, according to a recent study. However, the incidence of thyroid cancer is quite rare being 8.7 per 100000 people per year, which is seen increasing over the years. Hence it is important for the clinician to distinguish a benign nodule from a malignant one.

Ultrasound is usually the first imaging modality of choice for diagnosing thyroid nodules as the ultrasound is easily available and easy to perform but is not very accurate in differentiating the benign and malignant nodules. For this reason, in 2009 Horvath et al proposed a system for evaluation of thyroid nodules called TIRADS (Thyroid Imaging Reporting and Data System).

To improve the non-invasive diagnostic imaging modality in differentiating the thyroid nodules elastography was introduced and the technique in elastography that we will be using is Virtual Touch Tissue Quantification (VTQ) by Acoustic Radiation Force Impulse Technology (ARFI). This technique is defined on the simple principle that the target tissue generates small displacements when it is mechanically "pushed" by short duration acoustic radiation force impulse transmitted from the transducer. The displacement of the target tissue produces the shear wave which is detected by sonographic detection pulses and numeric value of the shear wave velocity (SWV) is calculated and displayed on the monitor to estimate tissue stiffness. According to pathologic fact that malignant nodules tend to be harder than the benign, so harder is the tissue greater is the shear wave velocity<sup>(3)</sup> (SWV) of the nodule and appears red on shear wave velocity map.

Fine needle aspiration cytology and biopsy of the thyroid gland has radically changed the management of patients with thyroid nodules. Fine needle aspiration cytology and biopsy are widely accepted to be sensitive, specific, accurate and a much cost-effective procedure in differentiating benign and malignant nodules.

## **OBJECTIVES**

- To characterize the thyroid nodules based on shear wave velocity and colour coding as measured by virtual touch tissue quantification technique (VTQ).
- To correlate the observations of elastography with cytological and/or histopathological diagnosis and establish a reference value of elastographic parameters for benignancy and malignancy.
- To compare the accuracy of elastography in differentiating benign and malignant thyroid nodules with that of grey scale and Doppler findings using pathological diagnosis as a reference standard.

## **REVIEW OF LITERATURE**

### **EMBRYLOGY**

The thyroid gland originates from a diverticulum located in the median ventral wall of the pharynx. During the 4<sup>th</sup> week of development, an endodermal thickening appears in the midline floor of the primitive pharynx between the first and second pharyngeal pouches, dorsal to the aortic sac (Fig 1). The primitive thyroid derived from the diverticulum initially is spherical and then assumes lobulated shape. For the next 3 weeks, the primitive thyroid tissue penetrates the underlying mesenchymal tissue and descends anterior to the hyoid and laryngeal cartilage to reach the lower neck (Fig 2). The pathway of the diverticulum retracts initially to form the thyroglossal duct (TGD) then later involutes <sup>(4)</sup>.

The thyroid gland is initially spherical and then assumes a more bilobed configuration as it enlarges. It reaches the pre-tracheal location by the 7<sup>th</sup> week of gestation. Early in the fifth week of gestation, the proximal part of the TGD retracts and can be identified in most adults as a permanent pit at the apex of the sulcus terminalis on the dorsum of the tongue known as the foramen cecum. Distally, the duct forms the pyramidal lobe of the thyroid gland. Part of the gland originates from fourth and fifth pharyngeal pouches. The neural crest cells (ultimobranchial bodies) of these pouches contribute parafollicular C cells that produce calcitonin. The thyroid gland is able to function by the end of third gestational month<sup>(4)</sup>.

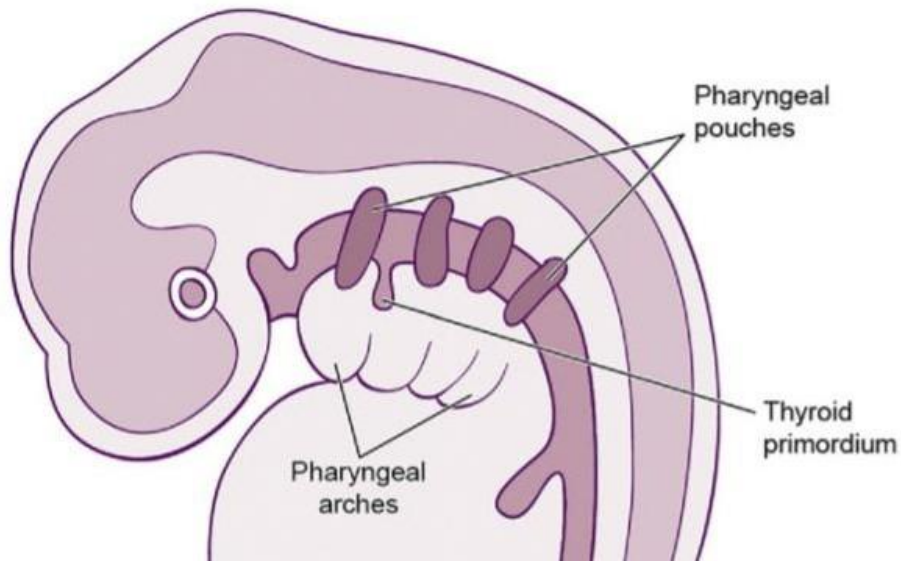


Fig 1 : Thyroid embryology. Thyroid primordium derives from an endodermal thickening that forms a diverticulum in the midline floor of the primitive pharynx between the first and second pharyngeal pouches. This will develop in the thyroid, which will migrate caudally along the thyroglossal duct (TGD)

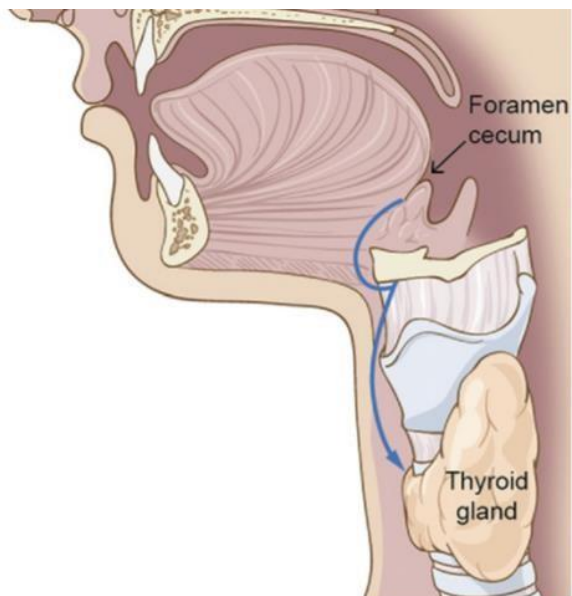


Fig 2 : Primitive thyroid tissue penetrates the underlying mesenchymal tissue and descends along the TGD. The duct travels just anterior to the hyoid bone and laryngeal

## **ANATOMY:**

The thyroid gland is located in the midline of the neck after its descent from the tongue. The gland has a right lobe and left lobe which are interconnected by the isthmus in the midline. The gland lies anterolateral to the larynx and trachea approximately at the level of 2<sup>nd</sup> and 3<sup>rd</sup> tracheal cartilage rings <sup>(5)</sup>. The thyroid gland weighs approximately 30 g, slightly heavier in females than in males and also gets enlarged during pregnancy<sup>(6)</sup>.

The thyroid gland resides within the visceral space, anterior to the prevertebral space, surrounding the trachea and lying posterior to the sternohyoid and sternothyroid (Fig 3)

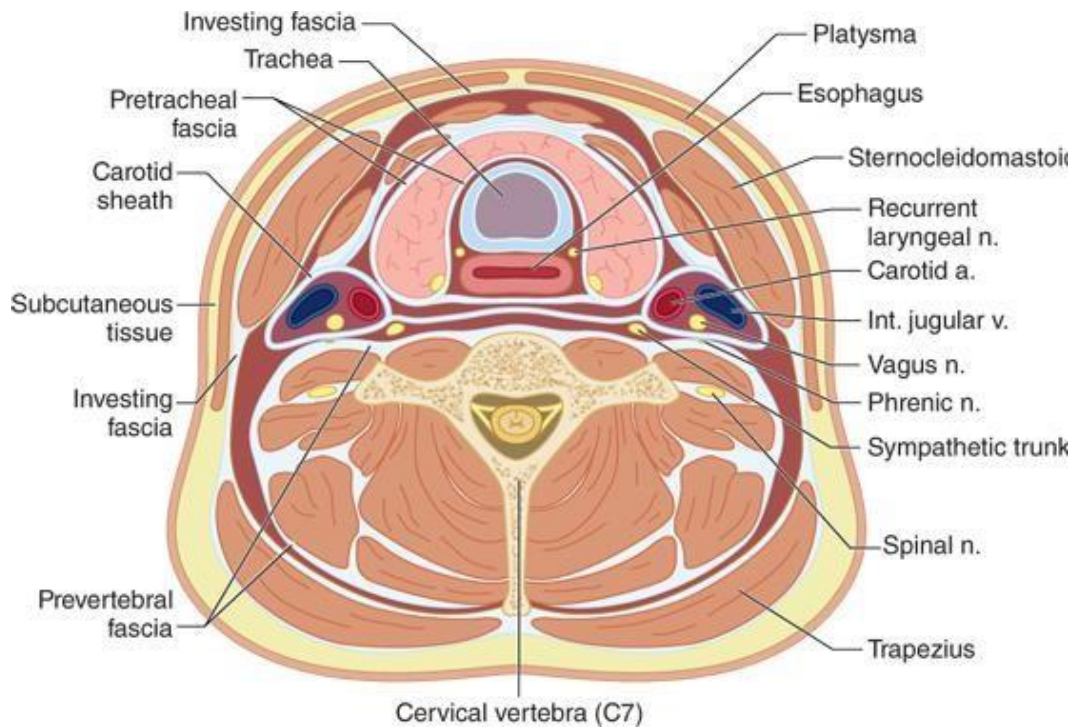


Fig 3 : Anatomical landmark and relations of the thyroid gland.

The thyroid gland is attached to the larynx and trachea within the visceral space and therefore moves with the larynx during swallowing<sup>(7)</sup>.



Superior and inferior thyroid arteries provide blood supply to the gland. The inferior thyroid artery is a branch of thyrocervical trunk that arises from the subclavian artery. The superior thyroid artery is the first branch of the external carotid artery, arising just below the hyoid bone<sup>(5)</sup>. Venous drainage is from the venous plexus that drains into the internal jugular and brachiocephalic veins<sup>(5)</sup>.

The middle and inferior cervical ganglia of the sympathetic innervates the thyroid gland, whereas the vagus nerve provides para-sympathetic regulation<sup>(5)</sup>.

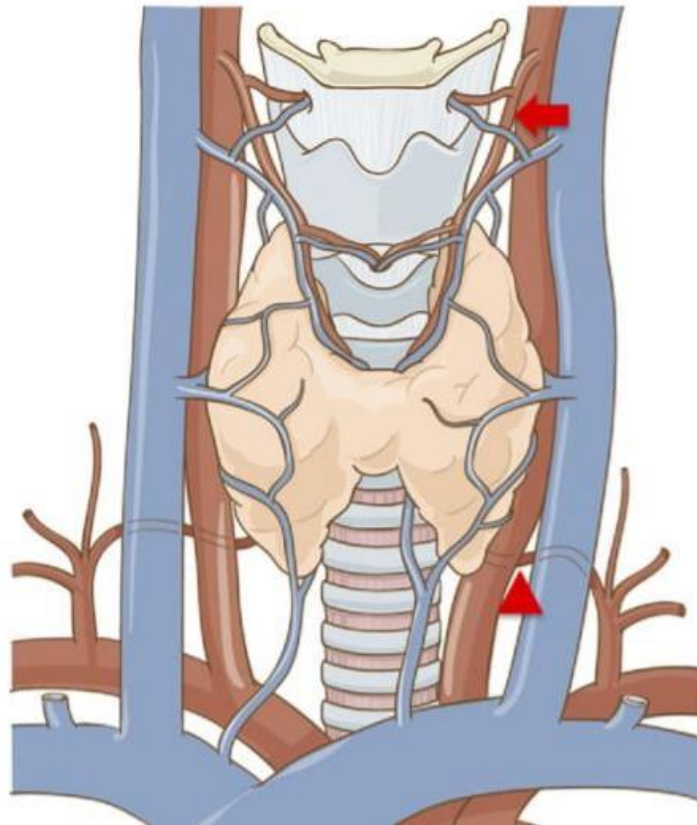


Fig 4: The arterial supply by the superior and inferior thyroid artery. The venous drainage is from the internal jugular and innominate veins bilaterally.

Microscopically the thyroid epithelial cells responsible for synthesis of the hormones released by gland are arranged in spheres called thyroid follicles. Follicles are filled with proteinaceous depot of thyroid hormone precursor. In addition to the epithelial

cells the thyroid houses another important endocrine cells, nestled in spaces between the thyroid follicles are the parafollicular or C cells, which secrete the hormone calcitonin.

The thyroid hormone is synthesized through iodination of the tyrosine residues in the glycoprotein thyroglobulin<sup>(8)</sup>. The thyroid stimulating hormone secreted by the anterior pituitary in response to feedback from the circulating thyroid hormone, acts directly on the TSH receptor (TSH-R) expressed on the thyroid follicular cell basolateral membrane<sup>(9)</sup>. The gland produces two types of hormones, thyroxine (T4) and triiodothyronine (T3), these being the derivative of the tyrosine.

The thyroid hormone is essential for the normal development, growth, neural differentiation and metabolic regulation in humans.

## **IMAGING OF THYROID GLAND**

### **ULTRASOUND :**

Most sensitive imaging technique used for assessment of the thyroid gland and its related abnormalities. Ultrasound scanning is non-invasive, widely available, less expensive and does not have any ionizing radiation. Real time ultrasound assists in diagnostic and therapeutic interventional procedures in cases of thyroid disease. The main drawback of ultrasound in thyroid imaging is that it cannot perceive thyroid function that is whether the thyroid gland is underactive, overactive or normally active; for which laboratory investigations like T3, T4 and TSH or radioactive isotope uptake test is generally required<sup>(10,11)</sup>.

### **INDICATION OF ULTRASOUND:**

According to American association of clinical endocrinologists (AACE) are as follows

(12):

- To verify the presence of a nodule when physical/ clinical examination is equivocal.
- To identify the thyroid nodule(s)
- To differentiate the benign and malignant thyroid masses.
- To differentiate and characterize these thyroid nodules from other cervical lesions such as lymphadenopathy, thyroglossal cyst, cystic hygroma etc.
- To identify diffuse changes in the thyroid parenchyma.
- To detect post-operative residual or recurrence of tumor in thyroid bed or metastases to neck lymph nodes.
- To screen cases at high risk for thyroid malignancies like cases having history of familial thyroid cancer, multiple endocrine (MEN) type II and irradiated neck in childhood.
- To guide diagnostic (FNA cytology/biopsy) and therapeutic interventional procedure.

### **TECHNIQUE**

Examined in the supine position with hyperextended neck, using a high frequency linear array transducer (7 to 15 MHz) that gives adequate penetration and high resolution image, scanning is performed in both transverse and longitudinal planes. The imaging is performed using both grey scale and color Doppler techniques. The imaging features of the mass to be identified and then FNAC may be advised if required<sup>(13,14)</sup>.

Normal thyroid gland consist of two lobes and a bridging isthmus (Fig 5). The thyroid shape, size and volume differs with age and sex. Normal thyroid gland measures<sup>(15)</sup>.

**New born**<sup>(15)</sup>

18-20 mm – longitudinal

8 to 9 mm – antero-posterior diameter

**One year**<sup>(15)</sup>

25 mm – longitudinal

12 - 15 mm – antero-posterior diameter

**Adult**<sup>(15)</sup>

40 to 60 mm – longitudinal

13 – 18 mm – antero-posterior diameter

Isthmus : < 3 mm

Volume : 10 to 15 ml in males and 12 to 18 ml in males.



Fig 5: normal ultrasound anatomy of thyroid gland.

Color and power Doppler are effective in determining the vascularity of the thyroid gland and local masses. As described earlier the thyroid gland receives blood supply from the

superior and inferior thyroid arteries (Fig 6). The thyroid arteries are visualized on color Doppler examination, while the flow velocity and pattern can be detected by the spectral Doppler examination. Normally, a low resistance flow with high peak systolic velocity (PSV) is seen in these vessels on spectral Doppler imaging (Fig 7). The normal PSV in intrathyroid arteries ranges from 15-30 cm/sec<sup>(15)</sup>.

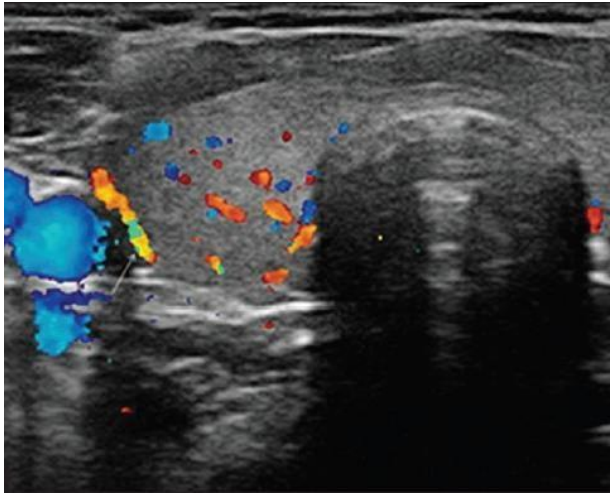


Fig 6: Normal thyroid gland on color Doppler.

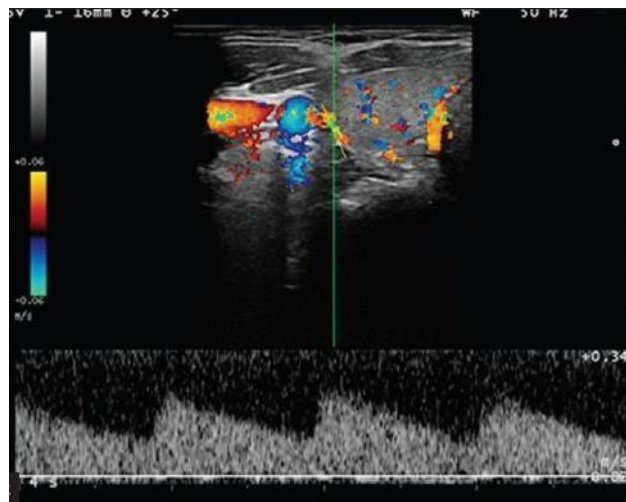


Fig 7: Normal spectral waveform of thyroid gland.

## **ADVANCES IN THYROID SONOGRAPHIC TECHNIQUES**

### **ELASTOGRAPHY:**

The palpation is a practical diagnostic technique, especially for thyroid evaluation and presence of hard thyroid nodule is associated with an increase risk of malignancy. The palpation is however the subjective and relies on the experience of the examiner. Small and deep nodules and those contained in the multinodular goiters cannot be palpated reliably.

The novel technology of ultrasound (US) elastography has been referred as "electronic palpation," because it provides a reproducible assessment of tissue consistency. US elastography was first proposed in 1991 by Ophir et al<sup>(17)</sup>, and was first used in thyroid applications in 2005 by Iyechik et al<sup>(18)</sup>. However the first use of shear wave elastography was first reported by Sebag et al in 2010<sup>(19)</sup>. Structural properties of the matrix decides the stiffness of the tissue, such as presence of pathology in the form of tumor or inflammation alters the composition of the tissue and structure with increase in stiffness of the tissue elasticity<sup>(20)</sup>.

TNs frequently pose a clinical dilemma, because only a few TNs harbor malignancy, while the majority of TNs are benign. The standard work-up of TNs consists of a US examination and fine-needle aspiration (FNA), but both have limitations for which a long-lasting search for suitable non-invasive diagnostic methods was done, that's when US elastography has emerged as an additional tool in combination with US and FNA for TN differentiation<sup>(16)</sup>.

The 2015 American Thyroid Association (ATA) management guidelines<sup>(21)</sup> stated that US elastography can be a helpful tool for preoperative accurate risk assessment in patients. The 2016 American Association of Clinical Endocrinologists, American College of Endocrinology, and Associazione Medici Endocrinologi Medical (AAACE/ACE/AME) guidelines<sup>(22)</sup> stated that US elastography provides stiffness information, which is complementary to grayscale findings, particularly in nodules with indeterminate US or cytologic characteristics. The 2013 European Federation of Societies for Ultrasound in Medicine and Biology (EFSUMB) guidelines<sup>(23)</sup> stated that US elastography can be used to

guide the follow-up of lesions diagnosed as benign at FNA. In 2017, the World Federation of Societies for Ultrasound in Medicine and Biology (WFSUMB)<sup>(20)</sup> launched few instructions for the use of elastography techniques on thyroid gland, with a detailed description of the procedure and its reproducibility, results, and limitations.

**PRINCIPLE :**

Depending on the physical quantities there are two main thyroid elastography methods in practice :

- Strain elastography (Fig 7A).
- Shear elastography (Fig 7B).

They can be classified based on various excitation method:

External force.

Internal force.

- Acoustic radiation force (ARF).

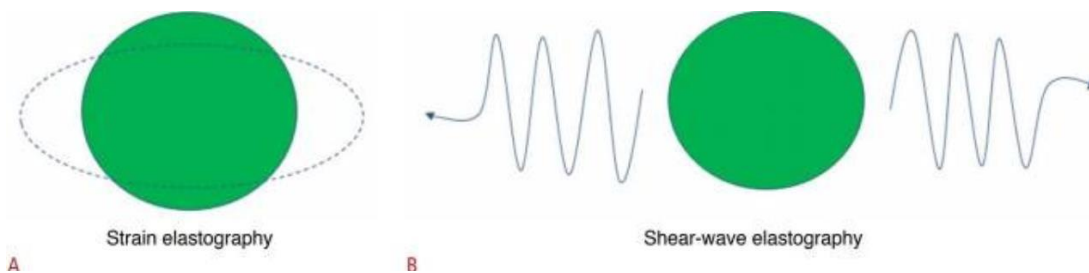


Fig 8: A. SE assesses tissue elasticity through tissue displacement induced by compression  
B. SWE assesses by measuring propagation speed of transverse shear

## **STRAIN ELASTOGRAPHY(SE)**

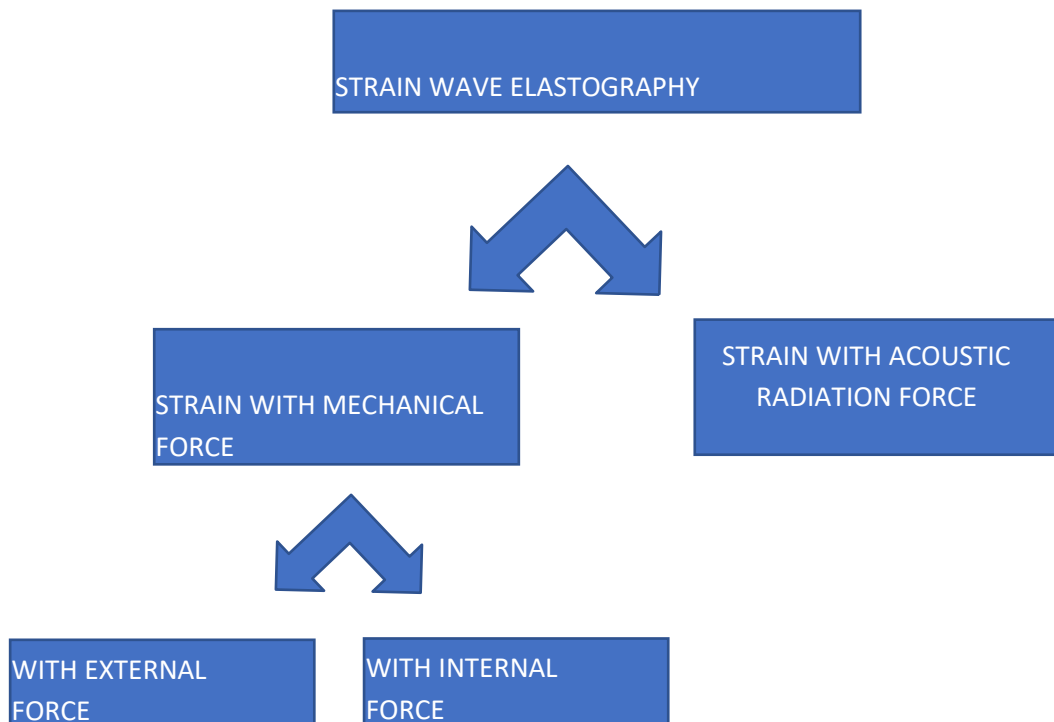
The relationship between the compression and strain, the young modulus (E), also known as the ratio of stress ( $\sigma$ ) to strain ( $\epsilon$ ), can be calculated using Eq:

$$E = \sigma / \epsilon$$

SE requires mechanical stress which results in axial displacement of the tissue<sup>(24, 25)</sup>

Tissue deformation from the stress is measured and visualized on a screen. The main limitations of SE are operator-dependence for the angle, strength, and duration of compression.

Two kinds of elasticity assessments can be obtained by SE. First, a visual scoring system of colors within and around the nodules can be used, with 4- and 5-point elasticity score (ES) systems. Second, two regions of interest (ROIs) are drawn over the target region and an adjacent reference region, respectively. Then, the strain ratio (SR) is automatically calculated<sup>(20)</sup>





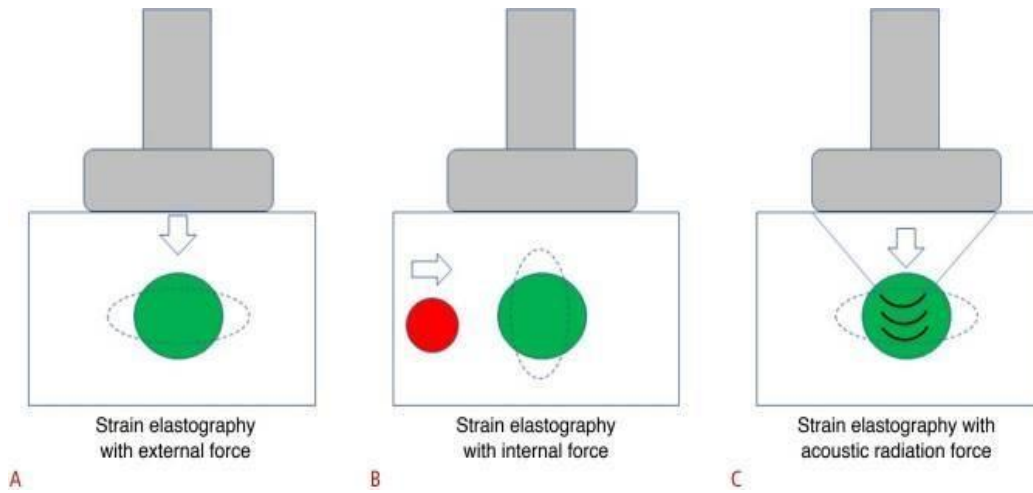


Fig 9 : A. Elastography Image by free hand compression.  
 B. Tissue displacement induced by compression caused by carotid artery pulsation.  
 C. Transducer is used to generate an acoustic radiation force push pulse

**SE with external force** : Free hand compression is continuously applied by a transducer on the neck followed by decompression (Fig 8A). Then tissue stiffness is displayed as a continuum of colors(Fig 9) from green (hard) to blue (soft), some operators give the coding vice versa<sup>(20)</sup>.

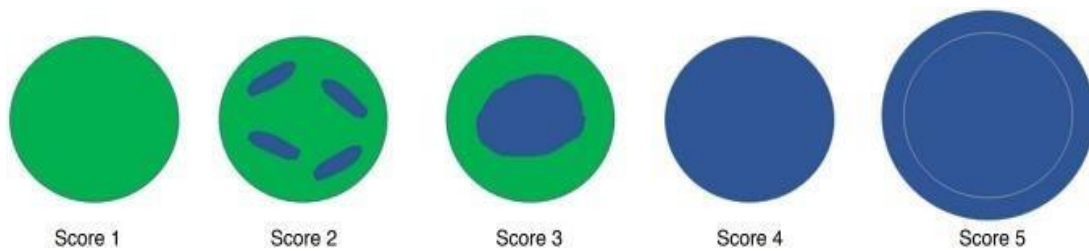


Fig 10 : Score of 1 - elasticity throughout the whole nodule; 2 - elasticity in a large part of the nodule; 3 - indicates elasticity only at the periphery of the nodule, 4 - no elasticity in the nodule, and 5 - indicates no elasticity in the nodule or in the area showing posterior shadowing.

**SE using internal force (carotid pulsation)** : In this technique, the compression source is carotid artery pulsation, while the operator holds the probe motionless(Fig 8B). Pre and post compression signals are generated and the hardness is expressed as thyroid

stiffness index(TSI) or the elasticity contrast index(ECI)<sup>(26)</sup>.

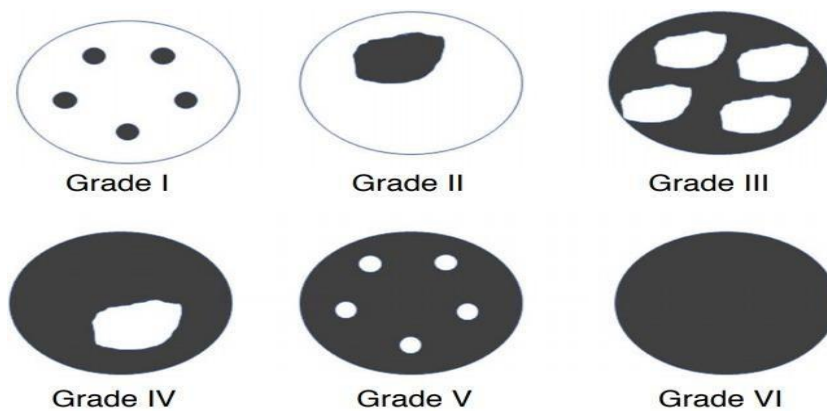
**SE using ARF** : Acoustic radiation force impulse (ARFI) imaging can image tissue deformation using a US beams. Imaging pulses before and after application of focused ARF "push" pulses are used to monitor tissue displacement within the region of the push.

ARFI is calculated by the equation

$$F = 2\alpha I / c$$

F- ARF;  $\alpha$  – acoustic absorption;  $I$  - average temporal intensity of the acoustic beam; c – speed of sound.

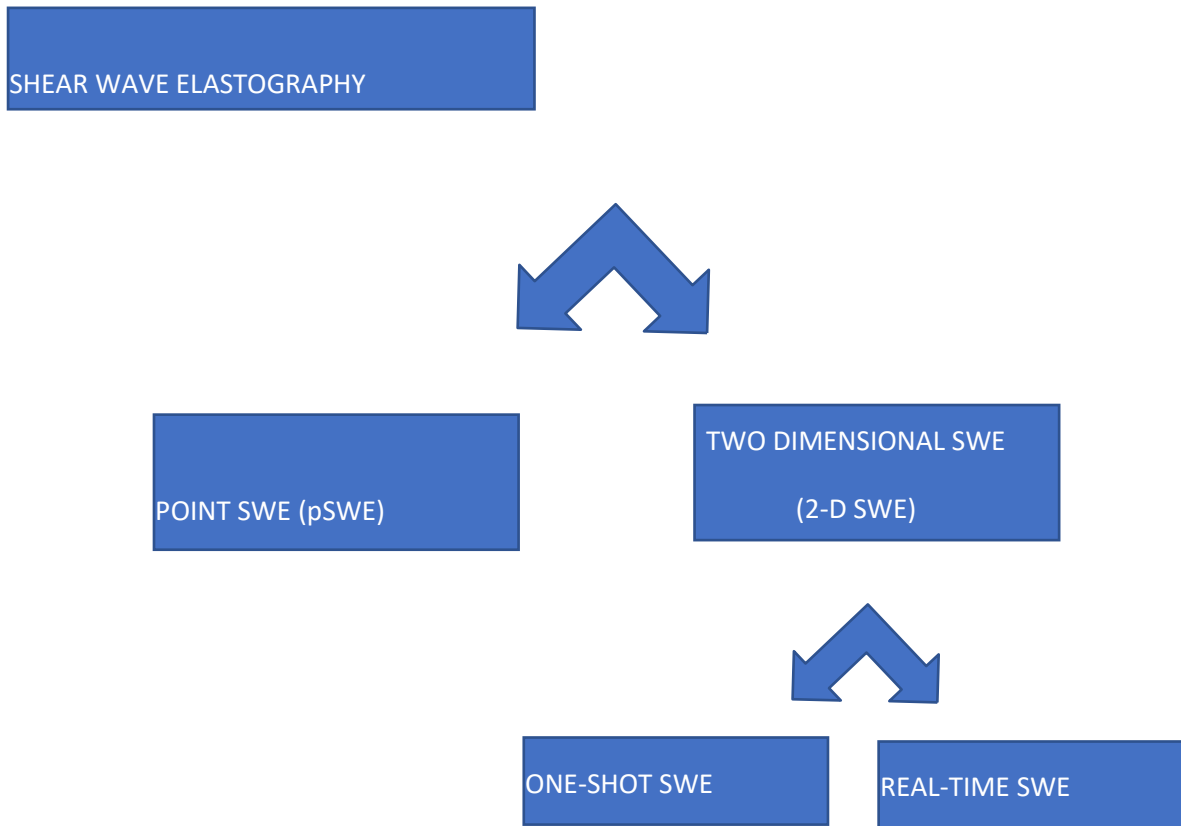
Strain changes are usually displayed as gray-scale images (Fig 10). A bright shade indicates relatively soft tissue, whereas a darker shade indicates relatively stiff tissue<sup>(27)</sup>.



## **SHEAR WAVE ELASTOGRAPHY**

Fig 11:

Grade I - the lesion is homogeneously white or with a few point-like areas of black;  
 Grade II - almost the whole lesion is white, with a small amount of black; Grade III- the black and white portions in the whole lesion are almost the same; Grade IV- almost the whole lesion is black, with a small amount of white; Grade V- the lesion is almost in black, with few point-like areas of white;



The acoustic pulses from the probe stimulate the target tissue, creating a shear wave (SW) that travels perpendicular to the conventional US waves. SWs are transverse components of particle displacement that are attenuated by the tissue. This component is detected and then measured as a numerical value which corresponds to the shear-wave speed (SWS). This speed measured is related to the Young modulus formula, according to which tissue elasticity is assessed from the SW propagation speed<sup>(24,25)</sup>.

$$E=3\rho c^2$$

E is the young modulus,  $\rho$  is the tissue density, and c is the SWS.

**Point SWE (pSWE)** : Uses short duration acoustic pulses that stimulate the tissue mechanically within a fixed size ROI, causing localized displacements that induce a lateral SW. Even though the amplitude of these SWs is small / minute, they can be detected with multiple laterally positioned US "tracking" beams and using appropriate algorithms SWS can be reconstructed by measuring time to peak. Elasticity is expressed as meters per second (m/sec)<sup>(27)</sup>.

## 2-D SWE :

### Two types

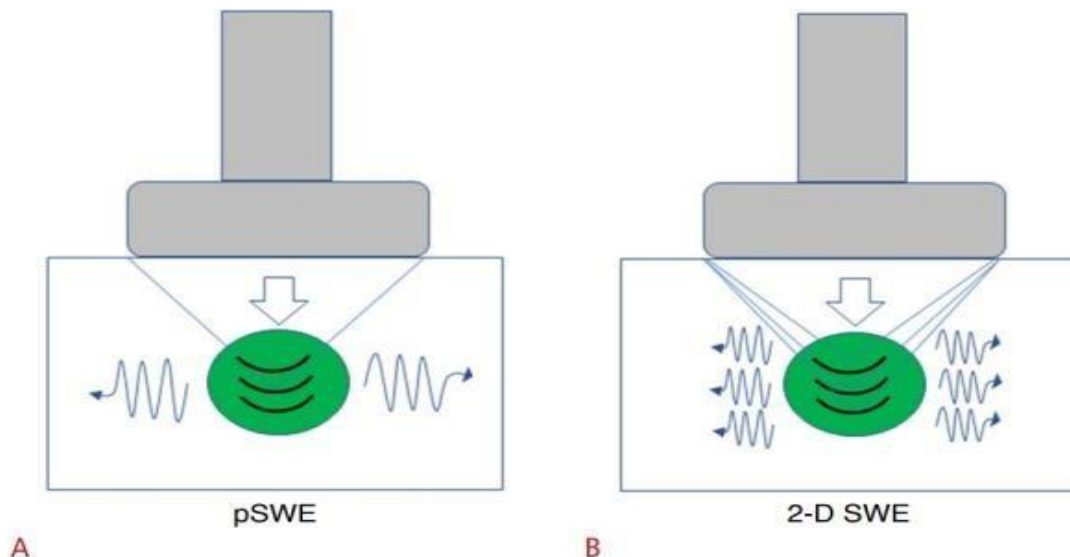


Fig 12 : A. pSWE uses ARF to mechanically stimulate the target tissue in a single focal location.

### “One shot” 2-D SWE technique (Fig 11A) :

The Virtual Touch Tissue Imaging and Quantification (VTIQ, Siemens Medical Systems, Mountain View, CA, USA) system is a representative means of performing the "one-shot" 2-D SWE technique. The VTIQ system can be used to measure the SWS

that propagates at various locations around the ARFI through a detection pulse. Time is required to allow the transducer to cool before another image can be generated after acquiring an image. Compared with pSWE, VTIQ provides more precise stiffness information within TNs because of its 2-D visualization of the SWS distribution in various colors and smaller SW ROIs. A SW-quality map is available to evaluate whether SWS propagation is reliable or adequate <sup>(27)</sup>.

This is the method which we will be using in this study.

This method can be used to calculate the shear wave velocity (SWV) (Table 1), black white virtual touch tissue imaging (Table 2) and shear wave velocity map <sup>(29)</sup> (SWV- map) (Table 3) of the nodules.

In the nodules with maximum size less than 1 cm, 5 measurements will be taken from ROI, the average value will be taken as the shear wave velocity for that nodule. For nodules larger than 1 cm, the ROI will be randomly measured in 3 regions; each region will be detected 3 times; and the average value will be calculated as the SWV for that nodule. Based on the above parameters, the thyroid nodule will then be characterized as being benign or malignant.


**TABLE1. SHEAR WAVE VELOCITIES <sup>(2,29)</sup> (SWV)**

Normal thyroid tissue	$2.106 \pm 0.392$ m/s
Benign thyroid nodule	$< 3$ m/s
Malignant thyroid nodule	$\geq 3$ m/s

**TABLE 2. BLACK AND WHITE VIRTUAL TOUCH TISSUE IMAGING <sup>(1)</sup>**

TYPE 1	If nodule appears more white than the surrounding tissue	BENIGN
TYPE 2	If nodule appears of the same colour as the surrounding tissue	BENIGN
TYPE 3	If > 50% of the nodule appears black as compared to surrounding normal tissue	MALIGNANT

**TABLE 3. SHEAR WAVE VELOCITY MAP <sup>(29)</sup>**

LIGHT BLUE	NEGATIVE	 SOFT     HARD
DARK BLUE		
GREEN	EQUIVOCAL	
ORANGE	EQUIVOCAL	
RED	MALIGNANT	

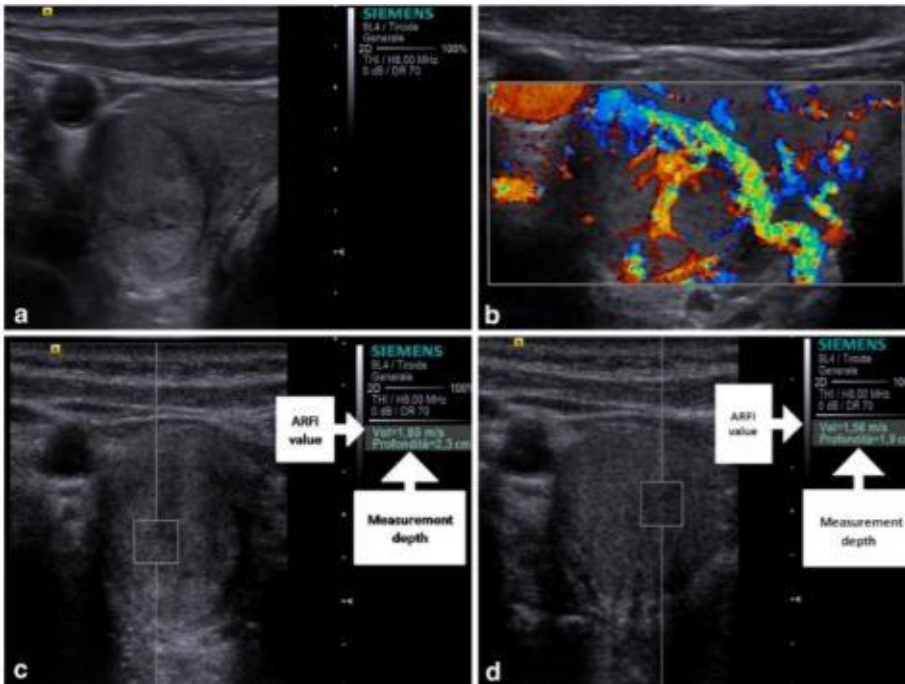


Fig 13 : A . hyperechoic nodule;

B. Color Doppler – Internal and peripheral vascularity.

C. Operator 1 – shear wave velocity – 1.89 m/s and D. operator 2 – SWE – 1.56 m/s

The lesion which was indeterminate on ultrasound showed benign SWV on elastography and the histopathology was benign nodular hyperplasia<sup>(29)</sup>.

### Real time 2-D SWE technique (Fig 11B):

Focused ultrasonic beams (so-called pushing beams) that propagate through the entire ROI, and ultrafast US is used to measure the velocity of the induced SWs. From this findings the elasticity can be quantitatively estimated. The stiffness of a particular ROI, including mean stiffness ( $E_{mean}$ ), maximal stiffness ( $E_{max}$ ), and standard deviation, can be expressed as SWS (m/sec) or elasticity (kPa). Soft tissue is displayed as blue and hard tissue is displayed as red<sup>(28)</sup> (fig 12)

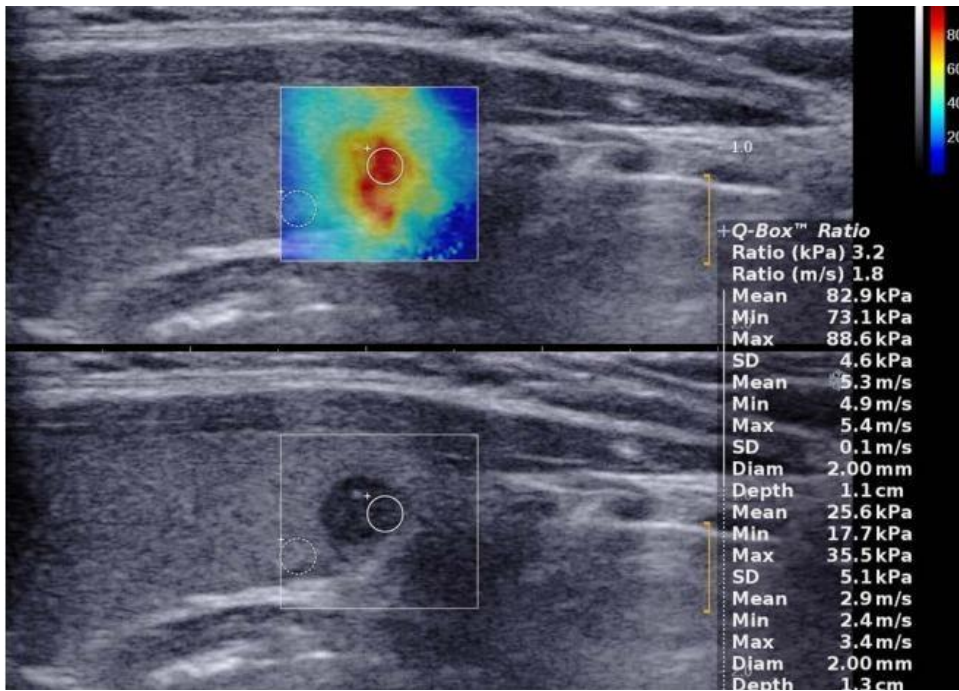


Fig 14 : a case of papillary thyroid carcinoma shows hypoechoic thyroid nodule with poor margin and macrocalcifications. On elastography the lesion is heterogenous (red and yellow) with a maximum velocity of 88.6 kPa.

#### RECENT DEVELOPMENT IN ELASTOGRAPHY:

Three-dimensional (3-D) SWE is a more recent development. High-resolution 3-D SWE images can be acquired using a 3-D volumetric probe (SSI) that provides 3-D elasticity maps of the entire TN and surrounding tissue<sup>(32)</sup>.

#### OTHER MODALITIES :

##### RADIONUCLIDE IMAGING :

Radionuclide imaging (RNI) is also been used as an alternative technique to assess thyroid gland for many years. Now, it plays a prime part in the identification of thyroid disease as it gives outstanding functional information about the gland. The most commonly used isotopes for thyroid scintigraphy are <sup>99m</sup> Technetium pertechnetate, <sup>131</sup> Iodine, <sup>18</sup> fluoro-deoxy-glucose, and gallium-67. Radionuclide scanning using <sup>99m</sup> Technetium pertechnetate and <sup>131</sup> Iodine is used in the differentiating focal nodule as hot, warm, or cold on the basis of



relative uptake of radioactive isotope by the nodule

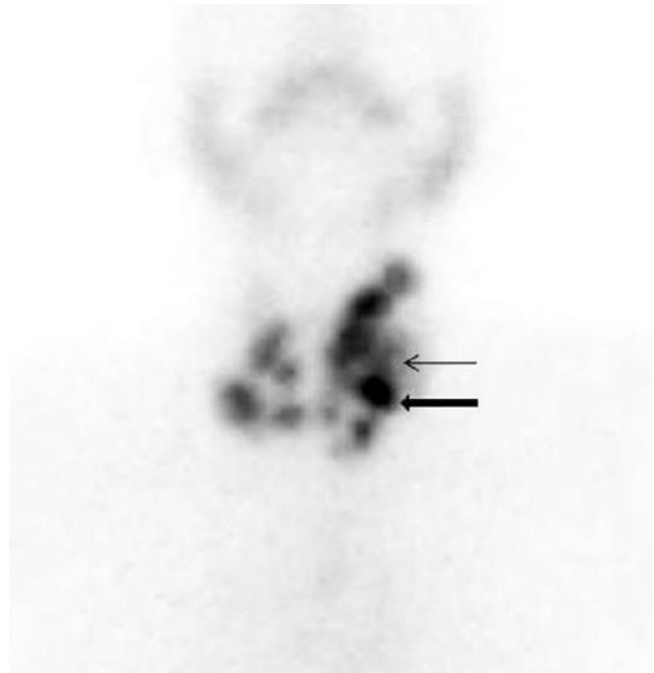


Fig 15 : Multinodular goiter. 99mTechnetium pertechnetate (Tc-99m) scintigraphy image of thyroid gland, of a 48-year-old female patient with multinodular goiter, shows multiple hot (thick arrow) and cold nodules (thin arrow) involving both the lobes of the gland (left>right).

### **POSITRON EMISSION TOMOGRAPHY:**

Positron emission tomography (PET) and single-photon emission computed tomography (SPECT) are latest techniques and are of great interest in imaging of the thyroid.

F18-fluorodeoxyglucose-PET (  $^{18}\text{F}$ -FDG-PET) is a well known imaging modality in oncology. Its special use is in evaluation of thyroid cancers with dedifferentiated tumors which are iodine scintigraphy negative but FDG-PET positive (in contrast to inactive slowly progressive tumors which are iodine scintigraphy positive but FDG- PET negative)<sup>(33,34)</sup>. F-FDG-PET is detected as the most precise method for identifying the recurrence or metastatic medullary thyroid carcinoma (MTC) in patients with an elevated

calcitonin level (tumor marker for MTC) postoperatively, when all other radionuclide and cross-sectional imaging techniques fail to depict the tumor or metastatic disease. It also has upper hand in localizing cervical and mediastinal lymph node involvement<sup>(35,36,37)</sup>

The use of PET scan with CT or MRI (PET/CT or PET/MRI) which allows fusion of functional and anatomical information has a predominant role in evaluating thyroid cancer. The Sn and Sp of FDG PET-CT to detect the suspected occult lesions and residual/recurrent well-differentiated thyroid cancer (DTC) is very high<sup>(11)</sup>.

Currently, whole-body FDG PET-CT is advised for evaluating the metastases of DTC in patients with radioiodine negative scans and elevated serum thyroglobulin (Tg) levels. This is mainly utilised for treatment decisions<sup>(39,40)</sup>, FDG PET is also helpful in differentiating incidentaloma (show focal uptake of FDG by the gland) from thyroiditis and/or hypothyroidism (show diffuse uptake of FDG by the gland); and malignant thyroid nodule (show high FDG avidity, approaching 100%) from benign nodule (show low FDG avidity, ~30%)<sup>(40,41)</sup>.

#### **SINGLE PHOTON EMISSION COMPUTED TOMOGRAPHY:**

SPECT is currently used with increased frequency due to its ability to provide the three-dimensional information which improves the overall sensitivity for detection and localization of a thyroid lesions. <sup>131</sup>I SPECT-CT has been found to be more accurate than FDG PET-CT in localizing the regional and distant metastases including detection of residual/recurrent disease in the case of well-differentiated thyroid cancer. The most important advantage of fusion FDG PET-CT and <sup>131</sup>I SPECT-CT is detection of metastasis in normal sized lymph nodes

**COMPUTED TOMOGRAPHY AND MAGNETIC RESONANCE IMAGING:**

Computed tomography (CT) and magnetic resonance imaging (MRI) have an adjuvant role in the evaluation of thyroid disease. CT and MRI are less sensitive than USG in detecting and characterizing intrathyroid lesions as benign and malignant. They are particularly used for staging thyroid cancer as they are useful in evaluating regional lymphadenopathy, assessing loco-regional extension of the tumor (particularly involving trachea and esophagus), spread of disease into the mediastinum or retrotracheal region and detecting pulmonary and hepatic metastases. CT and MR imaging are also recommended to determine the occult metastases (mediastinal or retropharyngeal) in post-thyroidectomy follow-up cases with elevated serum Tg level and negative sonographic finding<sup>(43,44)</sup>.

CT, in particular, is most sensitive in detecting intra-glandular calcification (Fig 13). Fusion PET-CT and PET-MRI play an important role in the evaluation of thyroid cancer. Diffusion-weighted imaging (DWI) may be helpful in differentiating benign and malignant nodules. Benign nodules have higher apparent diffusion coefficient (ADC) values than malignant ones<sup>(45)</sup> MR spectroscopy using long echo-time (TE) has been shown to be a sensitive method in differentiating thyroid carcinoma from benign follicular lesion. Choline peak is identified in almost all carcinomas, with raised choline/creatine ratio ranging from 1.6 in well differentiated carcinoma to 9.4 in anaplastic carcinoma. The normal thyroid tissue and benign follicular lesions generally demonstrate no choline peak<sup>(46)</sup>.



Fig 16 : Multinodular goiter. Plain axial (a) and contrast-enhanced axial (b) and coronal (c) CT scan neck region, of a 52-year-old female patient, shows enlargement of bilateral thyroid lobes due to presence of multiple non-enhancing hypodense (thin white arrows) and calcified thyroid nodules (thin black arrows)

### **OPTICAL COHERENCE TOMOGRAPHY AND OPTICAL COHERENCE MICROSCOPY:**

Optical coherence tomography (OCT) and optical coherence microscopy (OCM) are emerging imaging technologies based on inherent optical contrast. OCT provides high-resolution, real-time, cross-sectional imaging of tissues. OCM is extension of OCT and provides high magnification resulting in cellular imaging. OCT/OCM system uses infrared light in fiber active device that allows visualization of microstructures of gland (1-15  $\mu\text{m}$  cellular range) and provides high resolution images comparable with those obtained using histopathologic methods. OCT and OCM can clearly differentiate between benign and malignant thyroid tissue using intrinsic optical contrast<sup>(47,48)</sup>.

**PATHOLOGIES OF THE THYROID:**

<b>Benign lesions</b>
Benign follicular nodule
Adenomatoid nodule
Colloid nodule
Follicular adenoma
Hürthle cell adenoma
Thyroiditis
Chronic lymphocytic (Hashimoto) thyroiditis
<b>Malignant lesions</b>
Papillary carcinoma
Follicular carcinoma
Hürthle cell carcinoma
Poorly differentiated carcinoma
Anaplastic/undifferentiated carcinoma
Medullary carcinoma
Lymphoma
Metastasis

**MALIGNANT THYROID NODULES:**

The main pathologic types of thyroid carcinoma are papillary, follicular, medullary, and anaplastic. Papillary and follicular thyroid carcinomas both have an excellent prognosis, with a 20-year survival of 90%–95% and 75%, respectively. Medullary thyroid carcinoma is more aggressive, with a 10-year survival of 42%–90%. Anaplastic thyroid carcinoma has an extremely poor prognosis, with a 5-year survival of 5%<sup>(49)</sup>. Risk factors for thyroid carcinoma include age of less than 20 years or more than 60 years, a prior history of neck irradiation, and a family history of thyroid cancer<sup>(49)</sup>.

Thyroid lymphoma, usually of the non-Hodgkin type, is uncommon. It may occur as part of generalized lymphoma or as a primary tumor, usually in the setting of Hashimoto thyroiditis. Metastases to thyroid are rare and usually originate from primary lung,

breast, and renal cell carcinomas. Metastatic disease should be suspected when a solid thyroid nodule is found in a patient with a known nonthyroid malignancy.

### **PAPILLARY CARCINOMA OF THYROID:**

It is the most common malignancy of the thyroid and usually has a nodal metastases at presentation. It is typically seen in middle aged with a peak incidence in the third and fourth decade of life. Clinically the patient usually presents as a solitary palpable thyroid mass. Papillary carcinoma has a tendency to metastasize early to the lymph nodes at presentation. These metastases are usually to the ipsilateral jugular chain and are usually confined to the mid and lower lymph nodes level, level III and IV. The papillary carcinoma is associated with gardner syndrome, cowden syndrome and familial adenomatous polyposis. On ultrasound the papillary carcinoma usually has irregular outline, locted in the subcapsular region and demonstrates internal vascularity. Small punctate regions of echogenicity representing microcalcification (psammoma bodies) may be present.

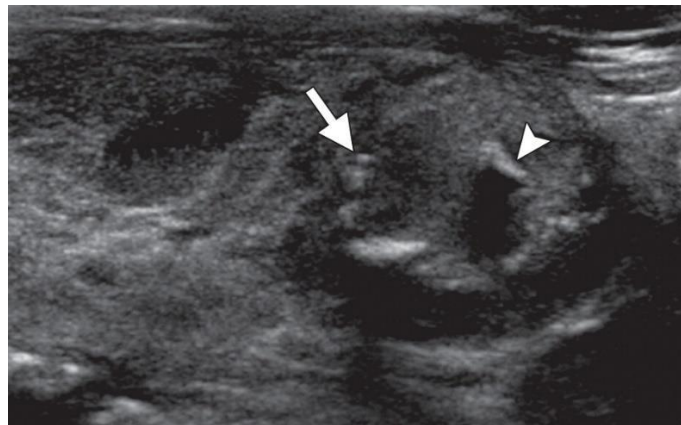


Fig 17 : Papillary carcinoma in a 60-year-old woman with nontoxic multinodular goiter. Longitudinal US image of the left lobe of the thyroid shows a 2.4-cm solid nodule in lower pole with ill-defined margins and microcalcifications (arrow), both of which are suspicious US features. A shadowing macrocalcification is also noted (arrowhead)

## **FOLLICULAR CARCINOMA :**

Follicular carcinoma is a 2<sup>nd</sup> most common malignant neoplasm composed of follicular cells. It constitutes about 11 % of all the primary thyroid malignancy<sup>(49)</sup>. Typically seen in women and older age group than papillary carcinoma. Unlike papillary it metastasizes late to the lymph nodes. FNA cannot differentiate between follicular thyroid adenoma and follicular thyroid carcinoma, surgery resection is necessary. On USG the lesions are typically hypoechoic and usually lacks cystic change.



Fig 18 : follicular carcinoma in woman the US image of the left lobe of the thyroid shows a well-defined solid nodule in left lobe with well-defined margins defined margins.

Hurthle cell carcinoma a variant of follicular carcinoma in which over 75 % of cells show oncocyctic or hurthle cell changes, accounts for 3 % of all the thyroid malignancy. The propensity of the hurthle cell carcinoma for locoregional nodal metastases may be higher than that of follicular carcinoma. The prognosis of the hurthle cell carcinoma is intermediate and is worse than that of follicular carcinoma.

## **ANAPLASTIC CARCINOMA**

Highly aggressive of the thyroid cancer accounts for 1 to 2 % of the primary thyroid malignancies. Typically seen in the elderly 6<sup>th</sup> to 7<sup>th</sup> decade. Patient tend to present late with compressive symptoms on the neighboring structures. On USG the lesion is an infiltrative with specs if microcalcification within . on CT the tumor shows extrathyroid tumor invasion as well as regional and distant lymph nodal metastases. There is no uptake of radio-iodine, therefore the radioactive iodine ablation and scintigraphy cannot be performed.



Fig 19: anaplastic carcinoma of in 55 year old woman the US image of the left lobe of the thyroid shows a ill-defined hypoechoic solid nodule with ill-defined margins and is taller than wide.

## **MEDULLARY CARCINOMA**

Accounts for 5 to 10 % of all the thyroid malignancies. Typically seen in 3<sup>rd</sup> to 4<sup>th</sup> decade of life. Medullary carcinoma is seen to arise from the parafollicular C cells of the thyroid. It is characterized by consistent production of a hormonal markers (calcitonin), calcification of both the primary and metastatic sites and association with the endocrine neoplasms. The carcinoma when familial is seen as a component of MEN 2 syndrome.

Other association includes von Hippel landau disease and neurofibromatosis type I. On USG the punctate high echogenic foci resembling calcification can be seen both within the primary thyroid lesion as well as metastatic regional lymph nodes and distant metastatic



sites.

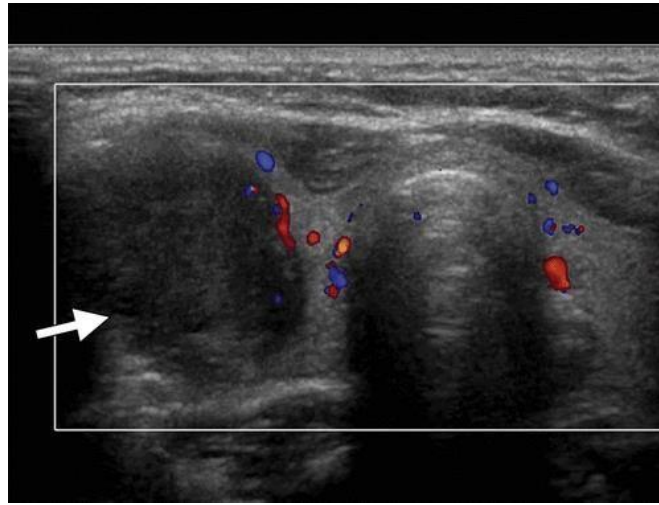


Fig 20: medullary carcinoma in 36 year old woman the US image of right lobe of the thyroid shows a well-defined hypoechoic solid nodule with ill-defined margins and is taller than wide<sup>(49)</sup>.

## **LYMPHOMA**

Thyroid lymphoma is a rare accounting for minority of both thyroid malignancies and lymphoma in general. The thyroid may be affected primarily or secondary to the lymphoma elsewhere. Accounting for less than 5 % of thyroid malignancies the incidence is common in age group of 50-70 years of age with strong female predominance. Hashimoto thyroiditis is major risk factor for development of thyroid lymphoma. The ultrasound pattern include nodular (hypoechoic mass), diffuse (mixed echotexture) or mixed. Calcification is uncommon. On CT the lesion is hypodense and on MRI it is iso to hyperintense.

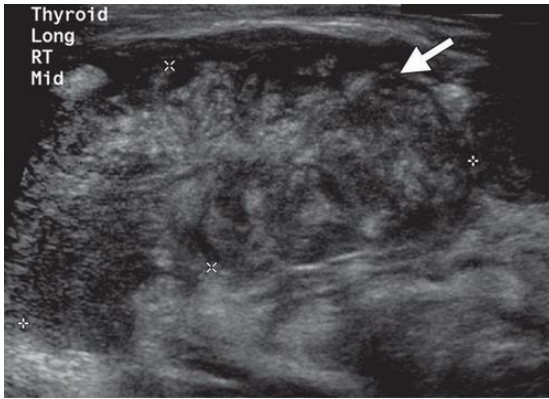


Fig 21: primary thyroid carcinoma in 5year old woman the US image shows diffusely enlarged thyroid with normal intervening parenchyma with infiltrative pattern and extracapsular extension.

### **METASTATIC TUMOR**

Metastatic tumor to the thyroid consist of both metastases from the distant organs and direct extension of the tumors from the adjacent structures. Metastatic tumor represent 5.5 % of the biopsied malignancies, usually originating from the primary lung, breast and renal cell carcinoma (49). On USG the lesion is predominantly hypoechoic lesion with poorly circumscribed margins (80 %), no calcification and concurrent cervical lymphadenopathy (80 %)

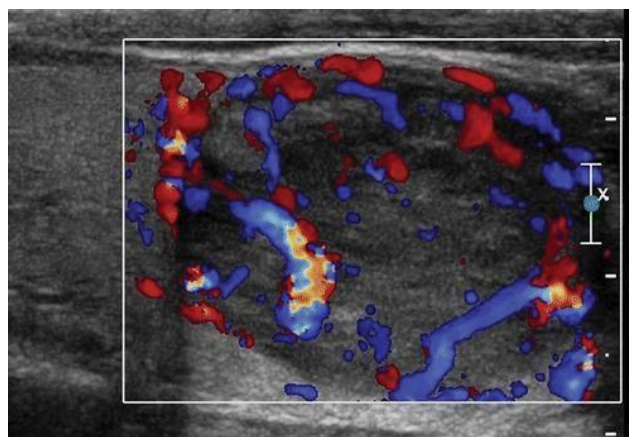


Fig 22: Metastatic lung carcinoma in a 63-year-old man with known lung carcinoma in whom a new thyroid nodule was discovered at staging CT. Longitudinal duplex US image shows a mildly heterogeneous, hypoechoic 3-cm solid nodule with increased peripheral and central vascularity. Increased central vascularity is a suspicious US feature.

### **BENIGN FOLLICULAR THYROID NODULE**

Benign follicular nodules are composed predominantly of colloid and benign appearing follicular cells. Benign nodules include nodular goiter, adenomatoid or hyperplastic nodules, colloid nodules, nodules of graves disease, and macrofollicular subtype adenoma. The different type of benign thyroid nodule cannot be differentiated by FNA.

### **ADENOMATOID OR HYPERPLASTIC NODULE:**

Non neoplastic lesion composed of follicles, colloid and variable amount of fibrosis and is generally unencapsulated. Although may be solitary, this nodule is usually found in setting of multinodular goiter.



Fig 23: Adenomatous nodule in 66-year-old man with a low thyroid-stimulating hormone level of 0.1  $\mu$ IU/mL. Transverse US image shows a predominantly solid 2.4-cm nodule with well-circumscribed margins and a surrounding halo (benign US features)

## **THYROIDITIS**

Thyroiditis is inflammation of the gland. It is categorized as chronic chronic lymphocytic thyroiditis (including autoimmune and Hashimoto thyroiditis), de Quervain (subacute or granulomatous) thyroiditis, acute (infectious) thyroiditis, Riedel (fibrous) thyroiditis, or, rarely, some other form of thyroiditis. Of these subtypes, chronic lymphocytic thyroiditis is the most common. These thyroiditis usually demonstrates as a diffusely enlarged thyroid lobe with heterogenous echotexture and diffusely increase vascularity but it may manifest with one or more nodules.

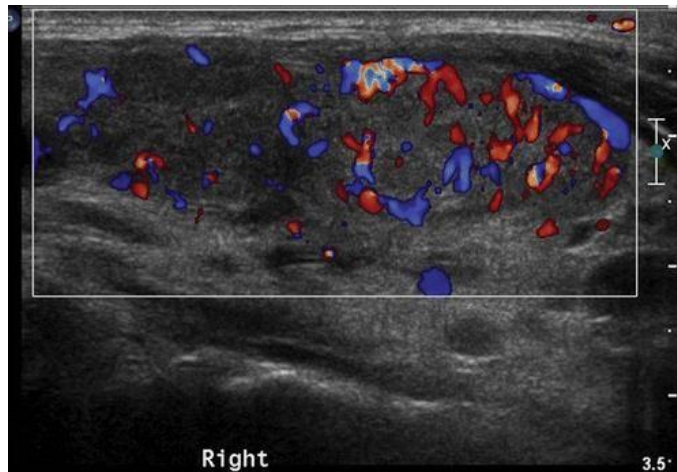


Fig 24: Chronic lymphocytic (Hashimoto) thyroiditis in a 53-year-old woman with a “swollen thyroid.” Longitudinal duplex US image shows diffusely heterogeneous thyroid parenchyma with abnormal diffusely increased vascular flow.

## **FOLLICULAR ADENOMA**

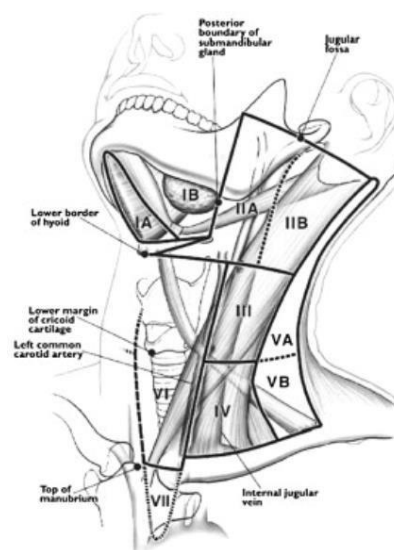
Follicular adenoma is a benign neoplastic proliferation of follicles surrounded by a complete capsule. It usually manifests as a solitary lesion in a background of normal- appearing thyroid tissue. If a nodule is reported to be a follicular neoplasm at FNA, there is a 70%–85% chance of its being a follicular adenoma and (as mentioned earlier) a 15%–30% risk to be malignant (51).



Fig 25 Hürthle cell neoplasm in a 53-year-old man with a palpable thyroid nodule at physical examination. Transverse US image shows a predominantly hypoechoic 1.5-cm solid nodule (arrow) that meets the criteria for biopsy.

### **CERVICAL LYMPH NODES**

On gray-scale sonography, normal and reactive nodes tend to be hypoechoic compared with adjacent muscles and oval (short axis-to-long axis ratio  $[S/L] < 0.5$ ) except for submandibular and parotid nodes, which are usually round ( $S/L \geq 0.5$ ), and to have an echogenic hilus<sup>(52)</sup>. The upper limit in minimal axial diameter of normal and reactive nodes is 9 mm for subdigastric and submandibular nodes and 8 mm for other cervical nodes.



Level I refers to nodes in the submental and submandibular regions. Levels II, III, and IV refer to nodes along the anterior cervical and internal jugular chains. Level II encompasses those nodes from the base of the skull to the lower border of the hyoid bone, Level III from the hyoid to the lower margin of the cricoid cartilage, and level IV from the cricoid to the clavicle. Level V nodes are those in the posterior compartment of the neck, along the course of the spinal accessory nerve, and are divided into upper (VA) and lower (VB) levels by the cricoid cartilage. Level VI nodes, the paratracheal nodes, are in the visceral or central compartment of the neck. This compartment extends from the hyoid bone superiorly to the suprasternal notch inferiorly. On each side of the neck, the lateral border of the central neck compartment is formed by the medial border of the carotid sheath. Level VII nodes are in the superior mediastinum.

### **FINE NEEDLE ASPIRATION AND CYTOLOGY**

**LOCAL ANESTHESIA :** approximately 1 to 2 ml of 1-2% lidocaine hydrochloride solution may be injected into the subcutaneous tissue over thyroid capsule using a small caliber needle.

**ASPIRATION TECHNIQUE:** Performed either parallel or perpendicular to the ultrasound probe. The needle tip is placed within the thyroid nodule, tissue sample is collected with 6 to 7 “to-and fro” needle movements over 5-10 seconds , with 2-3 ml suction applied.

**NEEDLE SIZE AND NUMBER OF NEEDLE PASSES:** Routinely 2 to 10 ml plastic syringe attached to a conventional 23-25 gauge needle<sup>(54,55,56,57,58)</sup>.

**PROCESSING OF FNA SAMPLES :** Proper methods should be applied during

smearing, fixation, and staining of samples to improve diagnostic yield. For conventional smear preparations, the syringe-needle unit is disassembled first<sup>(58)</sup>. The empty syringe is then filled with air, reconnected to the needle and the needle content is extruded onto glass slides. After that, FNA samples fixed in 95% ethyl alcohol for Papanicolaou staining can be used for immediate cytologic assessment<sup>(58, 59)</sup>.



Fig 26 Drawing illustrates FNAB technique, with parallel positioning of the needle relative to the US transducer and the thyroid<sup>(60)</sup>.

In a study conducted by Hektor grazhdani et al.,<sup>(2)</sup> 74 patients with nodules were examined on grey scale ultrasonography, elastography and then confirmation was either by cytology using FNAC and /or histology from thyroid surgery. This study shows VTQ values of 2.141 +/- 0.392 m/s for benign and VTQ values of 3.751 +/- 1.485 m/s for malignant nodules which was significantly higher than the value for benign. With a cutoff value of shear wave of 2.455 m/s the study shows a Sn of 90 % and Sp of 75 %.

Feng-juan, Ruo-Ling Han.<sup>(3)</sup> Analyzed 155 patients with nodules the mean value of shear wave velocity of benign and malignant thyroid nodules were 2.15 +/- 0.59 m/s and 6.34 +/- 2.58 m/s respectively. The sensitivity, specificity, PPV, NPV and Accuracy of differentiation of malignant and benign were 96.8%, 95.70%, 93.75%, 97.80% and 96.13% respectively considering a cutoff point at 2.84 m/s.

F.Sebag et al,<sup>(19)</sup> 93 patients and 39 control subjects were included in the study based on the characteristics on ultrasonographic findings sensitivity was 51.9 % and specificity was 97 % in characterization of nodules. Shear wave elastography showed a Sn of 85.2 % and Sp of 97 %. When both combined shows a Sn of 81.5 % and Sp of 97 %.

Jiying gu et al.<sup>(1)</sup> analyzed 98 nodules in 72 hospital patients in which 56 were SD of nodular goiter , 16 were thyrid adenoma , 4 were thyroiditis and 22 were thyroid malignancy, with a mean VTQ values 2.034 +/- 0.484 , 1.835 +/- 0.364 , 2.293 +/-0.787 and 3.941 +/- 1.393 m/s respectively .the study showed sensitivity of 86.36%, specificity of 93.42%, PPV OF 79.17%,NPV of 95.95% and diagnostic accordance of 91.84% in differentiating benign from malignant thyroid nodules with a standard VTQ of 2.555 m/s.



Hamidi et al<sup>(66)</sup> analyzed 95 patients with nodules using ARFI imaging in his prospective study and showed that SWV value of the malignant nodules ( $3.18 \pm 0.39$  m/s) was higher than that of the benign nodules ( $2.11 \pm 0.53$  m/s). There was significant difference between the mean SWV values of benign and malignant nodules ( $p < 0.001$ ). A SWV cutoff value of greater than 2.66 m/s yielded sensitivity and specificity values of 100 and 82.3 %, respectively, for diagnosis of malignant nodules.

Xu et al<sup>(30)</sup> evaluated 375 patients with 441 nodules among which there were 325 benign and 116 malignant nodules. Marked hypoechogenicity (odds ratio [OR]: 83.88; 95% confidence interval [CI]: 17.81, 394.99) was the strongest independent predictor for thyroid malignancy, followed by shape taller than wide (OR: 8.69; 95% CI: 2.87, 26.31), VTi (OR: 6.54; 95% CI: 3.61, 11.88), moderate hypoechogenicity (OR: 3.98; 95% CI: 1.13, 14.05), poorly defined margin (OR: 3.27; 95% CI: 1.22, 8.77), female sex (OR: 2.55; 95% CI: 1.33, 4.91), coarse background of surrounding thyroid tissue (OR: 2.01; 95% CI: 1.12, 3.62), and VTq (OR: 1.78; 95% CI: 1.28, 2.47) (all  $P < .05$ ). EI was not significantly associated with thyroid malignancy ( $P = .855$ ). Area under the ROC curve (Az) for VTq and VTi was greater than that with other significant independent variables. Az, sensitivity, and specificity were 0.91 (95% CI: 0.87, 0.94) and 0.86 (95% CI: 0.82, 0.90), 80% and 71.6%, and 93.8% and 83.4%, respectively, for VTi and VTq. VTq of at least 2.87 m/sec and VTi of at least grade IV were the best cutoff values for malignant thyroid nodules.

Calvette et al<sup>(67)</sup> evaluated 157 thyroid nodules using ARFI technique and found that mean SWV  $\pm$  SD on ARFI imaging in healthy, nodule-free thyroid glands was  $2.04 \pm 0.51$  m/s (range, 0.76-3.63 m/s). The mean SWV in benign thyroid nodules was  $1.70 \pm 0.55$  m/s (range, 0.50-2.80 m/s), and the mean SWV in malignant nodules was  $3.39 \pm$

1.15 m/s (range, 1.50-6.08 m/s). When we used an SWV greater than 2.50 m/s for the diagnosis of malignant nodules and less than 2.50 m/s for diagnosis of benign nodules, the Sn and Sp of ARFI imaging were 85.7% and 96.0%, respectively.

Deng et al<sup>(38)</sup> evaluated 175 nodules and found that there were no significant differences between individual groups (CEUS vs US, P=0.279, ARFI vs US, P=0.372, CEUS vs ARFI, P=0.849), combined use of US and CEUS (Contrast-enhanced US) or combined use of US and ARFI yielded significant difference compared to US. (combination of US & CEUS vs US, P=0.021; combination of US & ARFI vs US, P=0.036). The combination of three modalities significantly improved the diagnostic accuracy compared with either combination of conventional US and CEUS or combination of conventional US and ARFI (P=0.045 and P =0.027, respectively).

Hou et al<sup>(68)</sup> evaluated thyroid lesions and found that VTQ value of healthy thyroid tissue, the benign lesions, and the malignant lesions were  $1.69 \pm 0.41$  m/s,  $2.03 \pm 0.42$  m/s, and  $3.10 \pm 1.08$  m/s, respectively. The VTQ value of the malignant lesions was higher than that of the healthy thyroid tissue and the benign lesions (both  $p < 0.001$ ). The VTQ value of benign lesions was higher than the healthy thyroid tissue ( $p < 0.001$ ). With a cutoff value of 2.42 m/s, the sensitivity, specificity, accuracy, PPV and NPV for differentiating between the benign and the malignancy lesions were 80.00%, 89.23%, 87.05%, 69.56%, and 93.54%, respectively.

## **METHODOLOGY**

### **SOURCE OF DATA:**

This study was performed in the department of radio-diagnosis, Sri B M Patil medical college, Vijayapura on patients referred for ultrasound and elastography with clinically detected thyroid nodules.

**DURATION OF STUDY :** November 2018 to June 2020

### **INCLUSION CRITERIA :**

- Patients who were suspected of solitary/ multiple nodules in thyroid.
- Patients who were found to have thyroid nodule accidentally during neck USG.
- Patients undergoing B mode ultrasound, elastography and biopsy of the nodules.

### **EXCLUSION CRITERIA :**

- Thyroid nodules of size < 6mm
- Diffuse thyroid disease without nodules.
- Purely cystic lesions of thyroid without solid component.
- Patients who have undergone previous radiation, iodine ablation or surgery for thyroid on the same side of the lesion.

**STUDY DESIGN :** This is a hospital based prospective study.

### **METHOD OF COLLECTION OF DATA :**

The study was carried out on 60 patients based on the above mentioned inclusion and exclusion criteria.

Ultrasound and shear wave elastography was performed with Acuson S2000 diagnostic

ultrasound system (Siemens medical solutions) with ARFI imaging software and 9L4 high frequency probe with a frequency of 5 to 14 Hz for a ultrasound and 9 Hz of elastography.

All the patients were examined in the supine position. The image setting such as gain, focus, wall filter, color gain was utilized for optimal imaging quality. The nodules were evaluated for various features like location, number, shape, echogenicity, margins, internal composition, internal calcification , vascularity and involvement of neck lymph nodes. Based on these features the nodules are classified into different categories of TIRADS.

- Hypoechoogenicity
- Microcalcifications
- Partially cystic nodule with eccentric location of the fluid portion and lobulation of the solid component
- Irregular margins
- Perinodular thyroid parenchyma invasion
- Taller-than-wide shape
- Intranodular vascularity

TABLE 4: Sonographical suspicious criteria for malignancy. Each criterion is assigned a point. If suspicious cervical lymph nodes are detected, an extra point is added to the score for categorizing nodules on TI-RADS classification<sup>(61)</sup>.

**TI-RADS 1:** Normal thyroid gland. No focal lesion.  
**TI-RADS 2:** Benign nodules. Noticeably benign pattern (0% risk of malignancy)  
 Score of zero  
**TI-RADS 3:** Probably benign nodules (<5% risk of malignancy)  
 Score of zero  
**TI-RADS 4:**  
 • 4a – Undetermined nodules (5-10% risk of malignancy)  
 Score of 1.  
 • 4b – Suspicious nodules (10-50% risk of malignancy)  
 Score of 2.  
 • 4c – Highly suspicious nodules (50-85% risk of malignancy)  
 Score of 3-4  
**TI-RADS 5:** Probably malignant nodules (>85% risk of malignancy)  
 Score of 5 or higher  
**TI-RADS 6:** Biopsy-proven malignancy

TABLE 5: TI-RADS classification of thyroid nodules based on a scoring system according to ultrasound criteria for malignancy. <sup>(61)</sup>.

The patient also underwent shear wave elastography to determine the shear wave elastography for the velocity, black & white virtual tissue imaging of the nodule and the adjacent normal thyroid tissue of the same lobe or the other lobe. Then the nodule were characterized into benign or malignant based on the following.


**TABLE1. SHEAR WAVE VELOCITIES <sup>(2,29)</sup> (SWV)**

Normal thyroid tissue	$2.106 \pm 0.392$ m/s
Benign thyroid nodule	< 3 m/s
Malignant thyroid nodule	$\geq 3$ m/s

**TABLE 2. BLACK AND WHITE VIRTUAL TOUCH TISSUE IMAGING <sup>(1)</sup>**

TYPE 1	If nodule appears more white than the surrounding tissue	BENIGN
TYPE 2	If nodule appears of the same colour as the surrounding tissue	BENIGN
TYPE 3	If > 50% of the nodule appears black as compared to surrounding normal tissue	MALIGNANT

**TABLE 3. SHEAR WAVE VELOCITY MAP <sup>(29)</sup>**

LIGHT BLUE	NEGATIVE	SOFT 
DARK BLUE		
GREEN	EQUIVOCAL	
ORANGE	EQUIVOCAL	
RED	MALIGNANT	HARD

Then the findings of elastography were correlated with the histopathology. The findings of the elastography were correlated with the ultrasound with histopathology as the gold standard.

## **SAMPLE SIZE ESTIMATION**

Based on the study conducted by Hector Grazhdani et.al, it was seen that the sensitivity of Acoustic radiation force impulse imaging (ARFI) in differentiating thyroid nodules was 90%. Using expected incidence of thyroid nodules as 30%, expected sensitivity as 81% and expected specificity 82%, and desired precision as 20%, the minimum sample size is 51.

By using the formula:

$$n = \frac{z^2 p(1-p)}{d^2}$$

where,

Z= z statistic at 5% level of significance

d is margin of error

p is anticipated prevalence rate

### **STATISTICAL ANALYSIS:**

All the quantitative variables such as Age , SWV etc were summarized using descriptive statistics such as mean and standard deviation or median and inter quartile range. All the qualitative variables TIRADS etc were analysed using frequency and percentage.

Shear wave velocity values were compared between benign and malignant nodules using student T test or Mannwhitney U test.

Sensitivity, specificity, PPV, NPV , area under the curve were carried out for predicting the diagnostic accuracy of ARFI in comparison to Ultrasound and cytology/ histopathology.

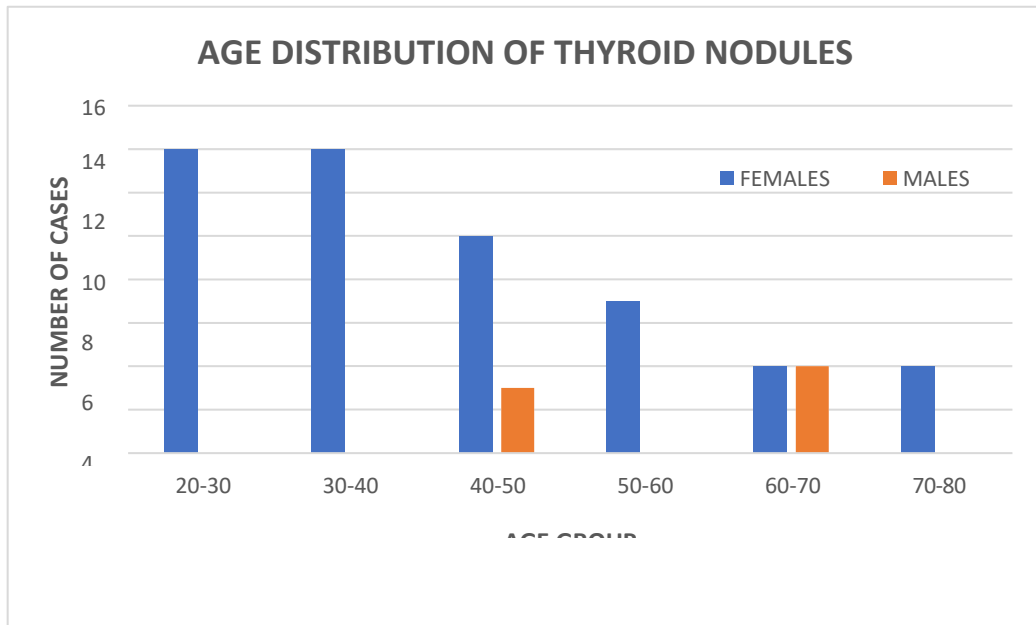
A p-value of <0.05 was considered statistically significant.

## RESULTS

**Table 6 : Tabular representation of age and gender distribution**

Age group		Gender		Total
		Female	Male	
10-19	F	0	0	0
20-29	F	14	0	14
30-39	F	14	0	14
40-49	F	10	3	13
50-59	F	8	0	8
60-69	F	4	4	8
>70	F	3	0	3
Total	F	53	7	60

**Chart 1 : Bar graph representing age and Gender distribution of thyroid nodules**

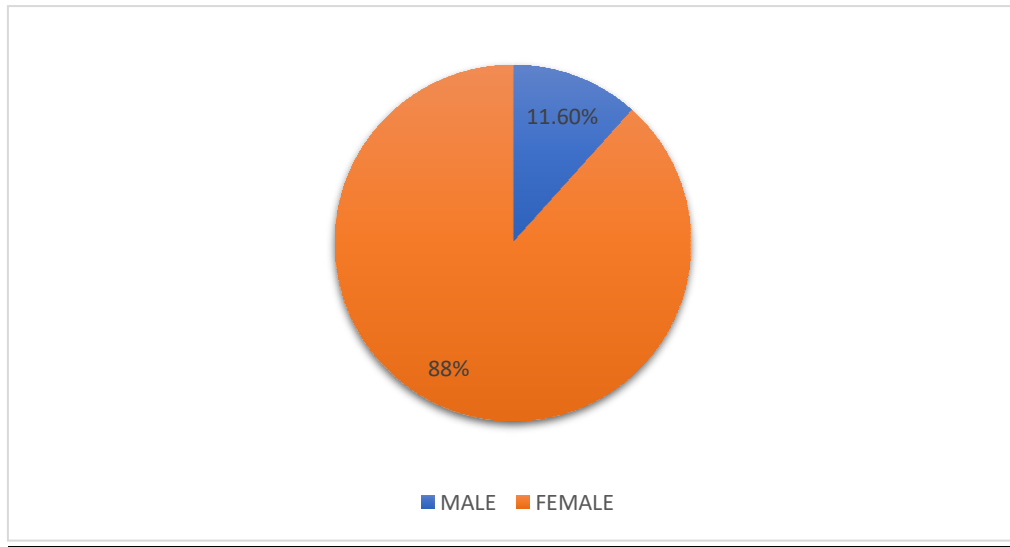


In the study, the thyroid nodules were most commonly seen in the age group between 20 to 40 years and predominantly in females.



**Table 7 : Tabular representation gender distribution of the study participants**

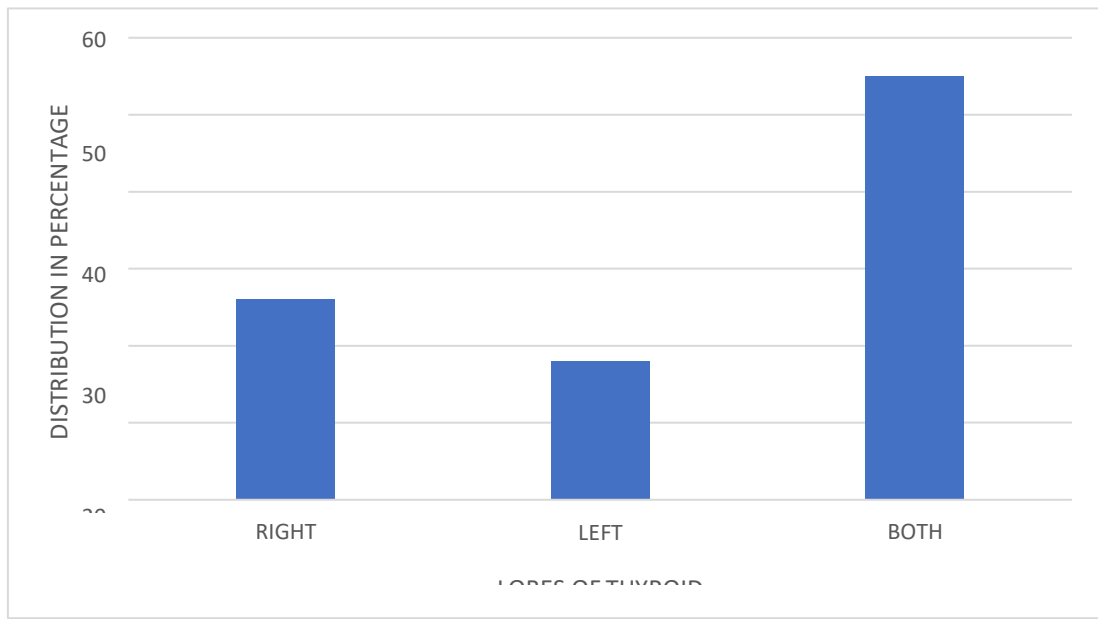
<b>Gender</b>	<b>Number</b>	<b>Percentage</b>
<b>Male</b>	<b>7</b>	<b>11.6 %</b>
<b>Female</b>	<b>53</b>	<b>88.3 %</b>
<b>Total</b>	<b>60</b>	<b>100 %</b>

**Chart 2 : Pie chart showing gender distribution of the study**

In the study out of the 60 patients, 53 were female patients and 7 were male patients with female to male ratio of 7.5 : 1.

**Table 8 : Tabular representation of lobe distribution of the thyroid nodules**

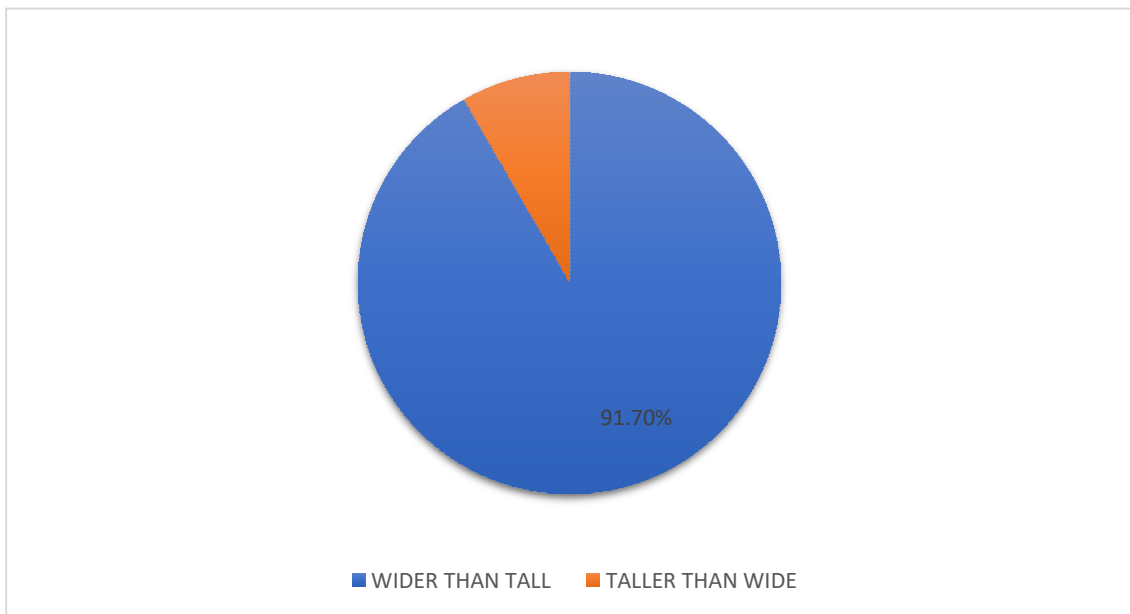
<b>Location</b>	<b>Number</b>	<b>Percentage</b>
<b>Right</b>	<b>16</b>	<b>26 %</b>
<b>Left</b>	<b>11</b>	<b>18.3 %</b>
<b>Both</b>	<b>33</b>	<b>55 %</b>
<b>Total</b>	<b>60</b>	<b>100 %</b>

**Chart 3 : Bar graph representation of distribution of the thyroid nodules**

In the present study, most of the nodules were multiple and distributed in both the lobes (55%).

**Table 9 : Tabular representation of shape of the thyroid nodules**

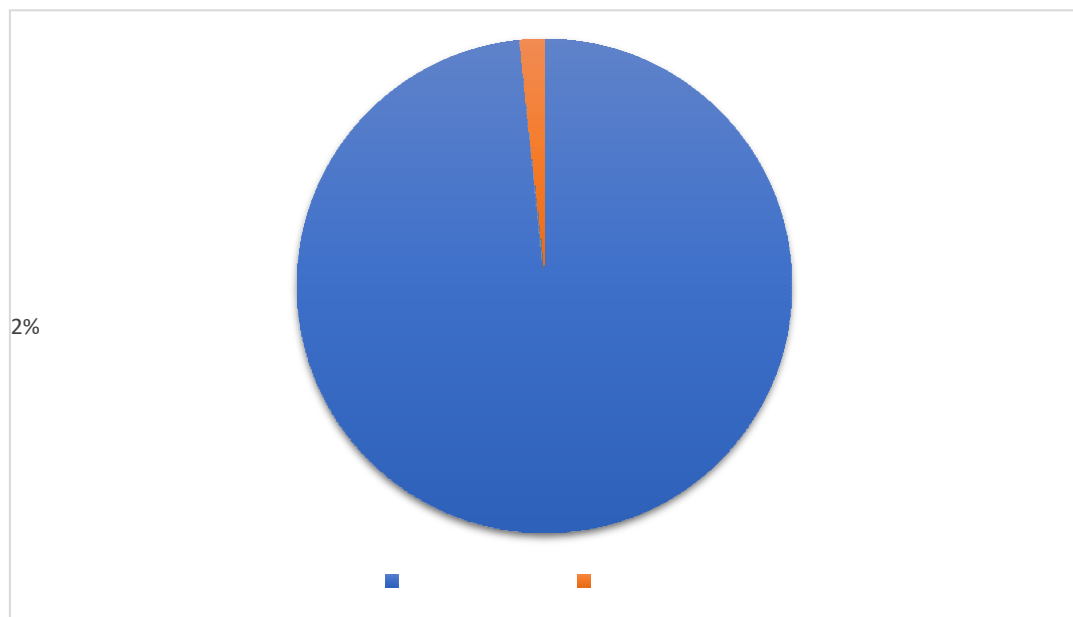
Shape	Frequency	Percentage
Wider than tall	55	91.7%
Taller than wide	5	8.3 %
Total	60	100 %

**Chart 4 : Pie chart representation of the shape of nodules**

In the study the shape of the nodules were predominantly wider than tall (91.7 %) than taller than wide (8.3 %)

**Table 10 : Tabular representation of the margins of the thyroid nodules**

<b>Margins</b>	<b>Frequency</b>	<b>Percentage</b>
<b>Well defined</b>	<b>59</b>	<b>98.3 %</b>
<b>Ill-defined</b>	<b>1</b>	<b>1.6 %</b>
<b>Total</b>	<b>60</b>	<b>100 %</b>

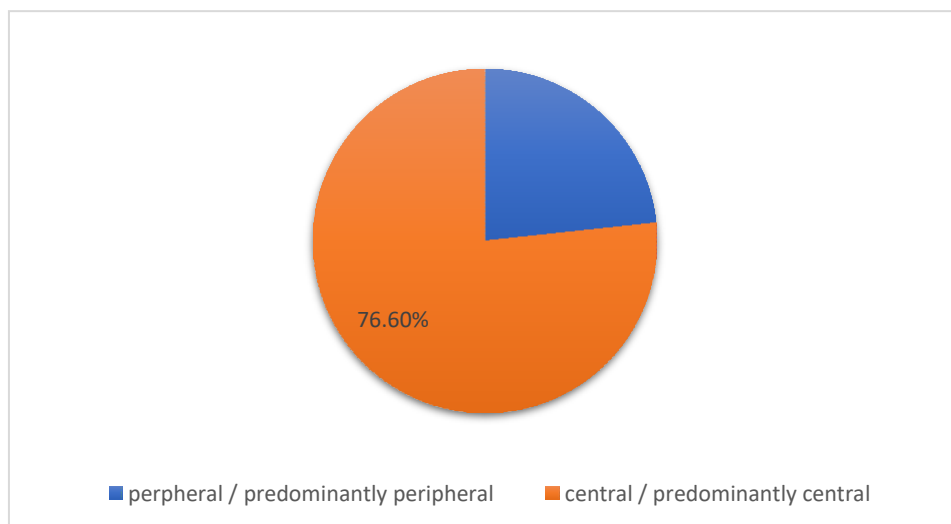
**Chart 5 : Pie chart representing margins of thyroid nodules**

In the study the nodules had predominantly well defined margins 98.3 % and only one case had ill-defined margins.

**Table 11 : Tabular representation of pattern of vascularity among the thyroid nodules.**

<b>Vascularity</b>	<b>Frequency</b>	<b>Percentage</b>
<b>Peripheral/ predominantly peripheral</b>	<b>14</b>	<b>23.4 %</b>
<b>Central / predominantly central</b>	<b>46</b>	<b>76.6 %</b>
<b>Total</b>	<b>60</b>	<b>100 %</b>

**Chart 6 : Pie chart representing pattern of vascularity among the thyroid nodules.**

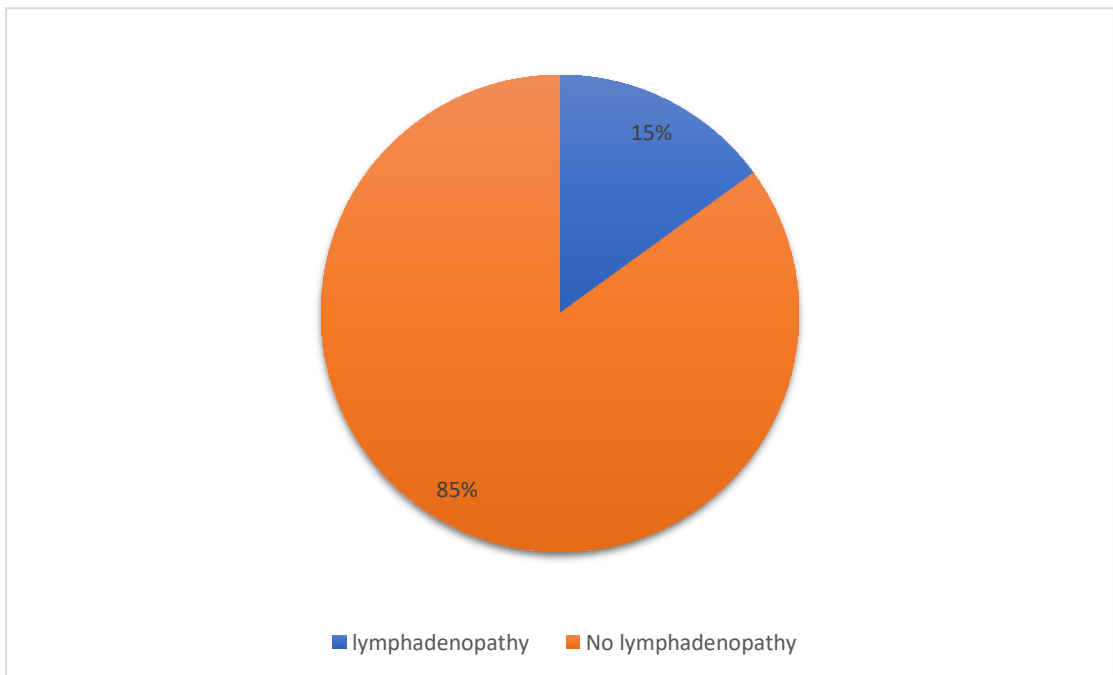


In the study most of the nodules had central or predominantly central vascularity (76.6 %) than peripheral or predominantly peripheral vascularity (23.4 %)

**Table 12 : Tabular representation of association of cervical lymphadenopathy with thyroid nodules**

<b>Lymph nodes</b>	<b>Frequency</b>	<b>percentage</b>
<b>present</b>	<b>9</b>	<b>15 %</b>
<b>absent</b>	<b>51</b>	<b>85 %</b>
<b>Total</b>	<b>60</b>	<b>100 %</b>

**Chart 7 : Pie chart representing association of cervical lymphadenopathy with thyroid nodules**

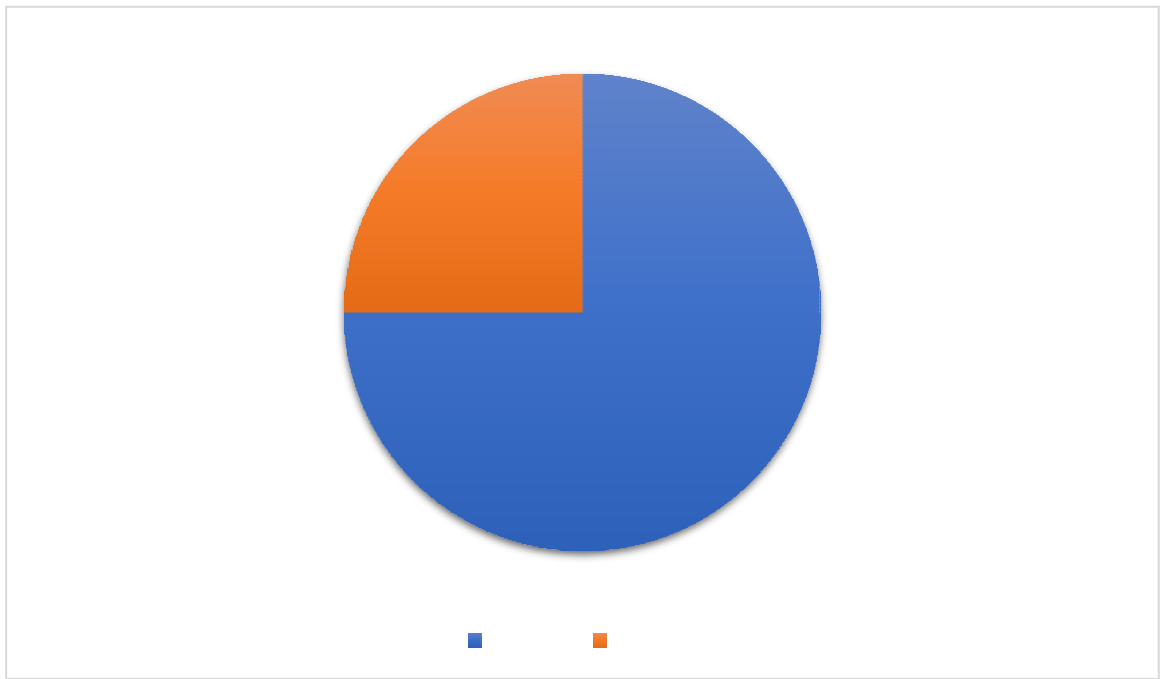


In the study out of 60 cases only 15 cases showed associated enlarged lymph nodes.

**Table 13 : Tabular representation of shear wave elastography among the thyroid nodules**

Shear wave velocity	Frequency	Percentage
< 3 cm/s	45	75 %
≥ 3 cm/s	15	25 %
total	60	100 %

**Chart 8 : Pie chart representing shear wave velocity among the thyroid nodules**

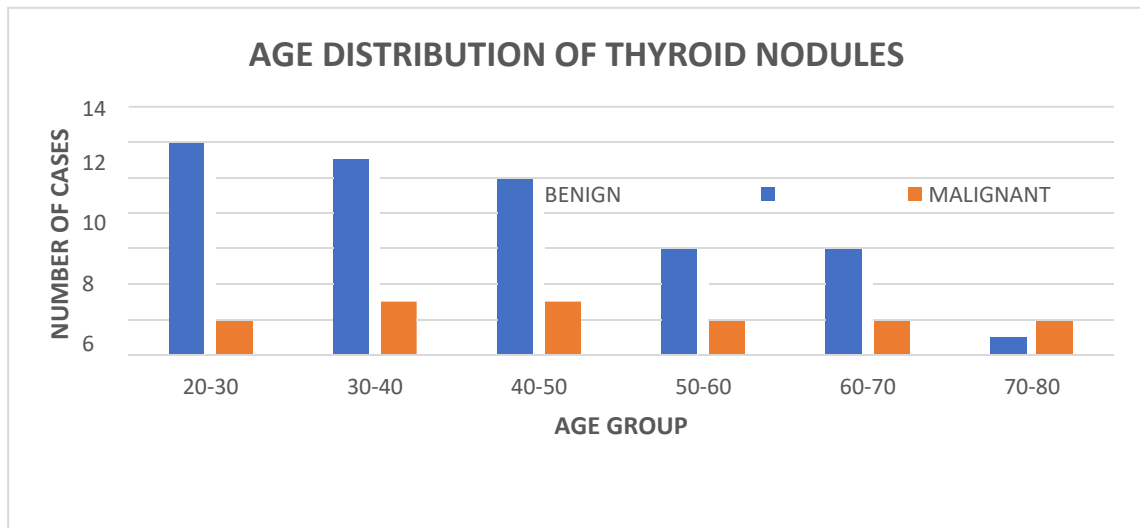


In the study among the 60 cases, 45 cases (75 %) showed a velocity < 3 cm/s and only 15 % cases showed a velocity of ≥3 cm/s.

**Table 14 : Tabular representation of age and gender distribution in thyroid nodules**

Age group		FNA/ HPR diagnosis		Total
		Benign	Malignant	
10-19	F	0	0	0
	%	0.0 %	0.0 %	0.0 %
20-29	F	12	2	14
	%	27 %	13.3 %	23.3 %
30-39	F	11	3	14
	%	24 %	20 %	23.3 %
40-49	F	9	4	13
	%	20 %	26.6 %	22 %
50-59	F	6	2	8
	%	13 %	13.3 %	13.3 %
60-69	F	6	2	8
	%	13 %	13.3 %	13.3 %
>70	F	1	2	3
	%	2 %	13.3 %	5 %
Total	F	45	15	60
	%	100 %	100 %	100 %

**Chart 9: Pie-chart representing age distribution in thyroid nodules**



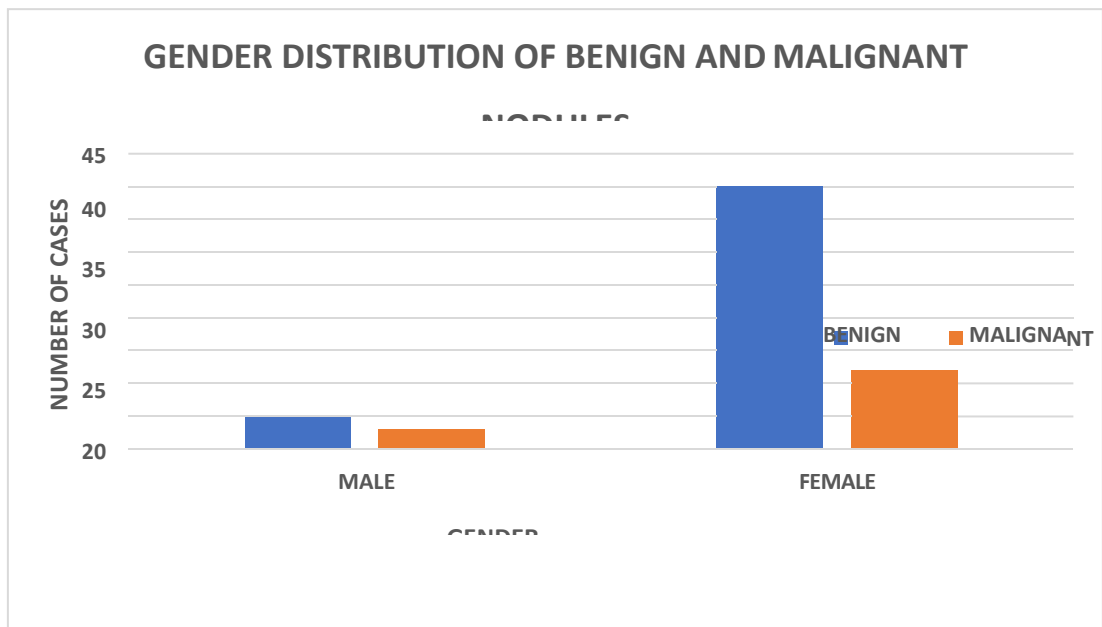
Majority of the benign and malignant nodules are noted in the age group of 30 to 50 years with mean average of 47.5 years for malignancy and 40.7 years for benign lesions. There is no significant between the age and presence of malignant nodules.



**Table 15 : Tabular representation of Gender distribution of malignant and benign thyroid nodules**

Gender		FNA / HPR diagnosis		Total
		Ben	Mal	
Male	F	4	3	7
	%	57.1 %	42.9 %	100 %
Female	F	41	12	53
	%	77.4 %	22.6 %	100 %
Total	F	45	15	60
	%	75 %	25 %	100 %

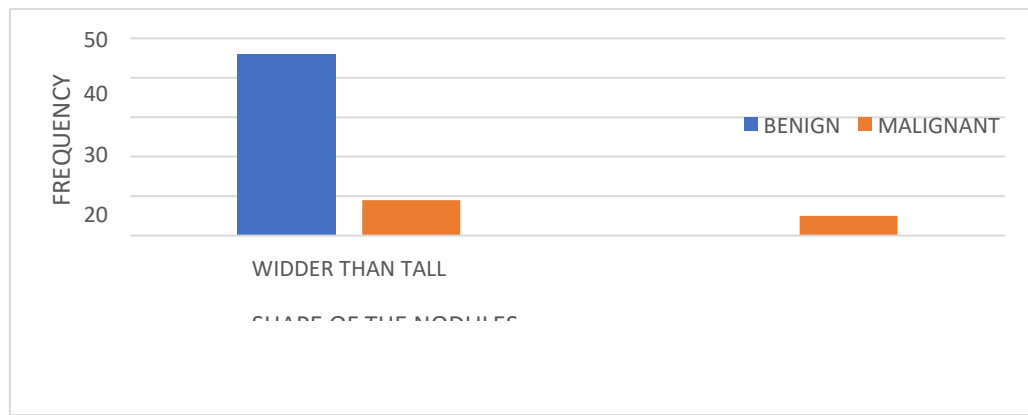
**Chart 10 : Pie chart representing gender distribution of malignant and benign thyroid nodules.**



In the study, Among the 53 females, 12 (22.6 %) had malignant nodules and among 7 males, 3 (42.9 %) had malignant nodules.

**Table no 16 : Tabular representation of shape of thyroid nodules.**

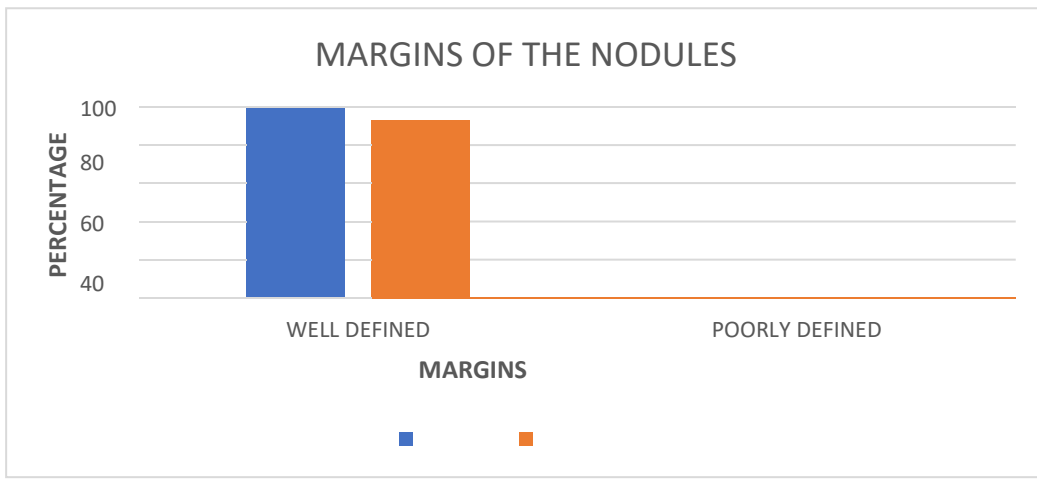
Shape		FNA / HPR diagnosis		Total	Odd's ratio (95% ci)	P
		Ben	Mal			
Wider than tall	F	46	9	55	53.84	0.008
	%	100 %	64.2 %	91.6 %		
Taller than wide	F	0	5	5		
	%	0 %	35.7 %	8.4 %		
Total	F	46	14	60		
	%	100 %	100 %	100 %		

**Chart no 11 : Tabular representation of shape of thyroid nodules.**

In the study the wider than tall was more commonly seen in benign nodules (100 %) with none of the benign nodules showing taller than wide shape. Of the 15 malignant nodules 5 of the nodules showed taller than wide and was found to be statistically significant.

**Table 17 : Tabular representation of margins of the thyroid nodules.**

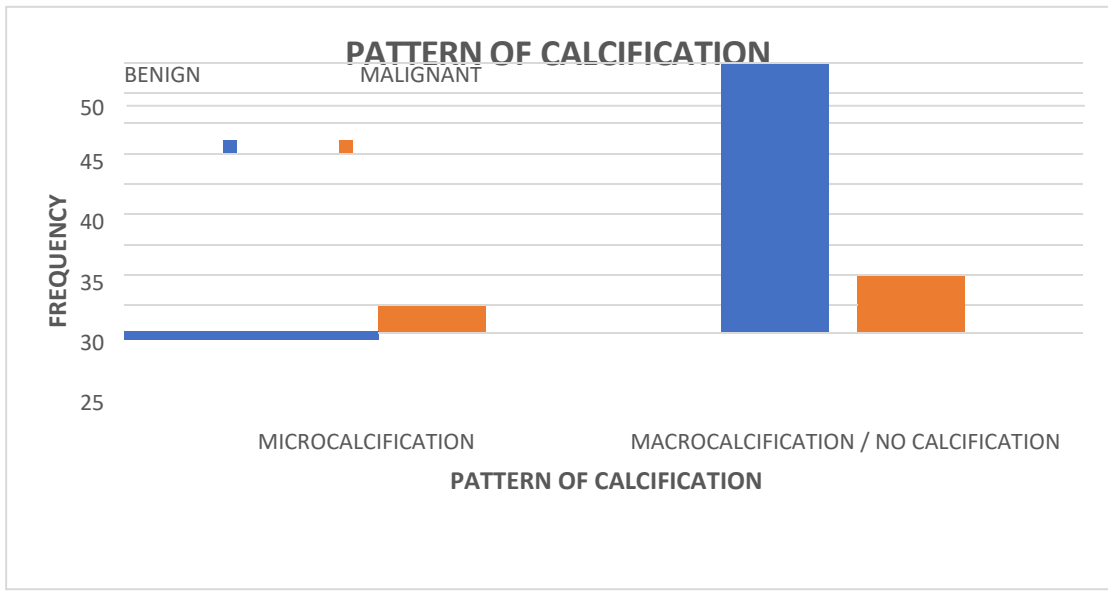
Margins		Histopathology		Total	P Value
		Benign	Malignant		
Well defined	No.	45	14	59	0.250
	%	100 %	93.3 %	98.3 %	
Ill defined	No.	0	1	1	
	%	0	6.7 %	1.6 %	
Total		45	15	60	
		100 %	100 %		

**Chart no 12 : Bar graph representation showing distribution of margins in benign and malignant nodules.**

Most of the benign and malignant nodules show well defined margins with none of the benign nodules showing ill-defined margins Hence the margins does not show statistical significance in differentiating benign and malignant nodules.

**Table 18 : Tabular representation of calcification in thyroid nodules**

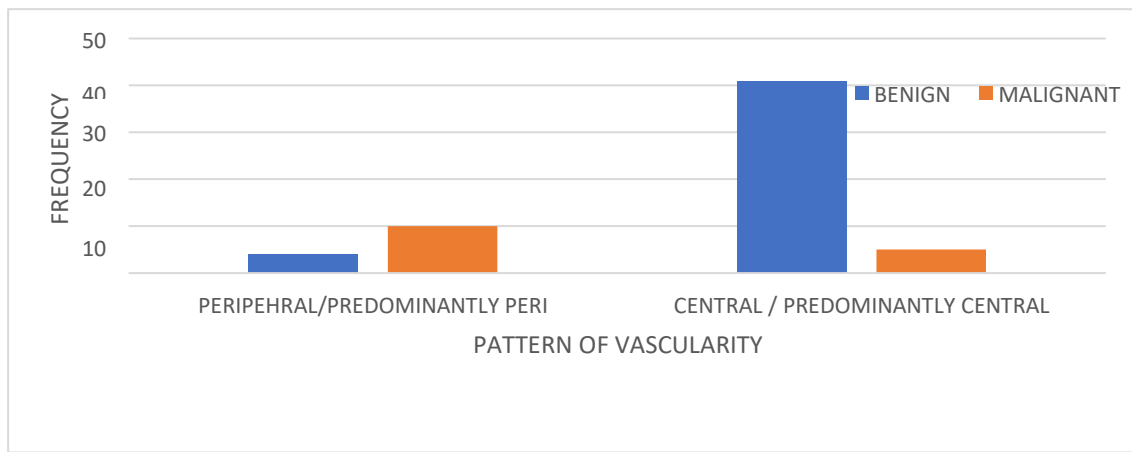
Calcification		Histopathology		Total	P Value
		Benign	Malignant		
Micro	No.	1	6	7	0.01
	%	2.2 %	40 %	11.6 %	
Macro	No.	6	0	6	
	%	13.3 %	0 %	10 %	
Absent	No.	38	9	47	
	%	84.4 %	60 %	78.3 %	
Total		45	15	60	
		100 %	100 %	100 %	

**Table 13 : Bar graph showing type of calcification in benign and malignant nodules**

Microcalcification was more commonly seen in malignant nodules ( n = 6) and macrocalcification more common in benign nodule. Classifying the nodules based on the type of calcification was statistically significant with  $p < 0.01$ .

**Table no 19 : Tabular representation of pattern of vascularity in thyroid nodules.**

PATTERN		FNA / HPR DIAGNOSIS		Total	odd	P
		BEN	MAL			
peripheral / predominantly peripheral	F	4	10	14	26.25	0.001
	%	8.8 %	66.7 %	%		
Central predominantly central	F	41	5	46		
	%	91.1 %	33.3 %	%		
Total	F	45	15	60		
	%	100.0%	100.0%	100.0%		

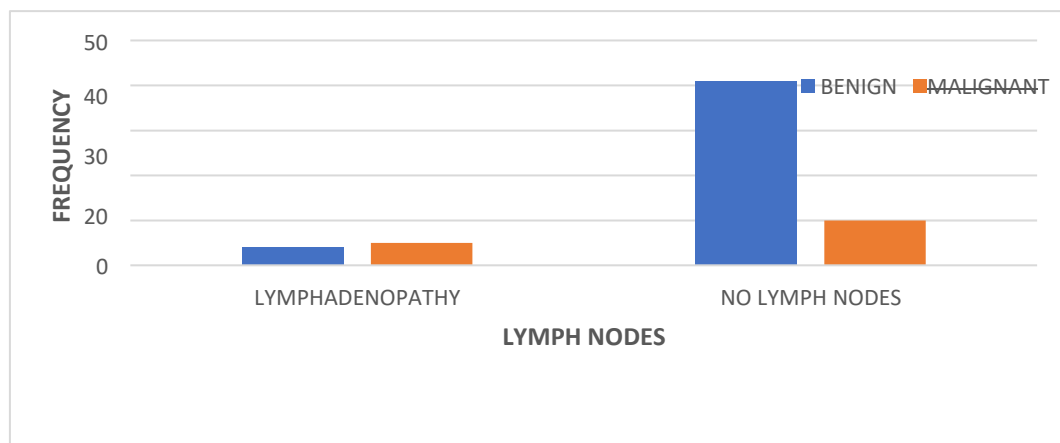
**Chart no 14 : Bar graph showing pattern of vascularity in thyroid nodules.**

The central / predominantly central vascularity was seen more commonly in benign nodules (91.1 %) and peripheral vascularity in malignant nodules with 66.7 % malignant nodules showing peripheral vascularity. There was statistical significance of peripheral vascularity in detecting malignant nodules.

**Table no 20 : Tabular representation of association of cervical lymphadenopathy with thyroid nodules**

Lymph nodes		FNA / HPR diagnosis		Total	Odd's (95% ci)	P
		Ben	Mal			
Present	F	4	5	9	0.17	0.02
	%	8.9 %	33.3 %	15 %		
Absent	F	41	10	51		
	%	81.9 %	66.7 %	85 %		
Total	F	45	15	60		
	%	100.0%	100.0%	100.0%		

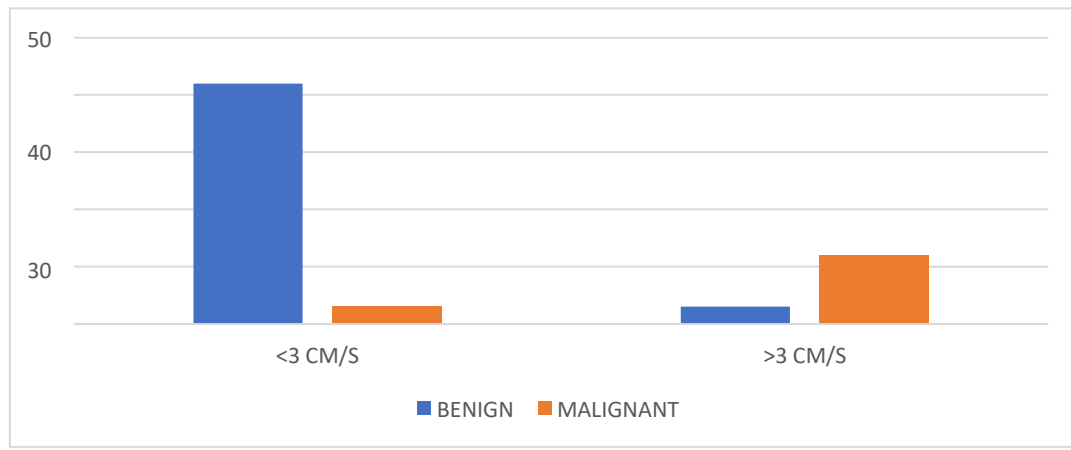
**Table no 15 : pie chart showing association of cervical lymphadenopathy with thyroid nodules.**



In the present study association of cervical lymphadenopathy was more frequently seen in malignant nodules (33.3 %) than in benign nodules (8.9 %). Characterization based on association of presence of lymphadenopathy is statistically significant.

**Table no 21 : Tabular representation of shear wave velocity of the nodules**

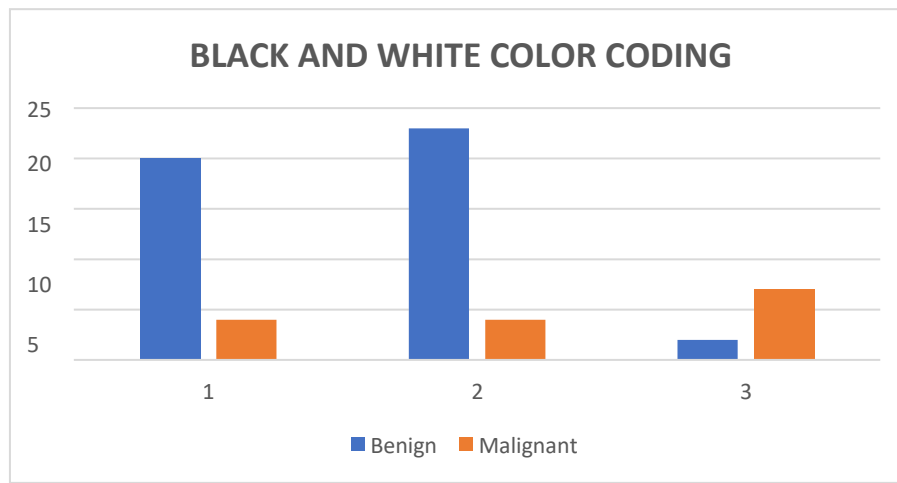
SWV		FNA / HPR DIAGNOSIS		Total	Odd's (95% CI)	P
		BEN	MAL			
<3	F	42	3	45	30.07	0.001
	%	93.3%	6.7%	100%		
≥3	F	3	12	15		
	%	20%	80%	100%		
Total	F	45	15	60		
	%	100.0%	100.0%	100.0%		

**Chart no 16: Bar diagram representing the SWV of the thyroid nodules**

Out of the 45 benign nodules 42 nodules (93.3 %) showed a velocity less than 3 cm/s and only 3 benign nodules showed velocity more than 3 m/s and out of 15 malignant nodules 12 nodules (80 %) showed a velocity of more than 3 cm/s and rest of the 3 malignant nodules showed velocity less than 3. Characterization of the malignant nodules by velocity more than 3 cm/s showed statistical significance.

**Table no 22 : Tabular representation of the black and white color coding.**

Black and white coding		FNA / HPR DIAGNOSIS		Total	P
		BEN	MAL		
1	F	20	4	24	0.001
	%	44.5 %	26.7 %		
2	F	23	4	27	
	%	51.1 %	26.6 %		
3	F	2	7	9	
	%	4.4 %	46		

**Chart no 17 : Bar diagram representing the black and white coding.**

Out of the 45 benign nodules 20 of the nodules show color more white as related to the normal parenchyma of the thyroid, while 23 nodules show similar color as the normal thyroid parenchyma. Out of the 15 malignant nodules 7 of them show color more black than the normal thyroid parenchyma which suggested that they were malignant nodules. Based on the black and white color coding , the nodules appearing more black than the surrounding parenchyma showed statistical significance in detecting malignant nodule.



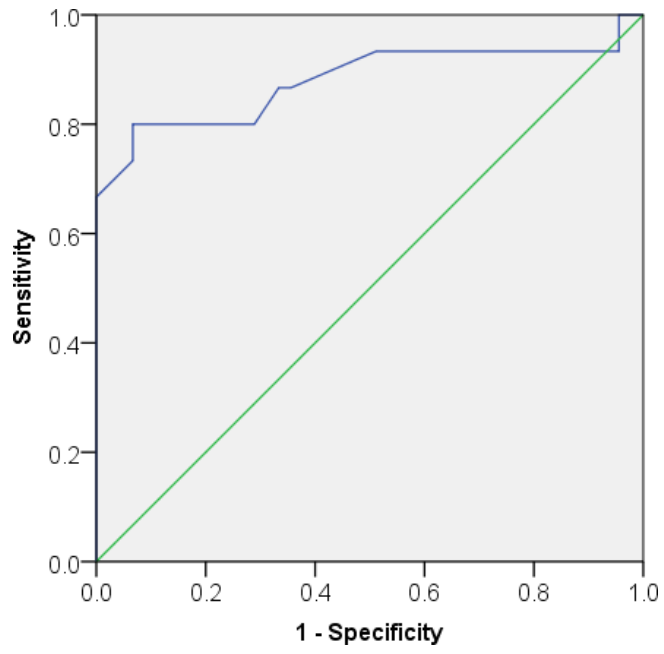
**Table no 23 : Tabular representation of the SWV color coding.**

SWV color coding		FNA / HPR DIAGNOSIS		Total	P value
		BEN	MAL		
LIGHT BLUE	F	0	0	0	0.128
	%	0 %	0 %	0 %	
DARK BLUE	F	3	2	5	
	%	6.7 %	13.3 %	8.3 %	
GREEN	F	40	10	50	
	%	88.9 %	66.7 %	83.3 %	
ORANGE	F	0	0	0	
	%	0 %	0 %	0 %	
RED	F	2	3	5	
	%	4.4 %	20 %	8.3 %	
TOTAL	F	45	15	60	
	%	100 %	100 %	100 %	

Most of the benign and malignant nodules demonstrates green color on SWV color coding.

There was no statistical significance of SWV color coding in differentiating benign and malignant nodules.

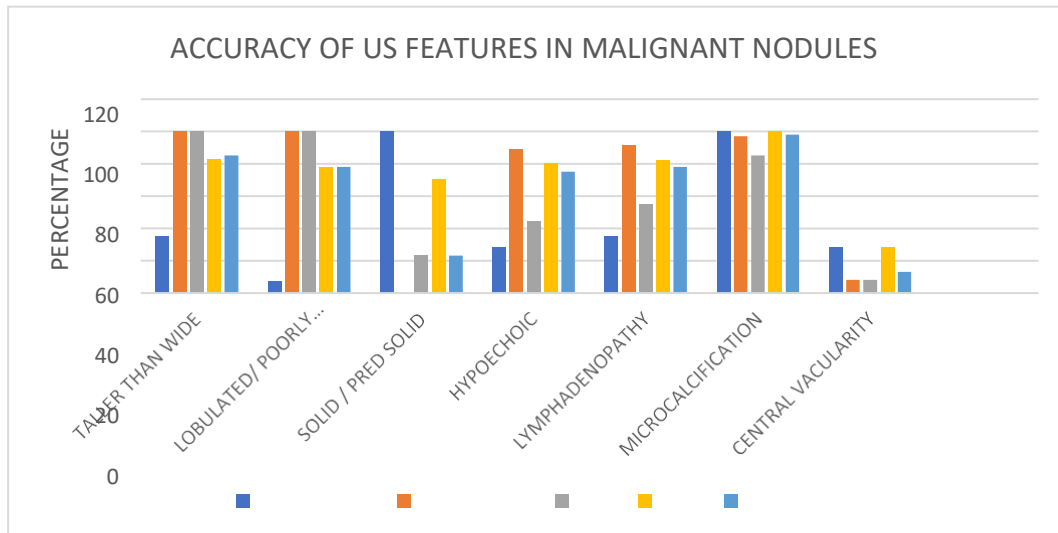
### ROC CURVE



The ROC curve of shear wave elastography in determining the thyroid nodules.

**Table 24: diagnostic accuracy of us findings for malignant nodules.**

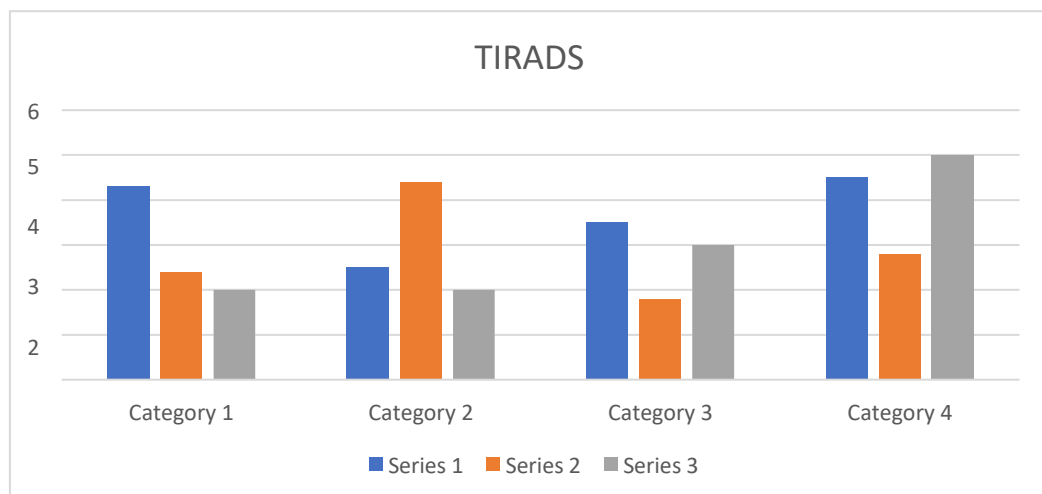
	Sensitivity	Specificity	PPV	NPV	Accuracy
TALLER THAN WIDE	35.71	100	100	83.64	85
LOBULATED/POORLY DEFINED MARGINS	7.14	100	100	77.97	78.33
SOLID/PREDOMINANTLY SOLID	100	0	23.33		23.33
HYPOECHOIC	28.57	89.13	44.44	80.39	75
LYMPHADENOPATHY	35.71	91.30	55.56	82.35	78.33
MICROCALCIFICATIONS	100	97.73	85.71	100	98
CENTRAL AND CENTRAL > PERINODULAR	28.57	8.70	8.70	28.57	13.33

**Chart 18 : Bar diagram representing US features in malignant nodules**

The diagnostic accuracy of taller than wide, lobulated/ poorly defined margins, solid / predominantly solid, hypoechogenicity, microcalcification, lymphadenopathy and central vascularity were 85%, 78%, 23.3%, 75%, 98%, 78% and 13.3% with highest accuracy seen in the microcalcification (98%).

**Table 25: tabular representing comparison of us diagnosis and FNA/HPR**

TIRADS		FNAC		Total
		Benign	Malignant	
TIRADS 2	Frequency	0	0	0
	%	0%	0%	0%
TIRADS 3	Frequency	32	3	35
	%	71.2%	20%	58.3%
TIRADS 4A	Frequency	12	3	15
	%	26.6%	20%	25%
TIRADS 4B	Frequency	1	5	6
	%	2.2%	33.3%	10%
TIRADS 4C	Frequency	0	4	4
	%	0%	26.7%	6.7%
TIRADS 5	frequency	0	0	0
	%	0%	0%	0%
TOTAL	Frequency	45	15	60
	%	100 %	100%	100%

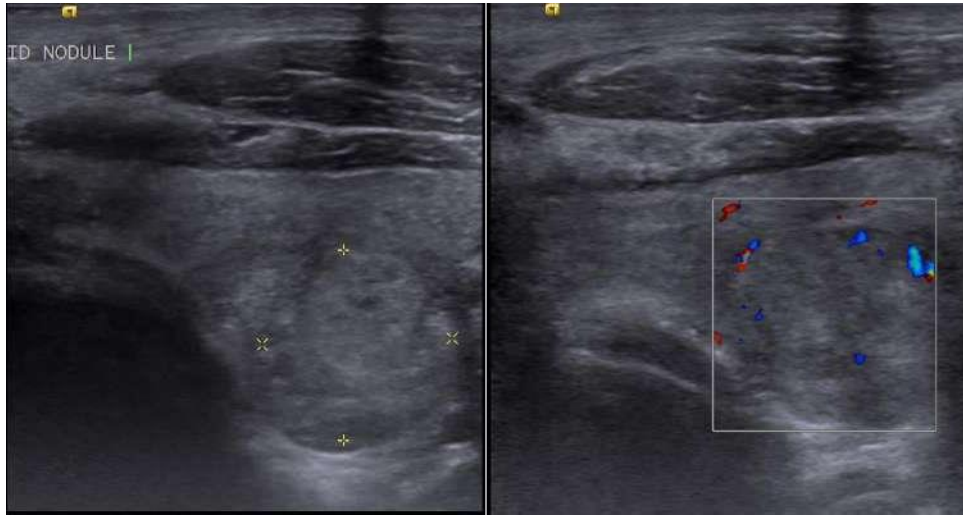
**Chart 19 : Bar graph comparing TIRADS with FNAC/ HPR**

TIRADS 4B and above have high sensitivity in detecting the malignant nodules.

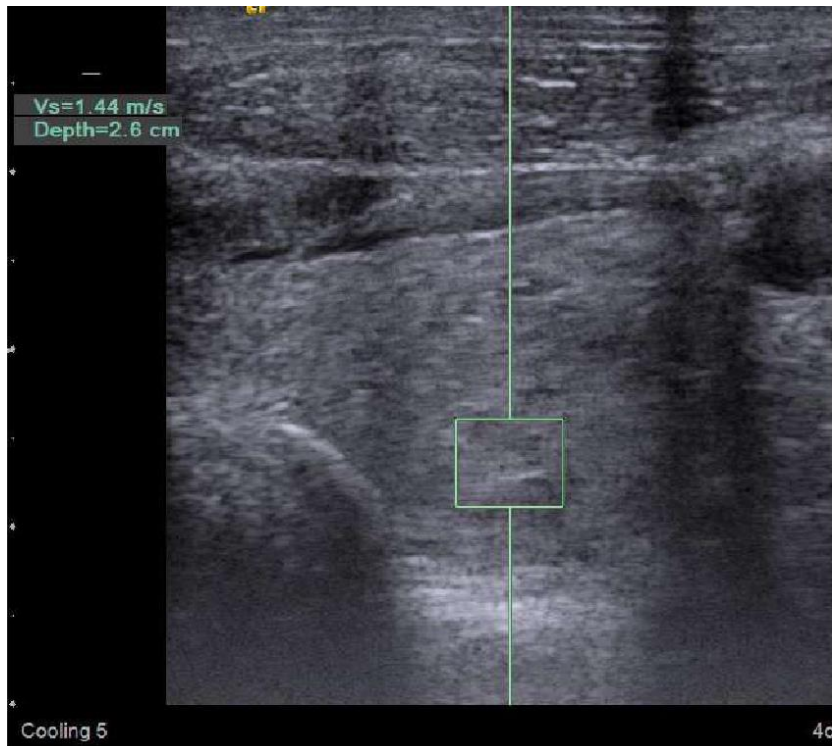
## REPRESENTATIVE IMAGES

### CASE 1:

ULTRASOUND AND DOPPLER :



ELASTOGRAPHY



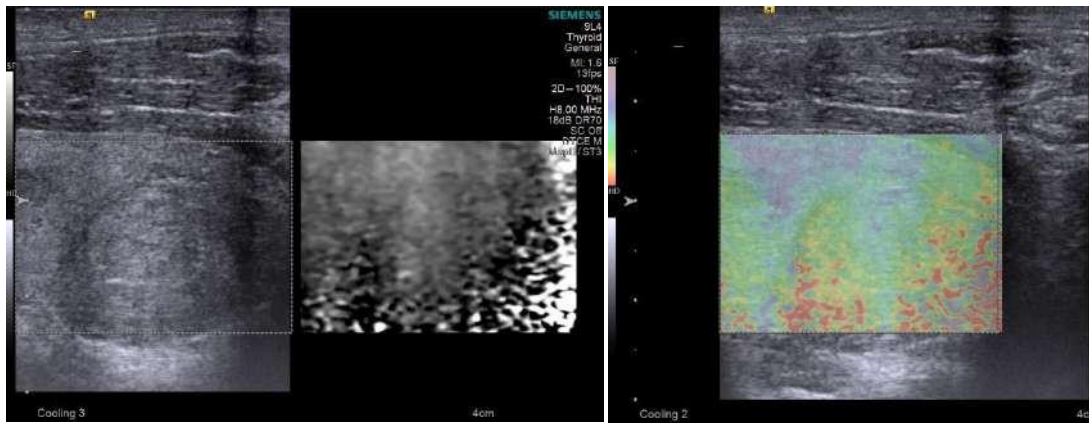


Fig 27 : A 44 year old female presented with swelling in the anterior aspect of the thyroid

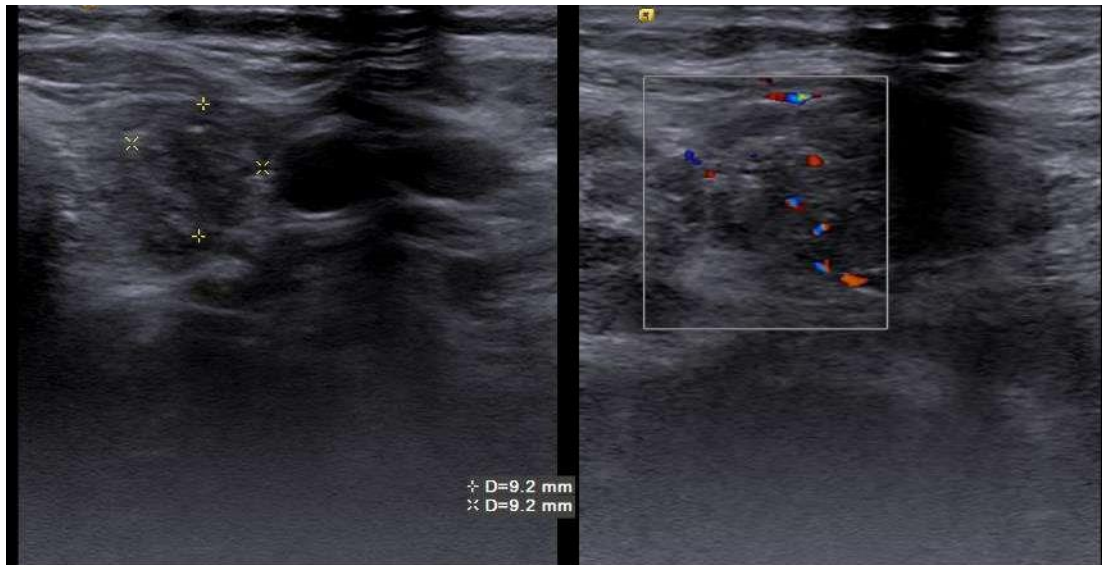
Ultrasound and doppler : A well defined isoechoic nodule was noted in the left lobe of the thyroid. The nodule showed predominantly peripheral vascularity. The nodule is wider than tall.

Shear wave elastography : The average velocity of the nodule was 1.33 m/s suggesting a benign nodule. On black and white color coding the lesion appears as white as the surrounding normal tissue. On SWV color coding the lesion shows predominantly blue color suggesting a benign nodule.

## **HISTOPATHOLOGY : COLLOID NODULE**

**CASE 2:**

## ULTRASOUND



## ELASTOGRAPHY

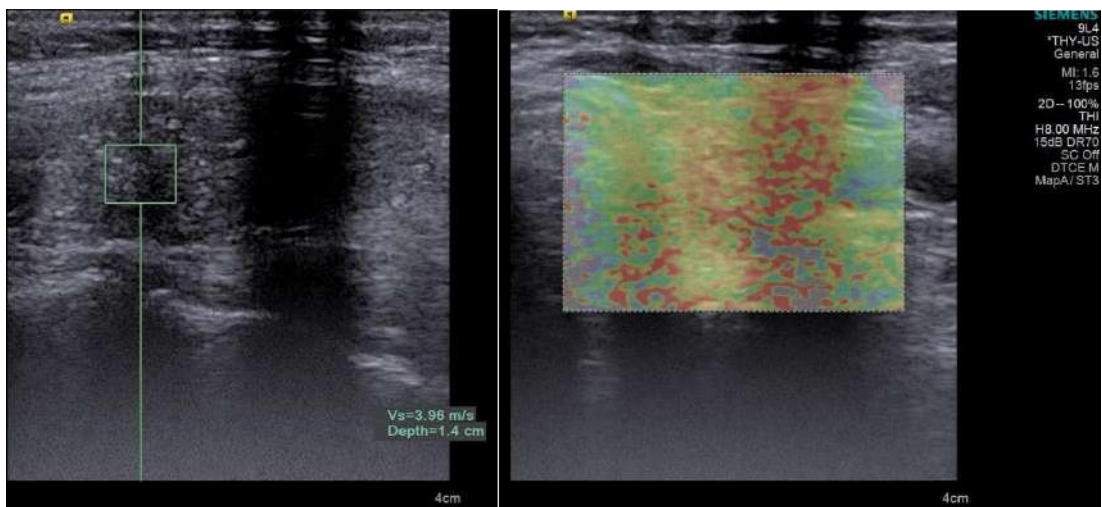


Fig 28 : 37 year old female presents with swelling of the neck

Ultrasound and Doppler : Well defined mixed echoic lesion in the left lobe of the thyroid, there few specs of microcalcification within the lesion. The lesion shows central and peripheral vascularity vascularity on Doppler.

Shear wave elastography : The velocity on shear wave elastography is 3.96 m/s, however the average velocity of the nodule is 3.16 m/s suggesting that it is a malignant

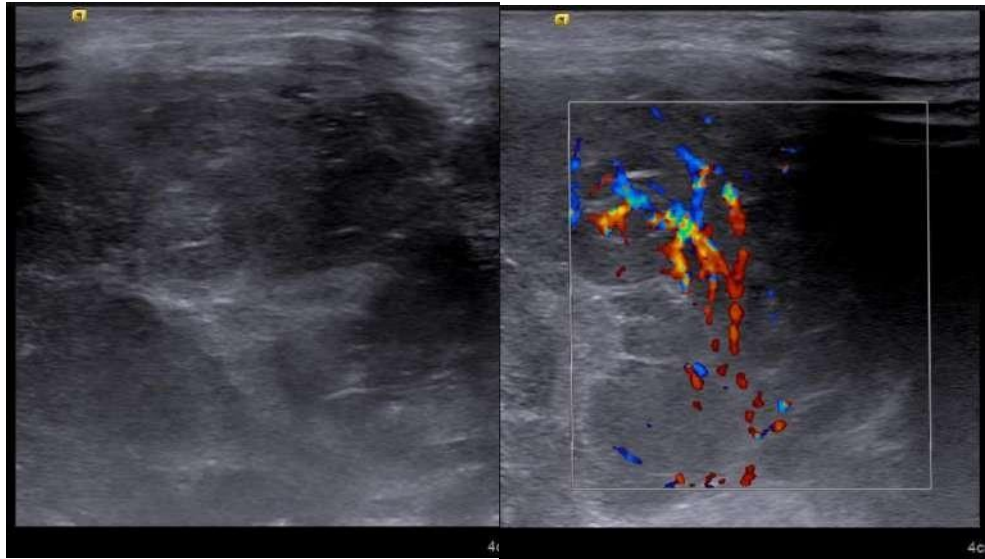
nodule. and on SWV color coding the lesion showed predominantly red color suggesting that malignant nodule.

## **HISTOPATHOLOGY : PAPILLARY CARCINOMA OF THYROID**

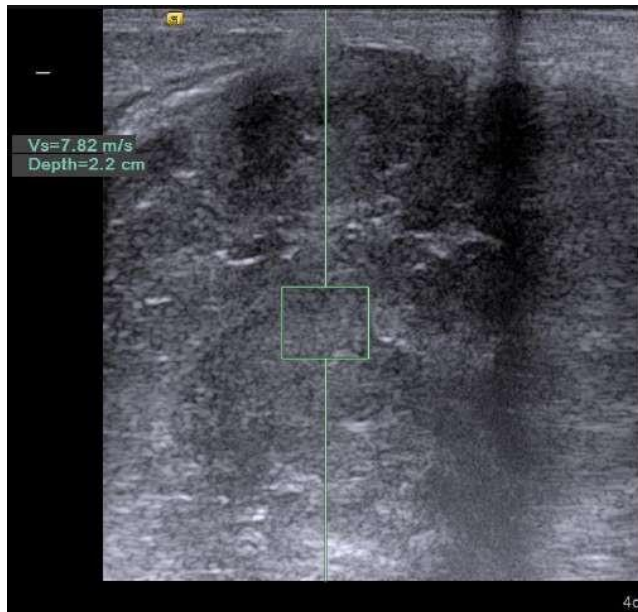


**CASE 3:**

ULTRASOUND AND DOPPLER :



ELASTOGRAPHY



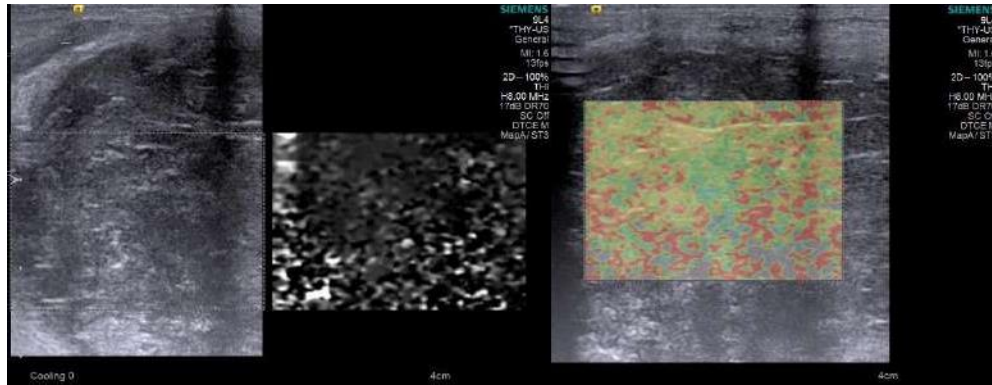


Fig 29 : A 70 Year old female presented with large swelling in the anterior aspect of the neck.

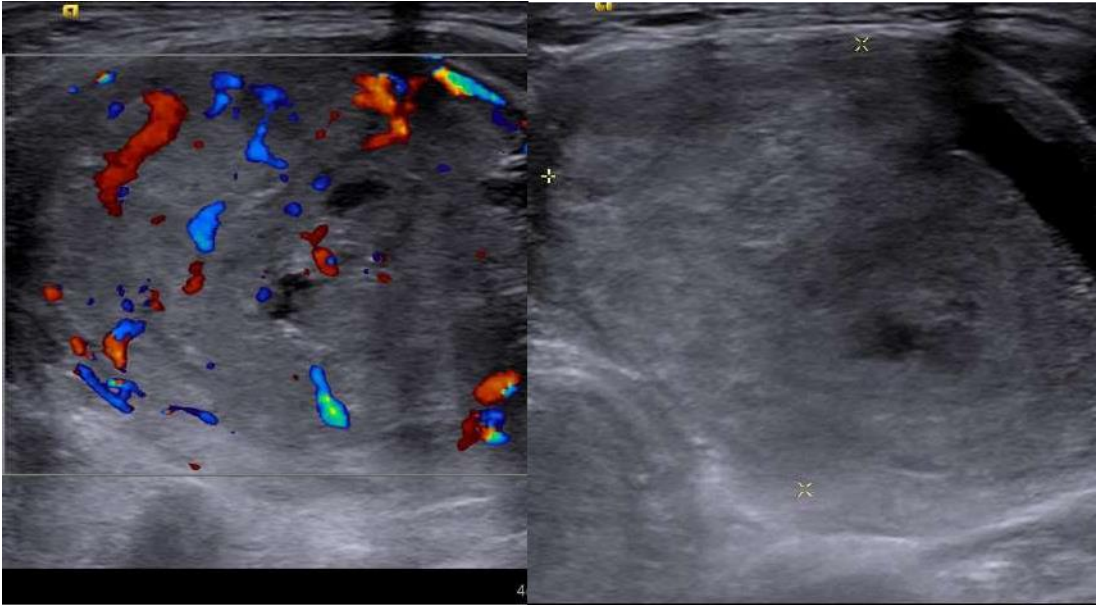
Ultrasound and doppler : an ill-defined predominantly hypoechoic nodule was noted in the right lobe of thyroid, the lesion showed internal vascularity on Doppler. The nodule appears taller than wide. There were evidence of microcalcification within the nodule,

Shear wave elastography : the nodule showed a maximum velocity of 7.86 m/s and an average velocity of 5.25 m/s suggesting of malignant nodule. The SWV color coding showed predominantly red color and the black and white color coding showed more black than the normal thyroid tissue.

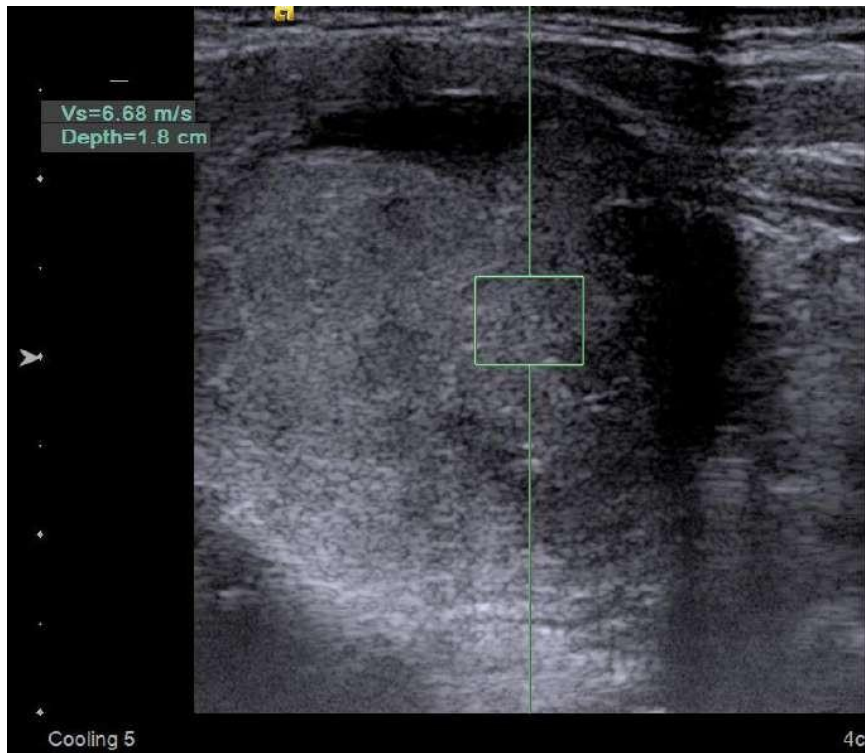
## **HISTOPATHOLOGY : ANAPLASTIC CARCINOMA OF THYROID**

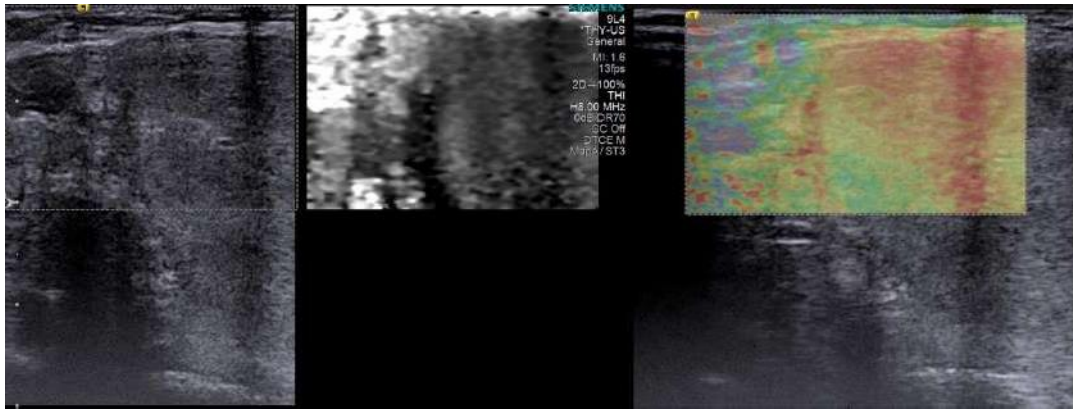
**CASE 4:**

ULTRASOUND AND DOPPLER :



ELASTOGRAPHY :





MRI:

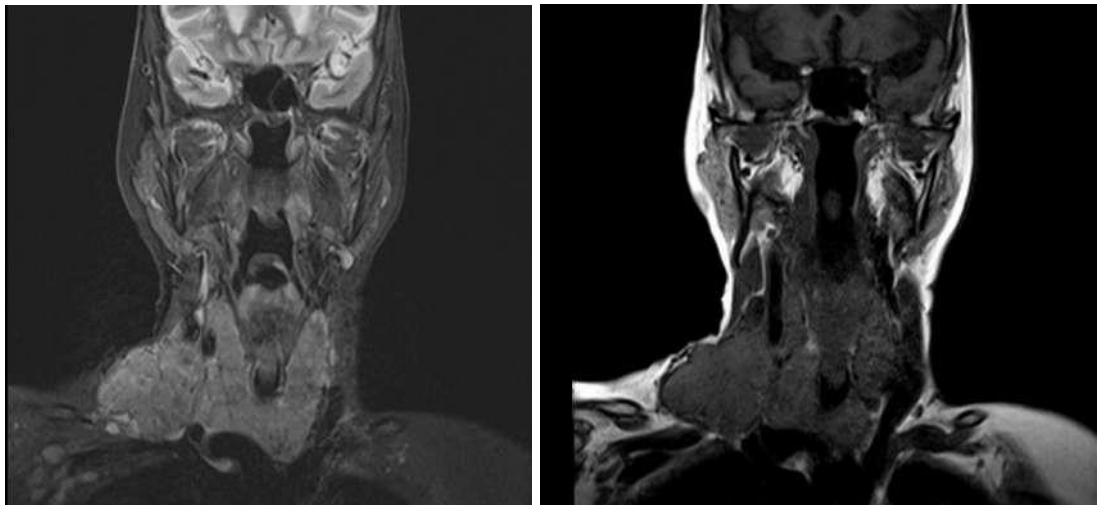


Fig 30 : A 50 year old female with swelling in the anterior aspect of the neck.

Ultrasound and doppler : A predominantly hypoechoic nodule is noted in the right lobe of thyroid. The nodule shows increase in internal vascularity on color doppler. Few cystic areas noted within the lesion.

Shear wave elastography : The nodule shows maximum velocity of 6.<sup>68</sup> m/s with an average velocity of 5.23 m/s. shows predominantly red color in SWV color coding and appears more black than the normal thyroid tissue.

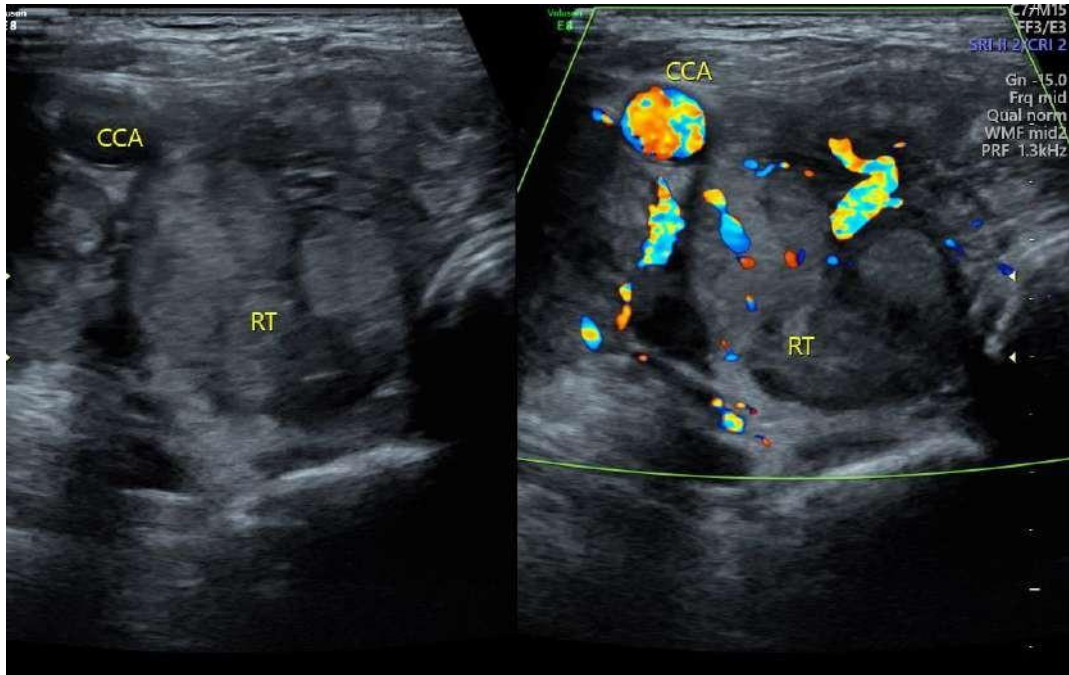
MRI : T1 isointense, T2 high signal intensity with diffusion restriction on DWI.

## **HISTOPATHOLOGY: HURTLE CELL CARCINOMA**

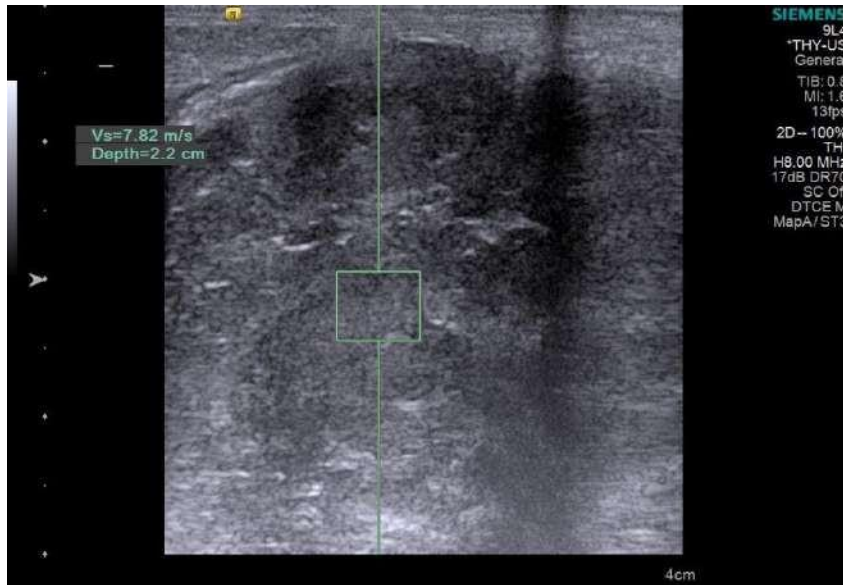


**CASE 5:**

ULTRASOUND AND DOPPLER :



ELASTOGRAPHY :



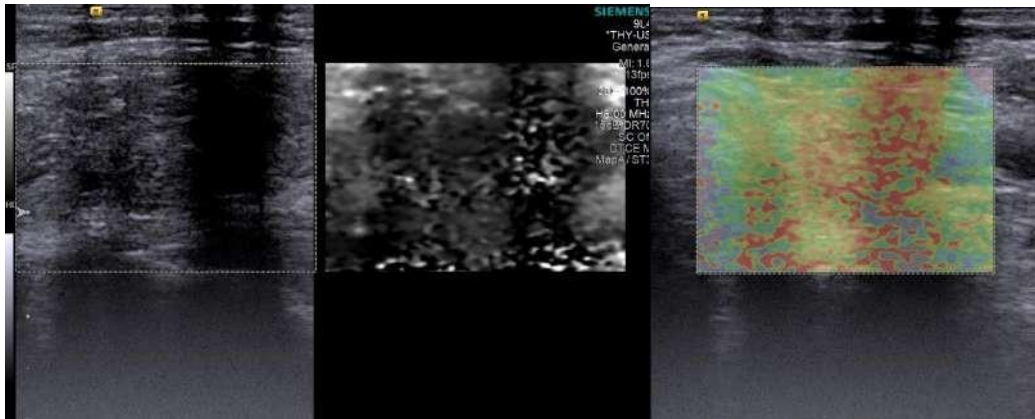


Fig 31 : A 29 Year female with swelling in anterior aspect of the neck.

Ultrasound and doppler : A ill-defined hyperechoic nodule in the right lobe of thyroid, taller than wide and shows central vascularity on doppler.

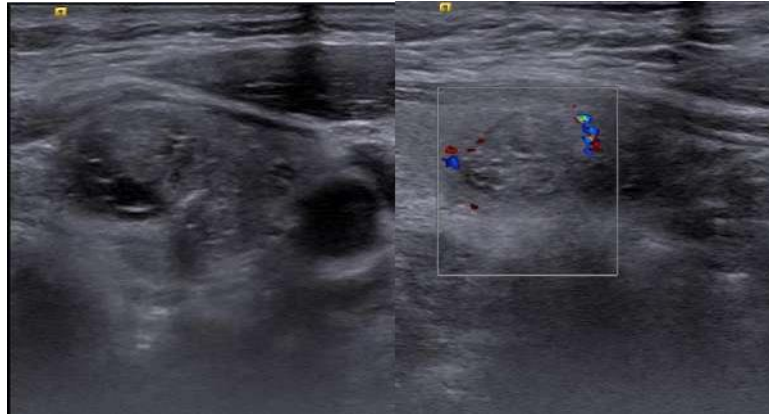
Elastography : a maximum of SWV of 7.82 m/s velocity. The nodule appears more black than the surrounding normal thyroid, and shows predominantly red color on SWV color coding.

Suggesting malignant nodule.

## **HISTOPATHOLOGY : FOLLICULAR CARCINOMA OF THYROID.**

**CASE 6:**

ULTRASOUND AND DOPPLER :



ELASTOGRAPHY



Fig 32 : Ultrasound and doppler : A ill-defined hyperechoic nodule in the right lobe of thyroid, taller than wide and shows central vascularity on doppler.

Elastography : a maximum of SWV of 7.82 m/s velocity. The nodule appears more black than the surrounding normal thyroid, and shows predominantly red color on SWV color coding. Suggesting malignant nodule.

**HISTOPATHOLOGY : MEDULLARY CARCINOMA OF THYROID.**

## **DISCUSSION**

The thyroid ultrasound is the safe and fast method to evaluate the thyroid nodules. There are several features which helps us to differentiate the benign and malignant nodules. However all the nodules cannot undergo biopsy / FNA for confirmation. Shear wave elastography is a novel technique with high Sn and Sp in evaluation of thyroid nodules and can potentially reduce unnecessary fine needle aspiration biopsies.

### **THE PRESENT STUDY**

Of the 60 nodules assessed, 45 nodules were benign and 15 nodules were malignant. Most of the benign and malignant nodules are found to be in the age group of 30-50 years with mean age of 40.7 years for benign and 47.5 years for malignant. The nodules are witnessed to be principally seen in females (53) than males (7) and with female to male ratio of 7.5:1. On histopathology, malignant nodules were found most commonly in females ie 12 of the 15 malignant nodules and less common in male ie 3 of the 15 malignant nodules.

There was no significance in distribution of the nodules in the lobes, most common being multiple and seen in both the lobes.

Of the 45 benign thyroid nodules most common histopathological diagnosis was colloid nodule followed by adenomatoid nodule. Among the 15 malignant thyroid nodules the papillary carcinoma was the most common followed by follicular carcinoma, medullary carcinoma of thyroid and the least common being anaplastic thyroid carcinoma. There was also a case of hurthle cell carcinoma.



Ultrasound being the first investigation for the thyroid nodule, we shall discuss the accuracy of grey scale and doppler ultrasound and then discuss accuracy of shear wave elastography, finally comparing both the modality considering histopathology as the gold standard.

## **THE ACCURACY OF ULTRASOUND IN EVALUATION OF THYROID**

### **NODULES**

In the study done by Moon et al<sup>(62)</sup> had found that the US features like taller than wide, spiculated margins, hypoechogenicity, microcalcification and macrocalcification were statistically significant in detecting the malignant thyroid nodules. Similar to the study done by moon et al our study also showed statistical significance in ultrasound features like taller than wide, hypoechogenicity and microcalcification in detecting the malignant nodules.

There were many studies considering shape of nodules as an indices in detecting malignancies. In the study done by Yoon s et al<sup>(63)</sup> on the taller than wide sign in thyroid malignancies found taller than wide as a marker of diagnosing malignancies showed a specificity of 60 to 100 % but a low sensitivity of 24.1 to 73 %. These results were similar to our results which showed than a Sp of 100 %, a low sensitivity of 35 % and a overall accuracy of 85 % of taller than wide criteria in detecting the malignant nodules.

According to the terminology of the internal content i.e. solid ( $\leq 10\%$  cystic portion), predominantly solid ( $> 10\%$  cystic and  $\leq 50\%$  cystic), predominantly cystic ( $>50\%$  cystic and  $\leq 90\%$  cystic portion) and cystic ( $>90\%$  cystic portion) suggested by moon et al<sup>(63)</sup> found that solid and predominantly solid component was observed in majority of malignant and benign nodules. But however in our study the presence of solid and predominantly solid component was not statistically significant in detecting the

malignant nodules.

In the present study the microcalcification was found to have a Sn of 100% and Sp of 97 % with high accuracy of 98 %. The microcalcification was statistically significant in detecting the malignant nodules these findings were similar to the study completed by Kim et al<sup>(64)</sup> who observed that microcalcification was statistically significant in detecting the malignant nodule with Sn and Sp of 60 % and 85 % respectively and overall accuracy of 77 %.

The US features of Wider than tall was statistically significant in determining benign nodule. This was again associated well with the study of Moon et al<sup>(63)</sup> who found that Wider than tall and Well defined margins are noteworthy to depict benignity. which is in contradiction to the study of Moon et al<sup>(62)</sup>.

In this study, we observed that the US findings like taller than wide, lobulated or poorly defined margins, hypoechogenicity and microcalcification showed a very high Sp of 100 %, 100 %, 89.3 and 97.7% which is similar to the study done by Popli et al<sup>(65)</sup> who had the Sp ranging from 80 to 98 % and also correlated with Moon et al<sup>(63)</sup> who had the Sp ranging between 90 to 93 %.

The central vascularity was not statistically significant for representation of malignant nodule. Which was in contradiction to the study done by moon et al<sup>(63)</sup> who found that central/ central > peripheral vascularity was statistically significant in noticing malignant nodules.

The individual US feature showed variable Sn and Sp but when all the US features were combined and classified into various TIRADS category based on the classification given by Sanchez et al<sup>(61)</sup>.

Considering TIRADS 3 as the cutoff showed very low accuracy in detecting the malignant nodules and considering TIRADS 4B showed a very high accuracy in detecting the malignant nodule.

### **THE ACCURACY OF SHEAR WAVE ELASTOGRAPHY**

The ARFI technique uses the ultrasound waves as mechanical waves which propagates at different speed based on the elasticity of the medium. These waves travels as longitudinal compressional waves and also as transverse vibrations known as shear waves. The velocity can be tracked by the small tissue displacements they cause. In the present study the shear wave elastography showed a significant correlation between the shear wave elastography in detection of the malignant nodule with Sn of 80 %, Sp of 93.3 %, PPV of 93.3 % and NPV of 80 % considering 3 cm/s as a cutoff velocity. The findings are similar to the result obtained by grazhdani et al<sup>(2)</sup> who had a sensitivity, specificity, PPV and NPV of 90%, 75 %, 90 % and 96.5 %.

Gu et al<sup>(1)</sup> in his study found that considering 2.55 m/s the sensitivity was 86.36 %, specificity was 93.42 % and a diagnostic accuracy was 91.84 % in detecting the malignant nodules. These findings also correlated with our study.

The study done by Hamidi et al<sup>(66)</sup> found that considering the cutoff of 2.66 m/s showed a Sn and Sp of 100 % and 82.4 %. Which correlated with our study.

Various other studies done by XU et al<sup>(30)</sup>, Calvete et al<sup>(67)</sup>, Deng et al<sup>(38)</sup>, Zhuo et al<sup>(58)</sup>, Bojunga et al<sup>(31)</sup>, Hou et al<sup>(68)</sup>, Zhang YF et al<sup>(27)</sup>, Zhang FJ et al<sup>(3)</sup> found that shear wave elastography showed high Sn and Sp ranging from 70 to 100 % as described in the table.

Table 26 : Comparison of shear wave elastography among different studies

S.no	Study	SWV	Sensitivity (%)	Specificity (%)
1	Liu BJ et al	2.58 m/s	76	70
2	Hamidi et al <sup>(66)</sup>	2.66 m/s	100	82.3
3	Xu et al <sup>(30)</sup>	2.87 m/s	71.6	83.4
4	Calvette et al <sup>(67)</sup>	2.50 m/s	85.7	96
5	Deng et al <sup>(38)</sup>	2.59 m/s	80.4	84
6	Zhuo et al <sup>(58)</sup>	2.54 m/s	96.3	96.2
7	Hou et al <sup>(73)</sup>	2.42 m/s	80	90.5
8	Gu et al <sup>(1)</sup>	2.55 m/s	86.4	93.4
9	Zhang YF et al <sup>(27)</sup>	2.87 m/s	75	82.2
10	Zhang FJ et al <sup>(3)</sup>	2.84 m/s	96.8	95.7
11	Present study	3 m/s	80 %	93.3 %

In the present study we found that the black and white color coding was statistically significant in detecting the malignant nodules, with 7 of the 15 nodules appearing more than 50 % black than the surrounding normal parenchyma which suggests malignancy and 4 of the 15 malignant nodules appearing same color as the normal parenchyma which suggests indeterminate and rest of the 4 nodules looking more white as compared to the normal parenchyma. Of the 45 benign nodules 23 of the nodules

displayed color same as the surrounding normal parenchyma while 20 of the nodules revealed color more white than the surrounding normal parenchyma.

In the present study, the most of the benign (40) and malignant (10) nodules displayed green color on SWV color coding suggesting indeterminate. While only 3 of the 15 malignant nodules showed red in SWV color coding, which suggests malignancy. There was no statistical significant of SWV color coding in characterization of benign and malignant nodules.

In the present study it was found considering the velocity of 3 m/s the sensitivity and specificity was 80% and 93.3% but however the similar sensitivity and specificity was seen when the velocity was taken as 2.77 m/s as there were no cases with mean velocity between 2.77 m/s and 3 m/s. Hence 2.77 m/s can be considered as the cutoff velocity in differentiating the benign and malignant nodules.

### **COMPARISON BETWEEN THE GREY SCALE ULTRASOUND AND SHEAR WAVE ELASTOGRAPHY:**

When each parameters of the ultrasound was considered as parameter to detect the malignant nodules there was variable sensitivity and specificity ranging from as low as 10 % to as high as 100 % with microcalcification showing the highest sensitivity, specificity and accuracy of 100%, 97 % and 98 % respectively and when the parameters were combined to give a TIRADS score TIRADS 3 which is considered as Intermediate between benign and malignant nodule for which the patient undergo FNAC showed a very low accuracy and risk stratification. However, considering TIRADS 4b as a cutoff the sensitivity was high.

The SWE considering 2.77 m/s as a cutoff the modality showed a high Sn and Sp of 80 % and 93.3 % respectively, which shows that it is a better modality in differentiating the benign and malignant nodules and can avoid unnecessary FNA/ Biopsy.

The black and white color coding indicated that out of the 15 malignant nodules, 7 (47 %) appear more than 50% black as compared to the surrounding normal parenchyma suggesting the nodule is hard, 4(26%) out of 15 malignant nodules appear same color as the surrounding normal parenchyma suggesting the finding is intermediate and 4(26 %) appear more white than the surrounding normal parenchyma suggesting the nodules appear benign on color coding on elastography. The black and white color coding indicated statistical importance in identifying malignant nodules considering more than 50 % black than the normal parenchyma as the criteria with p value <0.001.

The SWV color coding exhibited that majority of the benign and malignant nodules displayed green color on SWV color coding suggesting intermediate in differentiating benign and malignant nodules. Only 4 (26%) of the 15 malignant nodules showed red color on color coding suggestive of harder nodule malignant nodule. There was no statistical significance of SWV color coding in differentiating benign and malignant nodule.

Hence SWE can be used along with the ultrasonography to increase the confidence for better characterization and quantification of stiffness of the tissue, so that we avoid unnecessary FNA and Biopsy.

## **CONCLUSION**

The present study could demonstrate that the ultrasound features like Taller-than-wide shape, Lobulated/poorly defined margins, Hypoechoogenicity, Microcalcifications, and associated cervical lymphadenopathy suggests the presence malignancy with moderate to high Sn and Sp.

Among all the ultrasound feature microcalcification shows highest accuracy in predicting the malignant nodules. However presence of central or central > peripheral vascularity do not show any statistical significance.

Likewise the presence of Wider than tall shape, Well defined margins and Hyperechogenicity suggests benignity.

The TIRADS score considering TIRADS 3 or 4A as a cutoff of benignancy and malignancy showed low Sn and Sp but considering TIRADS 4B showed high sensitivity and specificity.

However the SWE considering shear wave velocity of 2.77 m/s showed more Sn and Sp in differentiating benign and malignant nodules than the ultrasound and Doppler.

The black and white color coding showed statistical significance in differentiating malignant and benign nodules, considering > 50 % black than the surrounding normal parenchyma as hard / malignant nodule and more white than normal parenchyma as a benign nodule.

The SWV color coding did not show statistical significance in differentiating benign and malignant nodule considering light and dark blue as benign nodules and orange and red suggesting hard / malignant nodule.

This suggested that SWE is an easy, non-invasive and rapid technique that can be used as an additional tool in the work-up of nodules to increase the confidence in differentiating the benign and malignant nodules and then to select cases for FNAC which would avoid unnecessary biopsies, and consequently decrease the complications related to it.



## **SUMMARY**

This study was a prospective study with objective to evaluate the thyroid nodules based on SWE into benign and malignant nodules and then compare it with the histopathological diagnosis. Then compare the efficacy of grey scale ultrasound and Doppler using TIRADS with the SWE to differentiate the benign and malignant nodules with histopathology as gold standard.

The study included 60 patients who underwent grey scale ultrasound and doppler and shear wave elastography for the thyroid nodules followed by fine needle aspiration cytology and /or histological examination.

Out of the 60 nodules, benign are 45 and 15 malignant. Majority of the benign and malignant nodules existed in the phase of 30-40 years. The thyroid nodules were detected to be largely seen in females (53) compared to males (7) with female to male ratio of 7.5:1. On histopathology, malignancy was found most commonly in females with 12 of the 15 malignant nodules and less common in male 3 of the 15 malignant nodules.

The ultrasound features including the hypoechogenicity, microcalcification, taller than wide and lobulated or poorly defined margins showed statistical significance in detecting malignant nodules with overall accuracy of 75 %, 98 %, 85 % and 78 % respectively.

Presence of lymph nodes in association with malignant thyroid nodules showed statistical significance with Sp of 91.3 % and accuracy of 78 %.

On classifying the thyroid nodules into various TIRADS classification based on Fernandez-Sanchez classification showed that most of the benign nodules were classified under TIRADS 2, 3 and 4A. Majority of the nodules classified under TIRADS 4B and 4C were malignant nodules. The risk of malignancy increases with increase in TIRADS score.

Then the nodules were classified into benign and malignant nodules based on shear wave elastography using ARFI technique 3 m/s as a cutoff value and also based on the SWV map and black & white color coding map. The shear wave velocity showed a high Sn of 80 % and Sp of 93.3 %. The black and white color coding system showed significant statistical difference in identifying malignant nodules bearing in mind more than 50 % black as compared to the normal parenchyma as hard / malignant nodule. But however the SWV map showed no statistical significance.

The limitation of the study includes the shorter duration of the study, small sample size compared to prior done studies.

## **BILBIOGRAPHY**

- 1 Gu J, Du L, Bai M, Chen H, Jia X, Zhao J et al. Preliminary Study on the Diagnostic Value of Acoustic Radiation Force Impulse Technology for Differentiating Between Benign and Malignant Thyroid Nodules. *Journal of Ultrasound in Medicine*. 2012;31(5):763-771.
- 2 Grazhdani H, Cantisani V, Lodise P, Di Rocco G, Proietto M, Fioravanti E et al. Prospective evaluation of acoustic radiation force impulse technology in the differentiation of thyroid nodules: accuracy and interobserver variability assessment. *Journal of Ultrasound*. 2014;17(1):13-20.
- 3 Zhang F, Han R. The value of acoustic radiation force impulse (ARFI) in the differential diagnosis of thyroid nodules. *European Journal of Radiology*. 2013;82(11):e686-e690.
- 4 Policeni B, Smoker W, Reede D. Anatomy and Embryology of the Thyroid and Parathyroid Glands. *Seminars in Ultrasound, CT and MRI*. 2012;33(2):104-114.
- 5 Ozgur Z, Celik S, Govsa F, Ozgur T. Anatomical and surgical aspects of the lobes of the thyroid glands. *European Archives of Oto-Rhino-Laryngology*. 2011;268(9):1357- 1363.
- 6 Gray H, Clemente CD. *Anatomy of the Human Body (American ed 30)*. Philadelphia, PA, Lea and Febiger, 1985
- 7 Som PM, Curtin HD: *Head and Neck Imaging (ed 4)*. St Louis, MO, Mosby, 2003
- 8 Rubio IG, Medeiros-Neto G *Curr Opin Endocrinol Diabetes Obes*. 2009 Oct;16(5):373-8.

- 9 Chiamolera M, Wondisford F. Thyrotropin-Releasing Hormone and the Thyroid Hormone Feedback Mechanism. *Endocrinology*. 2009;150(3):1091-1096.
- 10 Solbiati L, Charboneau JW, Osti V, James EM, Hay ID. The thyroid gland. In: Rumack CM, Wilson SR, Charboneau JW, editors. *Diagnostic Ultrasound*. 3rd ed. Vol. 1. St. Louis, Missouri: Elsevier Mosby; 2005. pp. 735–70.
- 11 Chaudhary V, Bano S. Imaging of the thyroid: Recent advances. *Indian Journal of Endocrinology and Metabolism*. 2012;16(3):371.
- 12 Nodules A. American association of clinical endocrinologists and associazione medici endocrinologi medical guidelines for clinical practice for the diagnosis and management of thyroid nodules. *Endocrine Practice*. 2006;12(1):63-102.
- 13 Baskin H. *Thyroid ultrasound and ultrasound-guided FNA biopsy*. Boston: Kluwer Academic Publishers; 2000.
- 14 Moon W, Jung S, Lee J, Na D, Baek J, Lee Y et al. Benign and Malignant Thyroid Nodules: US Differentiation—Multicenter Retrospective Study. *Radiology*. 2008;247(3):762-770.
- 15 Chaudhary V, Bano S. Thyroid ultrasound. *Indian Journal of Endocrinology and Metabolism*. 2013;17(2):219.
- 16 Zhao C, Xu H. Ultrasound elastography of the thyroid: principles and current status.

Ultrasonography. 2019;38(2):106-124.

17 Ophir J, Céspedes I, Ponnekanti H, Yazdi Y, Li X. Elastography: A Quantitative Method for Imaging the Elasticity of Biological Tissues. Ultrasonic Imaging. 1991;13(2):111-134.

18 Lyshchik A, Higashi T, Asato R, Tanaka S, Ito J, Mai J et al. Thyroid Gland Tumor Diagnosis at US Elastography. Radiology. 2005;237(1):202-211.

19 Sebag F, Vaillant-Lombard J, Berbis J, Griset V, Henry J, Petit P, et al. Shear wave elastography: a new ultrasound imaging mode for the differential diagnosis of benign and malignant thyroid nodules. The Journal of Clinical Endocrinology & Metabolism. 2010;95(12):5281-8.

20. Cosgrove D, Barr R, Bojunga J, Cantisani V, Chammas M, Dighe M et al.

WFUMB Guidelines and Recommendations on the Clinical Use of Ultrasound Elastography: Part 4.

Thyroid. Ultrasound in Medicine & Biology. 2017;43(1):4-26.

21. Haugen B, Alexander E, Bible K, Doherty G, Mandel S, Nikiforov Y et al. 2015 American Thyroid Association Management Guidelines for Adult Patients with Thyroid Nodules and Differentiated Thyroid Cancer: The American Thyroid Association Guidelines Task Force on Thyroid Nodules and Differentiated Thyroid Cancer. Thyroid. 2016;26(1):1-133.

22. Gharib H, Papini E, Garber J, Duick D, Harrell R, Hegedüs L et al. AMERICAN ASSOCIATION OF CLINICAL ENDOCRINOLOGISTS, AMERICAN COLLEGE OF ENDOCRINOLOGY, AND ASSOCIAZIONE MEDICI ENDOCRINOLOGI MEDICAL GUIDELINES FOR CLINICAL PRACTICE FOR THE DIAGNOSIS AND MANAGEMENT

OF THYROID NODULES – 2016 UPDATE. *Endocrine Practice*. 2016;22(Supplement 1):1-60.

23 Cosgrove D, Piscaglia F, Bamber J, Bojunga J, Correas J, Gilja O et al. EFSUMB Guidelines and Recommendations on the Clinical Use of Ultrasound Elastography. Part 2: Clinical Applications. *Ultraschall in der Medizin - European Journal of Ultrasound*. 2013;34(03):238-253.

24 Bamber J, Cosgrove D, Dietrich C, Fromageau J, Bojunga J, Calliada F et al. EFSUMB Guidelines and Recommendations on the Clinical Use of Ultrasound Elastography. Part 1: Basic Principles and Technology. *Ultraschall in der Medizin - European Journal of Ultrasound*. 2013;34(02):169-184.

25 Shiina T, Nightingale K, Palmeri M, Hall T, Bamber J, Barr R et al. WFUMB Guidelines and Recommendations for Clinical Use of Ultrasound Elastography: Part 1: Basic Principles and Terminology. *Ultrasound in Medicine & Biology*. 2015;41(5):1126-1147.

26. Andrioli M, Persani L. Elastographic techniques of thyroid gland: current status.

*Endocrine*. 2014;46(3):455-461.

27 Xu J, Xu H, Zhang Y, Guo L, Liu L, Bo X et al. Virtual Touch Tissue Imaging for Differential Diagnosis of Thyroid Nodules. *Journal of Ultrasound in Medicine*. 2016;35(5):917-926.

28 Liu B, Xie X, Liang J, Zheng Y, Huang G, Zhou L et al. Shear wave elastography versus real-time elastography on evaluation thyroid nodules: A preliminary study. *European Journal of Radiology*. 2014;83(7):1135-1143.

- 29 Yang Y, Xu X, Bo X, Liu B, Guo L, Xu J et al. Comparison of Virtual Touch Tissue Imaging & Quantification (VTIQ) and Virtual Touch Tissue Quantification (VTQ) for diagnosis of thyroid nodules. *Clinical Hemorheology and Microcirculation*. 2017;65(2):137-149.
- 30 Xu J, Xu X, Xu H, Zhang Y, Zhang J, Guo L et al. Conventional US, US Elasticity Imaging, and Acoustic Radiation Force Impulse Imaging for Prediction of Malignancy in Thyroid Nodules. *Radiology*. 2014;272(2):577-586.
- 31 Bojunga J, Dauth N, Berner C, Meyer G, Holzer K, Voelkl L et al. Acoustic Radiation Force Impulse Imaging for Differentiation of Thyroid Nodules. *PLoS ONE*. 2012;7(8):e42735.
- 32 Liu BJ, Li DD, Xu HX, Guo LH, Zhang YF, Xu JM, et al. Quantitative shear wave velocity measurement on acoustic radiation force impulse elastography for differential diagnosis between benign and malignant thyroid nodules: a meta-analysis. *Ultrasound Med Biol*. 2015;41:3035–3043.
- 33 Díaz Soto G, Halperin I, Squarcia M, Lomeña F, Puig Domingo M. Update in thyroid imaging. The expanding world of thyroid imaging and its translation to clinical practice. *HORMONES*. 2010;9(4):287-298.
- 34 Feine U, Lietzenmayer R, Hanke JP, Held J, Wöhrle H, Müller-Schauenburg W. Fluorine-18-FDG and iodine-131-iodide uptake in thyroid cancer. *J Nucl Med* 1996;37:1468-72.
- 35 Ersoy R, Karako A, Atasever T. Imaging techniques for metastatic thyroid medullary cancer. *Turk J Endocrinol Metab* 2002;4:149-53

36 Reading C, Gorman C. Thyroid Imaging Techniques. *Clinics in Laboratory Medicine*. 1993;13(3):711-724.

37 Heshmati H, Gharib H, van Heerden J, Sizemore G. Advances and Controversies in the Diagnosis and Management of Medullary Thyroid Carcinoma. *The American Journal of Medicine*. 1997;103(1):60-69.

38 Deng J, Zhou P, Tian S, Zhang L, Li J, Qian Y. Comparison of Diagnostic Efficacy of Contrast-Enhanced Ultrasound, Acoustic Radiation Force Impulse Imaging, and Their Combined Use in Differentiating Focal Solid Thyroid Nodules. *PLoS ONE*. 2014;9(3):e90674.

39 Hempel J, Kloeckner R, Krick S, Pinto dos Santos D, Schadmand-Fischer S, Boeßert P et al. Impact of combined FDG-PET/CT and MRI on the detection of local recurrence and nodal metastases in thyroid cancer. *Cancer Imaging*. 2016;16(1).

40 Wong K, Zanzhovsky N, Cahill J, Frey K, Avram A. Hybrid SPECT-CT and PET-CT imaging of differentiated thyroid carcinoma. *The British Journal of Radiology*. 2009;82(982):860-876.

41 Van den Bruel A, Maes A, De Potter T, Mortelmans L, Drijkoningen M, Van Damme B et al. Clinical Relevance of Thyroid Fluorodeoxyglucose-Whole Body Positron Emission Tomography Incidentaloma. *The Journal of Clinical Endocrinology & Metabolism*. 2002;87(4):1517-1520.

42 De Geus-Oei LF, Pieters GF, Bonenkamp JJ, Mudde AH, Bleeker-Rovers CP, Corstens FH, et al. <sup>18</sup>F-FDG PET reduces unnecessary hemithyroidectomies for thyroid nodules with



inconclusive cytologic results. *J Nucl Med* 2006;47:770-5.

43 Imanishi Y, Ehara N, Mori J, Shimokawa M, Sakuyama K, Ishikawa T et al. Measurement of Thyroid Iodine by CT. *Journal of Computer Assisted Tomography*. 1991;15(2):287-290.

44 Cooper D, Doherty G, Haugen B, Kloos R, Lee S, Mandel S et al. Revised American Thyroid Association Management Guidelines for Patients with Thyroid Nodules and Differentiated Thyroid Cancer. *Thyroid*. 2009;19(11):1167-1214.

45 Bozgeyik Z, Coskun S, Dagli A, Ozkan Y, Sahpaz F, Ogur E. Diffusion-weighted MR imaging of thyroid nodules. *Neuroradiology*. 2009;51(3):193-198.

46 King A, Yeung D, Ahuja A, Tse G, Chan A, Lam S et al. In vivo <sup>1</sup>H MR spectroscopy of thyroid carcinoma. *European Journal of Radiology*. 2005;54(1):112- 117.

47 Zhou C, Wang Y, Aguirre A, Tsai T, Cohen D, Connolly J et al. Ex vivo imaging of human thyroid pathology using integrated optical coherence tomography and optical coherence microscopy. *Journal of Biomedical Optics*. 2010;15(1):016001.

48 Pantanowitz L, Hsiung P, Ko T, Schneider K, Herz P, Fujimoto J et al. High- resolution imaging of the thyroid gland using optical coherence tomography. *Head & Neck*. 2004;26(5):425-434.

49 Hoang J, Lee W, Lee M, Johnson D, Farrell S. US Features of Thyroid Malignancy: Pearls and Pitfalls. *RadioGraphics*. 2007;27(3):847-860.

50. Cibas E, Ali S. The Bethesda System for Reporting Thyroid Cytopathology. *Thyroid*. 2009;19(11):1159-1165.
51. Tuttle R, Haddad R, Ball D, Byrd D, Dickson P, Duh Q et al. Thyroid Carcinoma, Version 2.2014. *Journal of the National Comprehensive Cancer Network*. 2014;12(12):1671-1680.
- 52 Ying M, Ahuja A. Sonography of Neck Lymph Nodes. Part I: Normal Lymph Nodes. *Clinical Radiology*. 2003;58(5):351-358.
- 53 Gharib H, Papini E, Paschke R, Duick D, Valcavi R, Hegedüs L et al. American Association of Clinical Endocrinologists, Associazione Medici Endocrinologi, and European Thyroid Association Medical Guidelines for Clinical Practice for the Diagnosis and Management of Thyroid Nodules: Executive Summary of Recommendations. *Endocrine Practice*. 2010;16(3):468-475.
- 54 Baloch Z, Cib53as E, Clark D, Layfield L, Ljung B, Pitman M et al. The National Cancer Institute Thyroid Fine Needle Aspiration State of the Science Conference: a Summation. *CytoJournal*. 2008;5(1):6. 55 Pitman MB, Abele J, Ali SZ, Duick D, Elsheikh TM, Jeffrey RB, Powers CN, Randolph G, Renshaw A, Scoutt L *Diagn Cytopathol*. 2008 Jun; 36(6):407-24.
- 56 Crockett JC. The thyroid nodule: fine-needle aspiration biopsy technique. *J Ultrasound Med*. 2011;30:685–694.
- 57 Kim M, Kim E, Park S, Kim B, Kwak J, Kim S et al. US-guided Fine-Needle Aspiration of Thyroid Nodules: Indications, Techniques, Results. *RadioGraphics*. 2008;28(7):1869-1886.

58 Zhuo J, Ma Z, Fu W, Liu S. Differentiation of benign from malignant thyroid nodules with acoustic radiation force impulse technique. *The British Journal of Radiology*. 2014;87(1035):20130263.

59 Fadda G, Rossi E. Liquid-Based Cytology in Fine-Needle Aspiration Biopsies of the Thyroid Gland. *Acta Cytologica*. 2011;55(5):389-400. 60 Hoang J, Lee W, Lee M, Johnson D, Farrell S. US Features of Thyroid Malignancy: Pearls and Pitfalls. *RadioGraphics*. 2007;27(3):847-860.

61 Fernandez-Sanchez J. TI-RADS classification of thyroid nodules based on a score modified according to ultrasound criteria for malignancy. *Rev Argent Radiol*. 2014;78:138–48

62 Moon W, Jung S, Lee J, Na D, Baek J, Lee Y et al. Benign and Malignant Thyroid Nodules: US Differentiation—Multicenter Retrospective Study. *Radiology*. 2008;247(3):762-770.

63 Seo Y, Yoon D, Yoon S, Lim K, Yun E, Choi C et al. Compressibility of Thyroid Masses: A Sonographic Sign Differentiating Benign From Malignant Lesions?. *American Journal of Roentgenology*. 2012;198(2):434-438.

64 Kim E, Park C, Chung W, Oh K, Kim D, Lee J et al. New Sonographic Criteria for Recommending Fine-Needle Aspiration Biopsy of Nonpalpable Solid Nodules of the Thyroid. *American Journal of Roentgenology*. 2002;178(3):687-691.

65 Popli M, Bhalla P, Rastogi A, Solanki Y. Utility of gray-scale ultrasound to differentiate benign from malignant thyroid nodules. *Indian Journal of Radiology and Imaging*. 2012;22(1):63.

66. Hamidi C, Göya C, Hattapoğlu S, et al. Acoustic Radiation Force Impulse (ARFI) imaging for the distinction between benign and malignant thyroid nodules. *Radiol Med*. 2015;120(6):579–83.
67. Calvete AC, Mestre JD, Gonzalez JM, et al. Acoustic radiation force impulse imaging for evaluation of the thyroid gland. *J Ultrasound Med*. 2014;33(6):1031–40.
- 68 Hou X, Sun A, Zhou X, Ji Q, Wang H, Wei H et al. The application of Virtual Touch tissue quantification (VTQ) in diagnosis of thyroid lesions: A preliminary study. *European Journal of Radiology*. 2013;82(5):797-801.
- 69 Deng J, Zhou P, Tian S, Zhang L, Li J, Qian Y. Comparison of Diagnostic Efficacy of Contrast-Enhanced Ultrasound, Acoustic Radiation Force Impulse Imaging, and Their Combined Use in Differentiating Focal Solid Thyroid Nodules. *PLoS ONE*. 2014;9(3):e90674.

**ANNEXURES**  
**CONSENT FORM**

**TITLE OF RESEARCH: ROLE OF ULTRASONOGRAPHY AND ULTRASOUND ELASTOGRAPHY IN THE EVALUATION OF THYROID NODULES.**

**GUIDE : DR. RAMESH C PATTANASHETTI**

**P.G. STUDENT : DR. SHABARISH.D.V**

**PURPOSE OF RESEARCH:**

I have been informed that the purpose of this study is to assess the role of ultrasonography and ultrasound Elastography in differentiating benign and malignant thyroid nodules.

**PROCEDURE:**

I understand that I will undergo history, clinical examination, ultrasonography and elastographic examination and Histopathological follow up.

**RISKS AND DISCOMFORTS:**

I understand that there is no risk involved and I may experience mild pain during the above mentioned procedures

**BENEFITS:**

I understand that my participation in this study will help to assess the role of Elastography in evaluating thyroid lesions.

**CONFIDENTIALITY:**

I understand that the medical information produced by the study will become a part of hospital record and will be subjected to confidentiality and privacy regulations of hospital. If the data is used for publications the identity of the patient will not be revealed.

**REQUEST FOR MORE INFORMATION:**

I understand that I may ask for more information about the study at any time.

**REFUSAL OR WITHDRAWAL OF PARTICIPATION:**

I understand that my participation is voluntary and I may refuse to participate or withdraw from study at any time

**INJURY STATEMENT:**

I understand in the unlikely event of injury to me during the study I will get medical treatment but no further compensations. I will not hold the hospital and its staff responsible for any untoward incidence during the course of study.

Date:

Dr. Ramesh C Pattanashetti  
(Guide)

Dr. Shabarish d v  
(Investigator)

**STUDY SUBJECT CONSENT STATEMENT:**

I/my ward confirm that Dr. Shabarish d v has explained to me the purpose of this research, the study procedure that I will undergo and the possible discomforts and benefits that I may experience, in my own language.

I/my ward have been explained all the above in detail in my own language and I understand the same. Therefore I agree to give my consent to participate as a subject in this project.

\_\_\_\_\_  
(Participant)

\_\_\_\_\_  
Date

\_\_\_\_\_  
(Witness to above signature)

\_\_\_\_\_  
Date

**PROFORMA**

**TITLE: ROLE OF SHEAR WAVE ELASTOGRAPHY IN EVALUATION OF  
THYROID NODULES**

**INVESTIGATOR: DR. SHABARISH D V**

**GUIDE: DR. RAMESH C PATTANASHETTI**

**CASE NO:**

**NAME:**

**AGE:**

**SEX:**

**HOSPITAL NO:**

**CLINICAL HISTORY:**

**PRESENT HISTORY:**

- 1. Neck swelling:**
- 2. Dysphagia:**
- 3. Dyspnea:**
- 4. Hoarseness of voice:**
- 5. Pain:**
- 6. Weight gain/ loss:**

**7. Rate of growth:**



**PAST HISTORY:**

**FAMILY HISTORY:**

**PERSONAL HISTORY:**

**GENERAL PHYSICAL EXAMINATION**

1. Pallor:
2. Icterus:
3. Cyanosis:
4. Clubbing:
5. Edema:

**LOCAL (THYROID & NECK) EXAMINATION:**

**I. PALPATION:**

1. Palpable: Solitary / Multiple-
2. Non-palpable:
3. Consistency: Soft / Firm / Hard
4. Tenderness:

**II. Movement with deglutition: Moves with deglutition / Doesn't move with deglutition**

**III. Fixity to underlying structures: Present / Absent.**

**IV. Lymphadenopathy: Number / Size / Consistency.**

**ULTRASOUND FINDINGS:**

**I. NUMBER OF NODULE/S:**

**II. SITE OF THE NODULE/S: Right lobe / Left lobe / Isthmus-**

**III. LOCATION: Upper pole / Mid portion / Lower pole.**

**IV. SIZE:**

**Measurements**

**Volume**

**1. Right lobe**

**2. Left lobes**

**3. Isthmus**

**4. Nodules**

**V. SHAPE:**

**1. Taller than wide-**

**2. Wider than tall-**

**VI. MARGINS:**

**1. Well defined-**

**2. Poorly defined-**

**VII.ECHOGENICITY:**

**1. Hyperechoic-1**

**2. Isoechoic-2**

**3. Hypoechoic-3**

**4. Anechoic-4**

**5. Mixed echogenicity-5**

**VIII. CONTENT :**

- 1. Cystic-1**
- 2. Solid-2**
- 3. Mixed-3**
- 4. Predominantly cystic4-**
- 5. Predominantly solid-5**

**IX. CALCIFICATION:**

- 1. Microcalcification- 3**
- 2. Macrocalcification-2**
- 3. Absent-1**

**X. LYMPHADENOPATHY:**

**COLOR DOPPLER FINDINGS-**

**I. VASCULARITY:**

- 1. Central-**
- 2. Peripheral-**
- 3. Predominantly central-**
- 4. Predominantly peripheral-**

**SUSPICIOUS CRITERIA FOR MALIGNANCY:**

**FEATURES**

**1. HYPOECHOGENICITY**

2. MICROCALCIFICATIONS
3. TALLER THAN WIDE SHAPE
4. THYROID PARENCHYMA INVASION
5. IRREGULAR MARGINS
6. INTRANODULAR VASCULARITY
7. PARTIALLY CYSTIC NODULE WITH ECCENTRIC LOCATION OF THE FLUID PORTION AND LOBULATION OF SOLID COMPONENT

**TOTAL SCORE:**

**TIRADS CATEGORY:**

**SHEAR WAVE ELASTOGRAPHY FINDINGS**

**I. SHEAR WAVE VELOCITY**

Velocity	Velocity1	Velocity2	Velocity3	Velocity4	Velocity5	Average velocity
<b>Nodules</b>						
<b>Nodule 1</b>						
<b>Nodule 2</b>						
<b>Nodule 3</b>						

**II. BLACK AND WHITE TOUCH TISSUE IMAGING:**

More white than the surrounding normal tissue	
Same colour as the normal thyroid tissue	
>50 black as compared to normal tissue	

**III. SHEAR WAVE VELOCITY MAP**

LIGHT BLUE	
DARK BLUE	
GREEN	
ORANGE	
RED	

**BLOOD INVESTIGATIONS:**

**THYROID FUNCTION TESTS:**

**FINE NEEDLE ASPIRATION CYTOLOGY:**

**HISTOPATHOLOGY (wherever available):**

**SIGNATURE OF THE INVESTIGATOR:**

**SIGNATURE OF THE GUIDE**

# MASTER CHART

	NAME	AGE	SEX	SWELLING	DYSPLAGIA	DYSPLNEA	HOARSENESS/OF VOICE	PAIN	WIEGHT_GAIN	WIEGHT_LOSS	RATE_OF_GROWTH	PALPATION	PALPATION_SOLITARY/MULTIPLE	CONSISTENCY_SOFT/FIRM/HARD	TENDERNESS	MOVES_WITH DEGLUTITION	FIXITY TO UNDERLYING STRUCTURE	LYMPHADENOPATHY	USC NUMBER OF NODULES	USCSITE
1	SHYAMOLIP	5	1	1	2	2	2	2	2	2	1	1	1	2	2	1	2	2	1	1
2	SUDHILA BA	6	1	1	2	2	2	2	2	2	1	1	1	2	2	1	2	2	2	3
3	NAVANTHA	4	1	1	2	2	2	2	2	2	1	1	2	1	2	1	2	2	2	3
4	MADAR BI	7	1	1	2	2	2	2	2	2	1	1	1	1	2	1	2	2	1	1
5	VISHVESHW	6	2	1	2	2	2	2	2	2	1	1	2	1	2	1	2	2	2	3
6	HARINAKSH	5	1	1	2	2	2	2	2	2	1	1	2	2	2	1	2	2	2	3
7	VASANTHA	2	1	1	2	2	2	2	2	2	1	1	2	2	2	1	2	2	2	3
8	GEETHA	3	1	1	2	2	2	2	2	2	1	1	1	2	2	1	2	2	1	2
9	VASANTHA	4	1	1	2	2	2	2	2	2	1	1	2	2	2	1	2	2	2	3
10	DEVIRAMM	2	1	1	2	2	2	2	2	2	1	1	1	2	2	1	2	2	1	4
11	ARUNAKU	M	4	1	1	2	2	2	2	2	1	1	2	2	2	1	2	2	2	3
12	ANITHA	3	1	1	2	2	2	1	2	2	1	1	2	2	2	1	2	1	2	2
13	TARANNUM	2	1	1	2	2	2	2	2	2	1	1	2	2	2	1	2	1	2	3
14	PALLAVI	2	1	1	2	2	2	2	2	2	1	1	1	2	2	1	2	2	1	1
15	LAVANYA	2	1	1	2	2	2	2	2	2	1	1	1	2	2	1	2	2	1	1
16	SHANTAMM	3	1	1	2	2	2	2	2	2	1	1	1	2	2	1	2	2	1	1
17	KAVITHA	4	1	1	2	2	2	2	2	2	1	1	2	2	2	1	2	2	2	3
18	JYOTI	2	1	1	2	2	2	2	2	2	1	1	2	2	2	1	2	2	2	3
19	NAGARATN	4	1	1	2	2	2	2	2	2	1	1	2	2	2	1	2	2	2	3
20	POORNIMA	2	1	1	2	2	2	2	2	2	1	1	1	2	2	1	2	2	1	1
21	MALA	3	1	1	2	2	2	2	2	2	1	1	1	2	2	1	2	2	1	1
22	JAYAMMA	4	2	1	2	2	2	2	2	2	1	1	2	2	2	1	2	2	2	3
23	GOLLARA	3	1	1	2	2	2	2	2	2	1	1	2	2	2	1	2	2	2	3
24	MUNILAKSH	4	1	1	2	2	2	2	2	2	1	1	2	2	2	1	2	2	2	3
25	AMBIKA	5	1	1	2	2	2	2	2	2	1	1	1	2	2	1	2	2	1	1
26	PARVATHI	3	1	1	2	2	2	1	2	2	1	1	2	2	2	1	2	1	2	2
27	KALAVATHI	2	1	1	2	2	2	2	2	2	1	1	2	2	2	1	2	1	2	3
28	KARUNA	2	1	1	2	2	2	2	2	2	1	1	1	2	2	1	2	2	1	1
29	DHANAMD	A	5	1	1	2	2	1	2	2	2	1	1	3	2	1	2	2	1	2
30	NARAYANA	7	1	1	2	2	2	1	2	2	1	1	1	3	1	2	1	2	1	2
31	LALA MUB	3	1	1	2	2	2	2	2	2	1	1	1	3	2	2	1	1	2	3
32	SWATHI	2	1	1	2	2	2	2	2	2	1	1	2	3	2	1	2	2	2	3
33	KRISHNA	4	2	1	2	2	2	2	2	2	1	1	1	2	2	1	2	2	1	1
34	ASHGARI	6	1	1	2	2	2	2	2	2	1	1	1	2	2	1	2	2	2	1
35	SHEELA	5	1	1	2	2	2	2	2	2	1	1	2	2	2	1	2	2	2	3
36	SATHEE	5	1	1	2	2	2	2	2	2	1	1	2	2	2	1	2	2	2	3
37	SRLATHA	3	1	1	2	2	2	2	2	2	1	1	1	2	2	1	2	2	2	3
38	PALLAVI	2	1	1	2	2	2	2	2	2	1	1	1	2	2	1	2	2	1	1
39	HEMA	3	1	1	2	2	2	2	2	2	1	1	1	2	2	1	2	2	1	1
40	JAYASHREE	4	2	1	2	2	2	2	2	2	1	1	2	2	2	1	2	2	2	3
41	PARVATHI	2	1	1	2	2	2	2	2	2	1	1	2	2	2	1	2	2	2	3
42	KAMALAKS	5	1	1	2	2	2	2	2	2	1	1	1	2	2	1	2	2	1	2
43	RUKSHAR B	3	1	1	2	2	2	1	2	2	1	1	1	2	2	1	2	2	1	2
44	MOHAMME	6	2	1	2	2	2	1	2	2	1	1	1	2	2	1	2	2	1	2
45	GOWRAMM	3	1	1	2	2	2	2	2	2	1	1	2	2	2	1	2	2	2	1
46	RAMATULA	4	1	1	2	2	2	2	2	2	1	1	2	2	2	1	2	2	2	3
47	RANI	6	1	1	2	2	2	1	2	2	1	1	2	2	2	1	2	2	2	2
48	TARANNUM	2	1	1	2	2	2	2	2	2	1	1	2	2	2	1	2	1	2	3
49	PALLAVI	2	1	1	2	2	2	2	2	2	1	1	1	2	2	1	2	2	1	1
50	APARNA	4	1	1	2	2	2	2	2	2	1	1	1	2	2	1	2	2	1	2
51	GANGAMMA	6	1	1	2	2	2	2	2	2	1	1	2	2	2	1	2	2	2	3
52	VRUNDA	4	1	1	2	2	2	2	2	2	1	1	2	2	2	1	2	2	2	3
53	VISHVESHW	6	2	1	2	2	2	2	2	2	1	1	2	1	2	1	2	2	2	3
54	HARINAKSH	5	1	1	2	2	2	2	2	2	1	1	2	2	2	1	2	2	2	3
55	SAVITHRAM	7	1	1	2	2	2	2	2	2	1	1	2	2	2	1	2	1	2	3
56	MANJULA	3	1	1	2	2	2	2	2	2	1	1	1	2	2	1	2	1	1	2
57	KAMAKRISH	6	2	1	1	2	2	2	2	2	1	1	1	2	2	1	2	1	1	1
58	DEVAMMA	4	1	1	2	2	2	2	2	2	1	1	2	2	2	1	2	2	2	3
59	VIJAYA	3	1	1	1	2	2	2	2	2	1	1	1	2	2	1	2	2	1	3
60	SUSHMA	3	1	1	1	2	2	2	2	2	1	1	2	2	2	1	2	2	2	3

NUMBER THAN TALLER THAN WIDE	BELL-BENDED MARGINS / POORLY BENDED MARG	USE ECHOSIMECTY	CONTENT	NO CALCULON MACRO MERO	ESULYMPHAGOSOMY	POPTER PERIPHERAL / CENTRAL	INTRAAGE SW	TEARS	BYE...osity	BLACK AND WHITE	SW VELOCITY MAP	HISTOPATHOLOGY
1	1	5	5	1	2	2	1	3	1.91			
1	1	3	5	1	2	2	1	3	1.97			
1	1	1	5	1	2	2	1	3	1.89			
1	1	1	5	1	2	2	1	3	1.57			
1	1	5	5	1	2	2	1	3	1.2			
1	1	5	5	1	2	2	1	4	1.53			
1	1	5	5	1	2	2	1	4	1.82			
1	1	5	5	1	2	2	1	3	1.74			
1	1	1	2	1	2	2	1	3	1.85			
1	1	5	5	2	2	2	1	4	2.03			
1	1	5	2	1	2	2	1	4	1.33			
1	1	3	2	1	1	1	2	4	3.15			
1	1	1	5	2	2	2	1	3	2			
1	1	5	5	1	2	2	1	3	1.87			
1	1	5	2	1	2	2	1	4	1.9			
1	1	5	5	1	3	2	1	3	1.77			
1	1	5	5	1	3	2	1	3	1.87			
1	1	5	2	1	2	2	1	4	1.82			
1	1	5	2	3	2	2	1	4	1.8			
1	1	5	5	1	2	2	1	3	1.87			
1	1	1	2	1	2	2	1	3	1.72			
1	1	5	2	1	2	2	1	3	1.78			
1	1	5	2	1	2	2	1	3	1.9			
1	1	5	2	1	2	2	1	4	2.01			
1	1	1	2	1	2	2	1	3	1.62			
1	1	3	2	1	1	1	2	5	3.15			
1	1	1	5	2	2	2	1	3	2			
1	1	5	5	1	2	2	1	3	1.87			
1	1	5	3	3	3	1	3	6	5.33			
2	1	5	2	1	1	1	2	6	5.25			
2	1	3	2	3	2	1	2	6	3.81			
1	1	5	2	3	2	1	2	5	3.13			
1	1	5	2	2	2	1	2	3	3.79			
1	1	1	2	1	2	2	1	3	1.76			
1	1	3	2	1	2	2	1	4	1.77			
1	1	5	2	1	2	2	1	3	1.87			
1	1	5	5	1	2	2	1	3	2.45			
1	1	5	5	1	2	2	1	3	1.87			
1	1	1	2	1	2	2	1	3	1.72			
1	1	5	2	1	2	2	1	3	1.78			
1	1	5	2	1	2	1	2	4	3.73			
1	1	3	2	1	2	1	2	5	3.33			
1	1	3	2	1	1	2	2	4	3.15			
1	1	5	5	3	2	2	1	4	1.29			
1	1	5	2	2	2	2	1	3	2.03			
1	1	5	5	1	2	2	1	3	1.33			
1	1	5	2	1	2	1	2	4	3.15			
1	1	1	5	2	2	2	1	3	2			
1	1	5	5	1	2	2	1	3	1.87			
1	1	5	2	3	1	2	1	6	1.9			
1	1	3	2	1	2	2	1	4	1.77			
1	1	5	2	1	2	2	1	3	1.87			
1	1	5	5	1	2	2	1	3	1.2			
1	1	5	5	1	1	2	1	3	1.55			
2	1	5	2	1	2	1	2	5	5.5			
2	1	1	2	3	1	1	2	5	3.16			
2	1	5	2	1	1	1	2	3	3.4			
1	1	3	2	1	2	1	2	5	3.48			
1	1	1	2	1	2	2	1	3	2.2			
1	1	1	2	1	1	2	2	3	1.68			